

KATYAYANI SINGH

Neuropsychiatric endophenotypes –
focusing on IgLON adhesion molecules in
the mouse brain



KATYAYANI SINGH

Neuropsychiatric endophenotypes –
focusing on IgLON adhesion molecules in
the mouse brain



Department of Physiology, Institute of Biomedicine and Translational Medicine, University of Tartu, Tartu, Estonia

Dissertation was accepted for the commencement of the degree of Doctor of Philosophy (Neurosciences) on June 20, 2019 by the Joint Council for the Curriculum of Neurosciences.

Supervisors: Eero Vasar, MD, PhD, Professor, Department of Physiology, Institute of Biomedicine and Translational Medicine, University of Tartu, Tartu, Estonia

Mari-Anne Philips, PhD, Senior Research Fellow, Department of Physiology, Institute of Biomedicine and Translational Medicine, University of Tartu, Tartu, Estonia

Kersti Lilleväli, PhD, Senior Research Fellow, Department of Physiology, Institute of Biomedicine and Translational Medicine, University of Tartu, Tartu, Estonia

Reviewers: Džamila Safiulina, PhD, Associate Professor, Senior Research Fellow, Department of Pharmacology, Institute of Biomedicine and Translational Medicine, University of Tartu, Tartu, Estonia

Mari Palgi, PhD, Chief Officer, Department of Chemistry and Biotechnology: Division of Gene Technology, Tallinn University of Technology, Tallinn, Estonia

Opponent: Osborne Almeida, PhD, Professor, Department of Stress Neurobiology and Neurogenetics, Max Planck Institute of Psychiatry, Munich, Germany

Commencement: August 22, 2019

This research was supported by the institutional investigation grant from the Estonian Research Council IUT20-41 (E. Vasar) and personal investigation grant from the Estonian Research Council PUT129 (M.-A. Philips). This research was also supported by the European Union through the European Regional Development Fund (Project No. 2014-2020.4.01.15-0012) and from the European Union's Horizon 2020 research and innovation programme under grant agreement 692202.

ISSN 1736-2792
ISBN 978-9949-03-114-6 (print)
ISBN 978-9949-03-115-3 (pdf)



European Union
European Regional
Development Fund



Investing
in your future

Copyright: Katyayani Singh, 2018

University of Tartu Press
www.tyk.ee

CONTENTS

LIST OF ORIGINAL PUBLICATIONS	8
ABBREVIATIONS	9
INTRODUCTION	11
REVIEW OF LITERATURE	13
1. General description of Immunoglobulin superfamily of cell adhesion molecules (IgLONs)	13
2. Expression of IgLONs in mouse brain	15
3. Functional regulations of IgLONs in the mouse brain	16
4. IgLONs in association with human diseases	18
AIMS OF THE STUDY	21
MATERIALS AND METHODS	22
1. Experimental Animals	22
1.1 <i>Lsamp</i> deficient mice	22
1.2 <i>Ntm</i> deficient mice	22
1.3 <i>Lsamp Ntm</i> double deficient mice	23
1.4 <i>Negr1</i> deficient mice	23
2. Morphological study	23
2.1 Primary hippocampal neuronal culture preparation and neurite-genesis stages	23
2.2 Immunofluorescent staining and image analysis	24
2.3 Scanning electron microscopy	25
2.4 Transfection	25
2.5 Neuronal imaging and neurite analysis	25
2.6 Apoptosis Assay	26
2.7 qRT-PCR analysis	26
3. Neuroanatomical analysis	26
3.1 Nissl staining	26
3.2 Neurofilament immunohistochemical staining	27
3.3 <i>In situ</i> RNA hybridisation for <i>Negr1</i> transcript	27
3.4 Magnetic resonance imaging	28
3.5 Immunohistochemical analysis of hippocampus	29
4. Behavioral testing	29
4.1 Open field test	29
4.2 Elevated plus-maze	30
4.3 Light-dark box test	30
4.4 Morris water maze test	30
4.5 Barbering behavior testing	31
4.6 Three-chamber test	31
4.7 Social dominance tube test	32
4.8 Direct social interaction test	32

4.9 Marble burying test	32
4.10 Tail suspension test	33
5. Data presentation and Statistical Analysis	33
RESULTS	34
1. Role of IgLONs in morphology of developing neurons.....	34
1.1 <i>Lsamp</i> and <i>Ntm</i> are expressed in developing hippocampus	34
1.2 Complementary interaction of <i>Lsamp</i> and <i>Ntm</i> in the regulation of neuritogenesis.....	34
1.3 Coordinated regulation of <i>Lsamp</i> and <i>Ntm</i> in neuronal homeostasis	38
1.4 Implications of <i>Negr1</i> during neuritogenesis	40
2. Neuroanatomy of IgLONs deficient mice	42
2.1 Gross anatomy of <i>Lsamp</i> ^{-/-} , <i>Ntm</i> ^{-/-} , <i>Lsamp</i> ^{-/-} <i>Ntm</i> ^{-/-} and <i>Negr1</i> ^{-/-} brains.....	42
2.2 <i>Negr1</i> expression in the mice brain.....	42
2.3 MRI analysis of <i>Negr1</i> ^{-/-} brain.....	43
2.4 Impact of <i>Negr1</i> on hippocampal neuronal population.....	45
3. Effect of IgLONs deficiency on the mouse behavior.....	46
3.1 Coordinated interaction of <i>Lsamp</i> and <i>Ntm</i> in the regulation of behavior	46
3.1.1 Open field test	46
3.1.2 Elevated plus-maze	47
3.1.3 Morris water maze	48
3.2 Implications of <i>Negr1</i> on mouse behavior	49
3.2.1 Barbering behavior test	49
3.2.2 Three-Chamber test	50
3.2.3 Social dominance tube test	51
3.2.4 Direct Social Interaction test between <i>Negr1</i> ^{-/-} mice	51
3.2.5 Morris Water Maze test	52
3.2.6 Deficits in social behavior correlate with changes in the brain structure of <i>Negr1</i> ^{-/-} mice	54
DISCUSSION	58
1. <i>Lsamp</i> and <i>Ntm</i> interact with each other in establishing neuronal morphology and homeostasis	58
2. Of IgLON members, only <i>Negr1</i> has a profound effect on neuroanatomy	61
3. IgLON members cooperate the patterning of complex mouse behavior .	63
3.1 <i>Lsamp</i> and <i>Ntm</i> interactions in mouse behavior	63
3.2 <i>Negr1</i> is involved in regulation of social and cognitive behavior	65
4. IgLONs deficient mice in relation to neuropsychiatric endophenotypes ..	68
5. Concluding remarks and future prospects	68
CONCLUSIONS	71
REFERENCES	73

SUMMARY IN ESTONIAN	86
ACKNOWLEDGEMENT	87
PUBLICATIONS	89
CURRICULUM VITAE	141
ELULOOKIRJELDUS	144

LIST OF ORIGINAL PUBLICATIONS

- I. **Singh K**, Lilleväli K, Gilbert SF, Bregin A, Narvik J, Jayaram M, Rahi M, Innos J, Kaasik A, Vasar E, Philips MA (2018). The combined impact of IgLON family proteins Lsamp and Neurotrimin on developing neurons and behavioral profiles in mouse. *Brain Research Bulletin*, 140, 5–18. doi: 10.1016/j.brainresbull.2018.03.013.
- II. **Singh K**, Loreth D, Pottker B, Hefti K, Innos J, Schwald K, Hengstler H, Menzel L, Sommer CJ, Radyushkin K, Kretz O, Philips MA, Haas CA, Frauenknecht K, Lilleväli K, Heimrich B, Vasar E, Schäfer MKE (2018). Neuronal Growth and Behavioral Alterations in Mice Deficient for the Psychiatric Disease-Associated *Negr1* Gene. *Frontiers in Molecular Neuroscience*, 11 (30), 1–14. doi: 10.3389/fnmol.2018.00030.
- III. **Singh K**, Jayaram M, Kaare M, Leidmaa E, Jagomäe T, Heinla I, Hickey M A, Kaasik A, Schäfer MKE, Innos J, Lilleväli K, Philips MA, Vasar E (2019). Neural cell adhesion molecule *Negr1* deficiency in mouse results in structural brain endophenotypes and behavioral deviations related to psychiatric disorders. *Scientific Reports*, 1, 9(1), 5457. doi: 10.1038/s41598-019-41991-8.

Contribution of the author:

- I. The author participated in breeding of mice, designing the study, performed most of the *in vitro* experiments and wrote the manuscript.
- II. The author participated in breeding and genotyping of mice, designed and performed the behavioral tests, and was involved in writing the manuscript.
- III. The author participated in breeding and genotyping of mice, designed and performed all the experiments, wrote the manuscript and handled correspondence.

ABBREVIATIONS

129Sv	129S6/SvEv mouse strain
aa	amino acid
AD	Alzheimer's disease
Amy	amygdala
ASD	autism spectrum disorders
ADHD	attention-deficit hyperactive disorder
B6	C57BL/6 mouse strain
BP	bipolar disorder
BSA	bovine albumin serum
CA1-3	cornu Ammonis
CAM	cell adhesion molecules
Cb	cerebellum
cDNA	complementary DNA
CLA	claustrum
CNS	central nervous system
CP	caudate putamen
DAPI	4',6-diamidino-2-phenylindole
DG	dentate gyrus
DLPFC	dorsolateral prefrontal cortex
DIV	days <i>in-vitro</i>
DNA	deoxyribonucleic acid
dUTP	2'-deoxyuridine 5'-triphosphate
E	embryonic period
E/I	excitatory/inhibitory ratio
Epd	endopiriform cortex
F-actin	filamentous actin
FGFR	fibroblast growth factor receptors
GWAS	genome wide association studies
GAPDH	glyceraldehyde 3-phosphate dehydrogenase
GPI	glycosylphosphatidylinositol
HA	hypothalamus
IGL	inter geniculate lateral geniculate complex
IgLONs	immunoglobulin superfamily of cell adhesion molecules
iSI	island of Cajella
LacZ	beta-galactosidase gene
LacZNeo	beta-galactosidase/neomycin fusion gene
Lcn2	lipocalin-2
LGD/V	dorsal/ventral part of lateral geniculate complex
Lsmp	limbic system associated membrane proteins
LSM	laser scanning microscopy
MAP2	microtubule-associated protein2
MDD	major depressive disorders

MG	medial geniculate
MO	somatomotor cortex nucleus
MRI	magnetic resonance imaging
NDS	normal donkey serum
Negr1	neuronal growth regulator 1
NF	neurofilament
NPC2	Niemann-Pick disease Type C2
Ntm	neurotrimin
OB	olfactory bulb
Obcam	opioid-binding cell adhesion molecules
OsO ₄	osmium tetroxide
OT	olfactory tubercle
P	post natal day period
pAAV-hSyn-RFP	plasmid adeno-associated virus with human Synapsin I promoter driving DsRedExpress
PB	phosphate buffer
PBS	phosphate buffered saline
PFA	paraformaldehyde
PFC	prefrontal cortex
PD	Parkinson's disease
Pir	piriform cortex
PTLP	posterior parietal association
qRT-PCR	quantitative real-time polymerase chain reaction
RARE	rapid imaging with refocused echoes
RFP	red fluorescent protein
RIPA	radioimmunoprecipitation assay
RsPD	retrosplenial cortex
RTn	reticular nucleus of thalamus
RT	room temperature
SCZ	schizophrenia
SDS	sodium dodecyl sulphate
SEM	scanning electron microscopy
SS	somatosensory cortex
SSC	saline-sodium citrate
Sub	subiculum
Syp	synaptophysin
TdT	terminal deoxynucleotidyl transferase
Th	thalamus
TUNEL	terminal deoxynucleotidyl transferase dUTP nick end labeling
VIS	visual area
Wt	wild type

INTRODUCTION

Neurons are the basic units of the nervous system. Morphology of neurons is an important determinant of their functioning. Understanding how neurons acquire intricate morphologies during development, as well as how altered morphology of neurons can modify the functional connectivity of adult brain, is the key to decipher the formation and function of the nervous system. A functional brain constitutes networks of neurons that require tightly controlled and coordinated interactions between the cellular molecules during development (Casey et al. 2000). Brain development is the most complex biological process, organised by accurately regulated expression of diversified genes. During development, differentiating neurons migrate and elongate the neurites en routing their targets via synapse to form neuronal networks. Definite control of neurite sprouting during neuritogenesis is crucial to establish neuronal networks and proper functioning of the nervous system (Munno and Syed 2003; Flynn, 2013). Each of these events is dependent on cues generated by cell surface proteins like cell adhesion molecules (CAMs) (Togashi et al. 2009). Numerous families of CAMs including glycosylphosphatidylinositol (GPI) anchored immunoglobulin superfamily (IgLON) are located in the developing neurons (Zacco et al. 1990; Tan et al. 2017). Five members of the IgLON superfamily of CAMs include *Lsamp*, (limbic system associated membrane proteins), *Ntm* (neurotrimin), *Opcml* (opioid-binding cell adhesion molecule), *Negr1/ Kilon* (neuronal growth regulator 1) and *IgLON 5* (Horton and Levitt, 1988; Struyk et al. 1995; Schofield et al. 1989; Funatsu et al. 1999; Grimwood et al. 2004; Sabater et al. 2014). These adhesion molecules are important in the formation of neuronal circuits and remarkably regulate brain functions like learning and social behavior (Innos et al. 2011, 2012; Philips et al. 2015). Disruptions in CAM gene family may lead to abnormal neuronal connectivity with manifested neuropsychiatric endophenotypes and thus increase the possibility of neuropsychiatric conditions such as schizophrenia (SCZ), autism spectrum disorders (ASD), major depressive disorders (MDD), attention-deficit hyperactive disorder (ADHD), bipolar disorder (BP) and mental as well as cognitive symptoms present in neurodegenerative disorders like Alzheimer's disease (AD) and Parkinson's disease (PD) (Koido et al. 2014; Vawter, 2000; Corvin, 2010).

In order to explore the potential endophenotypes of psychiatric disorders, this study analysed the biological determinants at cellular, anatomical and behavioral levels in mice models of IgLON superfamily molecules. IgLONs assist the congregation of synaptic connections during the establishment of neuronal circuits through inter-family interactions (Reed et al. 2004; Hashimoto et al. 2009; Tan et al. 2017). At the cellular level, these molecules interact with each other, reconcile specific neuronal projections and can further inflect the behavioral responses (Gil et al. 2000; Innos et al. 2011, 2012; Mazitov et al. 2017). Among all the five members of the IgLON superfamily, *Lsamp* and *Ntm* have been shown to have maximum affinity for trans-interactions (Reed et al. 2004).

Hence, it was an intriguing question to decipher how these two different IgLON molecules are regulated and interact to affect morphology during development, structural anatomy and behavior at adulthood.

Basic *in vitro* studies elucidating the functional properties of IgLON adhesion molecules were performed using overexpression or viral induced knockout of IgLON superfamily genes in the neuronal or secondary cell lines (Miyata et al. 2003; Yamada et al. 2007; Hashimoto et al. 2009; Akeel et al. 2011; Pischedda et al. 2014; Sanz et al. 2017). Thus, morphological description of neuronal development under realistic situation which is comparable to deficient mice of IgLON molecules is still lacking. Dissociated primary neuronal culture from IgLONs deficient mice has the potential to recapitulate the same phenotypic properties of the corresponding *in vivo* neuronal cell type. Our study is the first to outline the early neurite sprouting from the dissociated primary neurons derived from a mouse model. In this thesis, we used single or combined deletional mouse model of *Lsamp*, *Ntm* to evaluate the interacting effects, and *Negr1* deletional mouse model for comprehensive investigations in manifold behavioral assessment and neuroanatomical examinations. In order to perform morphological phenotyping of growing neurons, we chose hippocampal dissociated neuronal culture as *Lsamp* and *Ntm* coexpression and *Negr1* expression were seen during development of hippocampal formation.

Double knockout mice were created from *Lsamp*^{-/-} and *Ntm*^{-/-} mice and experiments were done in parallel to understand their potential interaction at early neuronal development. We showed that neurogenesis process and balance in tissue homeostasis is regulated through complementary interactions between *Lsamp* and *Ntm*. Similarly, *Negr1* is also involved in early neurogenesis, indicating the role of IgLON family proteins during neurite initiation which is independent of their regulation of cell-cell adhesion. Neuroanatomical analysis of *Lsamp*^{-/-}, *Ntm*^{-/-} and double deletional *Lsamp*^{-/-}*Ntm*^{-/-} mice revealed no gross changes. *Negr1*^{-/-} mice displayed several neuroanatomical abnormalities potentially related to neuropsychiatric endophenotypes and apparent imbalanced E/I (excitation/inhibition) ratio in hippocampus which are reminiscent of cross-disorder neuropsychiatric disorders like SCZ, ASD, BP, ADHD etc. These neuropsychiatric disorders are highly heritable, share common polygenic traits with distinct set of partially overlapping symptoms (Lee et al. 2013; Wang et al. 2017; Gandal et al. 2018). Finally, behavioral phenotyping of mice with same genotypes allowed us to interpret how morphological and anatomical data could influence the behavioral manifestations and promote the endophenotype approach to study the gene to behavior pathways. This thesis is an attempt to understand how different organisational levels are integrated to generate specific behavioral changes due to different gene doses. Among all the studied genotypes, *Negr1*^{-/-} mice data warrant further study of *Negr1* in the pathogenesis of neuropsychiatric disorders. Mouse models displaying relevant endophenotypes of neuropsychiatric disorders can advance translational research in understanding the possible etiology of disorders and help to develop new active compounds for potential treatments.

REVIEW OF LITERATURE

1. General description of Immunoglobulin superfamily of cell adhesion molecules (IgLONs)

IgLON superfamily of cell adhesion molecules (CAMs) assembles the tuned group of cells for the fundamental development, communication, maintenance and functioning of the adult brain (Tan et al. 2017). IgLONs are most abundantly expressed neural cell surface glycosylated proteins (Salzer et al. 1996). Five members of the IgLON family are Limbic system associated membrane proteins (*Lsamp*; IgLON3; Levitt, 1984; Horton and Levitt, 1988; Pimenta et al. 1996), Opioid-binding cell adhesion molecules (*Opcml*; IgLON1; Schofield et al. 1989), Neurotrimin (*Ntm*; IgLON2; Struyk et al. 1995), Neuronal growth regulator 1 (*Negr1/Kilon*; IgLON4; Funastu et al. 1999) and IgLON 5 (Grimwood et al. 2004; Sabater et al. 2014). These molecules are mainly clustered at pre and post synaptic sites at different brain regions (Zacco et al. 1990; Miyata et al. 2003).

Table 1. IgLON superfamily genes in *Homo sapiens* (hu), *mus musculus* (mu), their genomic location, protein size in amino acid (aa) and molecular mass in kilodaltons (kDa) of the proteins.

	Lsamp	Ntm	Opcml	Negr1	IgLON 5
Genomic location(hu)	3q13.31	11q25	11q25	1p31.1	19q13.41
Genomic location(mu)	16qB4	9qA4	9qA4	3qH4	7qB3
Protein size (aa)	338	344	337	348	336
Mol. Mass (kDa)	64-68	65	46-51	46	36

Phylogenetic analyses indicate the first divergence of IgLON family by duplication over the time of Arthropod emergence around 555Mya (Kubick et al. 2018). IgLON homologous genes found to be present in all vertebrates as well as invertebrates (Garver et al. 2008; Kubick et al. 2018). High levels of intra family homology were found in the IgLON superfamily. All the five IgLONs share the same structure, contain three C2 type immunoglobulin (Ig) like domains, and one conserved disulphide bond with each Ig domain through which they adhered to the plasma membrane via GPI anchor depicted in Fig. 1 (Pimenta et al. 1996, Miyata et al. 2003). *Ntm* and IgLON5 contains one extra non conserved cysteine inside the first 90 aa (C45 and C83, respectively), attributing to form covalent dimers (Struyk et al. 1995). The sequence of alternative promoter of *Lsamp* 1a and 1b transcript were initially provided by Pimenta and Levitt, 2004 and later detailed analysis was performed by our group in Vanaveski et al. 2017. Similar genomic structures were found in *Ntm* and *Opcml* with two alternative promoters 1a and 1b. *Negr1* and IgLON 5 possess uniform 5' regions implying to have single promoter (Vanaveski et al. 2017).

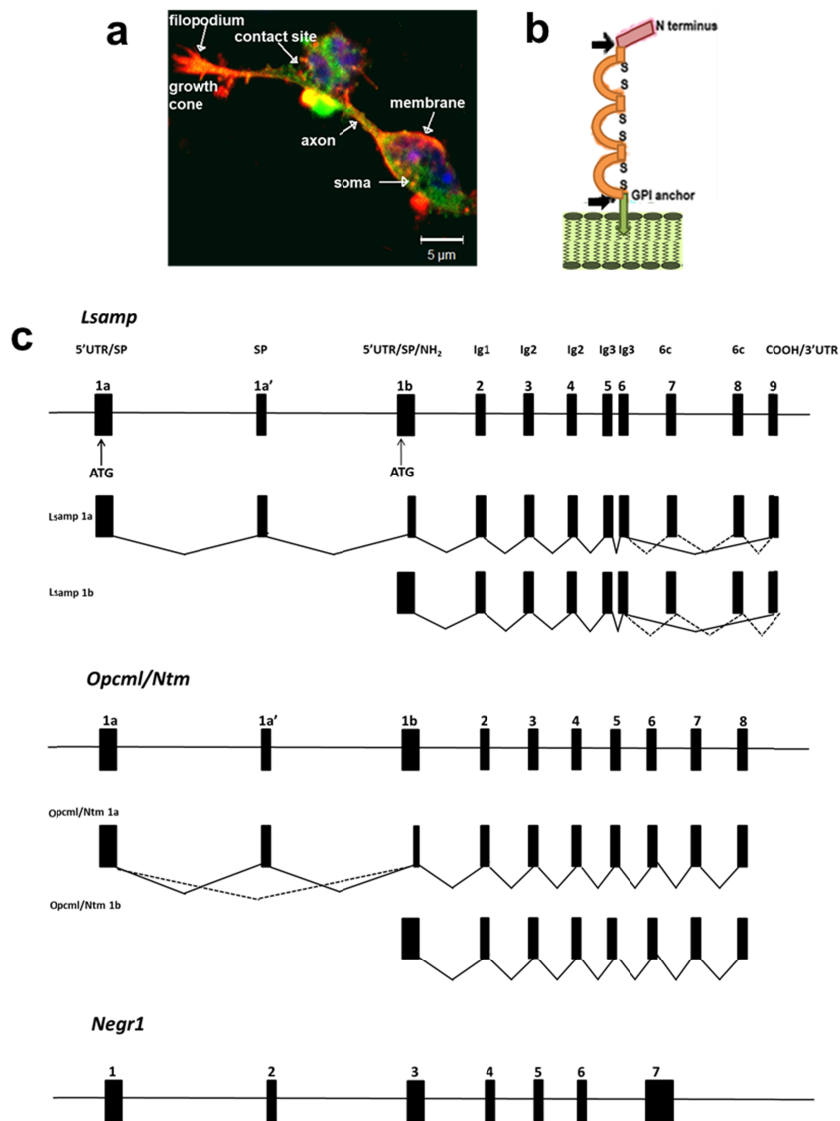


Figure 1. (a) Localisation of CAMs in the developing neurons. Red: CAM labelling in the growth cone, filopodium, axons, at cell membrane and contact site with other neurons, green: cell soma, blue: nucleus (adapted from G. Pollerberg/ Cells). **(b) Molecular structure of IgLONs.** Three C2 type Ig- domains adhered to plasma membrane with GPI anchor. **(c) Structure of *Lsamp*, *Ntm/Opcml* and *Negr1* gene.** Genomic structure and assembly of the of 1a and 1b promoter derived transcripts of *Lsamp*, *Ntm* and *Opcml* and single transcript of *Negr1* gene. Exons are illustrated as boxes (adapted from Pimenta and Levitt, 2004; Vanaveski et al. 2017).

2. Expression of IgLONs in mouse brain

In the mice brain *Lsamp*, *Opcml* and *Negr1* were expressed both in neurons and oligodendrocytes (Sharma et al. 2015). *Ntm* has been found to express specifically in neurons, *Opcml* and *Lsamp* has also shown to be expressed in astrocytes (Sugimoto et al. 2010; Zhang et al. 2014; Sharma et al. 2015). IgLON5 and *Ntm* were also expressed in microglia (Zhang et al. 2014). Among all IgLONs, only *Ntm* was expressed in endothelial cells (Petryszak et al. 2014).

The neuroanatomical distribution of *Lsamp*, *Ntm*, *Opcml* and *Negr1* is extremely diverse throughout the brain with coexpression at few sites (Philips et al. 2015; Gil et al. 2002; Hachisuka et al. 2000; Schafer et al. 2005). The timing of their first mRNA expression in the developing nervous system was almost identical and starting from embryonic period (E) 12.5-15 (Philips et al. 2015; Struyk et al. 1995; Hachisuka et al. 2000). During this embryonic period the majority of neurons establish their neural circuits indicating IgLONs involvement in formation of variety of diverse neural circuit.

The first described IgLON family member was *Lsamp* in the rat brain showing expression in the limbic cortex and medial nucleus of the thalamus thus suggesting its role in the limbic system circuitry (Levitt, 1984; Horton and Levitt, 1988; Pimenta et al. 1996; Reinoso et al. 1996). The mRNA expression in the developing and adult rat brain showed the expression of *Lsamp* in hippocampus, amygdala, ventral and dorsal striatum, and preoptic and hypothalamic areas, somatosensory, motor cortex, thalamic nuclei, midbrain, hindbrain, superior and inferior colliculus, dorsal and ventral cochlear nuclei, nucleus of lateral lemniscus, superior olive and spinal trigeminal nucleus (Pimenta et al. 1996b; Reinoso et al. 1996). In cat, *Lsamp* expression was also observed in the caudate nucleus and substantia nigra (Chesselet et al. 1990). Basal ganglia, hippocampus and amygdaloid area (Cote et al. 1995; 1996) were labelled with *Lsamp* in primates brain. Previous study from our lab confirmed the remarkable variety in the twin promoters activity of *Lsamp1a* and *1b* in the mice brain (Philips et al. 2015). *Lsamp 1a* was highly expressed in classical limbic structures like hippocampal formation, temporal cortex, amygdaloid area, ventral striatum, olfactory tubercle, limbic cortex, cingulate cortex, insular cortex, anterior thalamus, anterior hypothalamus and pre optic areas. On the contrast, *Lsamp 1b* promoter was strongly expressed in the sensory pathways like brain stem, sensory nucleus in thalamus, layer 4 and 6 of cortex, sensory areas like visual, auditory and somatosensory cortex. *1b* promoters were also expressed in regions regulating stress and arousal like mammillary bodies, paraventricular nucleus of hypothalamus and regions important in olfactory and gustatory regulation like insular and piriform cortices (Philips et al. 2015).

Ntm expression was first described in the developing rat brain (Struyk et al. 1995). *Ntm* expression emerges to be restricted to post-mitotic neurons. *Ntm* were highly expressed in somatosensory areas between E18 to post natal day (P) 10 in the developing thalamus, cortical subplate, V, VI laminae of forebrain cortex, pontine nucleus, internal granule cells and Purkinje cells of cerebellum.

Expression in these neurons suggests Ntm involvement in the development of these projections. It is interesting to note that Lsamp and Ntm possess complementary expression pattern in the brain with few similar coexpressions. The brain regions expressing both Lsamp and Ntm include sensory and sensory motor cortex, entorhinal cortex, hippocampus, amygdala, thalamus (ventral posteromedial, lateral geniculate nucleus and lateral dorsal nuclei), piriform cortex, cerebellum, brain stem nuclei, spinal cord and dorsal root ganglia (Phillips et al. 2015; Struyk et al. 1995; Gil et al. 2002). In cultured hippocampal neurons, the coexpression of Lsamp and Ntm has been also shown at the level of single neurons (Gil et al. 2002).

At first Opcml was considered as a key protein for an opioid receptor in rat brain (Cho et al. 1986). Opcml expression was first reported in the developing rat brain on cortical plate apparently at subplate, spinal cord and is limited to grey matter (Struyk et al. 1995; Hachisuka et al. 2000). Opcml is expressed at very restricted set of neurons, high expression in the developing hippocampus (Ammon's horn), cerebral cortex, developing hippocampus, piriform cortex, and the mitral cell layer of the olfactory bulb. Opcml and Ntm coexpressed within cornu Ammonis (CA) 1, 2 and 3, with lesser expression in presubiculum, subiculum and no expression in the dentate gyrus (DG) by P14 and in coexpressed in the mitral cell layer of the olfactory bulb and the piriform cortex (Struyk et al. 1995). Opcml presents more restricted distribution pattern compared to Lsamp and Ntm (Struyk et al. 1995; Miyata et al. 2003). Detailed characterization of alternative twin promoter activity has not been described so far.

The Negr1 expression levels were detected in developing rat brain in the ventricular zone of telencephalic neuroepithelium, diencephalon and basal forebrain, cortex, developing entorhinal hippocampal formation, caudate putamen, thalamic nuclei, superior, inferior colliculi, cerebellum (Brauer et al. 2000). In the adult brain the expression was detected on the neuronal processes in the layer IV of cerebral cortex specially to somatosensory and visual cortex, layers II/III of entorhinal cortex, DG, amygdala, hypothalamus, (Schafer et al. 2005; Szczurkowska et al. 2018). Negr1 and Lsamp possess similar distribution on dendrites and soma of pyramidal neurons (Zacco et al. 1990).

3. Functional regulations of IgLONs in the mouse brain

IgLONs are located at the surfaces of neuronal somata, dendrites, axons and synaptic sites during the first post natal weeks suggesting its important role during synaptogenesis (Chen et al. 2001; Miyata et al. 2003; Zacco et al. 1990). Accumulative evidence based on overexpression and knock down of IgLON family members showed that IgLONs can regulate neurite outgrowth, promote growth cone migration, axon target guidance, and dendritic tree formation, throughout development and adulthood (Pimenta et al. 1995; Zhukareva and Levitt, 1995; Mann et al. 1998; Gil et al. 1998, 2002; Miyata et al. 2003; Akeel et al. 2011; Pischedda et al. 2014; Sanz et al. 2017). IgLON family members

differentially affect the formation and maintenance of excitatory synapses and synaptogenesis (Chen et al. 2001; Yamada et al. 2007; Hashimoto et al. 2009). Among all IgLON members, only *Opcml* has ability to regulate the morphology and proliferation of cerebral astrocytes (Sugimoto et al. 2010, 2012). *Lsamp* has been shown to negatively regulate myelination process whereas *Negr1* is positive regulator of myelination (Sharma et al. 2015; Poplawski et al. 2018).

Functional studies have shown that each members of the IgLON family such as *Lsamp*, *Ntm*, *Opcml* and *Negr1*, form homo- and heterophilic dimers through cis and trans interaction along the cell membrane as part of a larger signalling complex (Reed et al. 2004; McNamee et al. 2011). Recent study demonstrates that all IgLONs perform basic homodimeric interactions via their first Ig domain through calcium independent fashion. *Ntm* and *Negr1* have capacity to uphold homo- and heterodimers via trans interactions over different cells or synaptic cleft (Ranaivoson et al. 2019). It has been also shown that *Ntm* and *Negr1* are particularly shed from the cell surface in regulating neurite outgrowth in cortical neurons (Sanz et al. 2015).

The distinct expression and differential function of IgLON cell adhesion molecules suggest its vital contribution into the development of neural circuits (Gil et al. 1998; Funastu et al. 1999; Miyata et al. 2003; Takamori et al. 2006). *Lsamp* is involved in the establishment of septo and intrahippocampal, and thalamic circuits; an essential role for *Lsamp* has also been shown in the fasciculation process of dopaminergic afferents from midbrain to lateral habenula (Schmidt et al. 2014). *Ntm* has been shown to participate in directing the thalamocortical and pontocerebellar projections (Keller et al. 1989; Pimenta et al. 1995; Mann et al. 1998; Struyk et al. 1995; Chen et al. 2001). *Negr1* has been shown to collaborate during hippocampal denervation through its interactions with fibroblast growth factor receptor 2 (FGFR2) for cortical layering during cortical development (Schafer et al. 2005; Szczurkowska et al. 2018). Recent study indicated significance of *Negr1* during adult neurogenesis in hippocampus (Noh et al. 2019).

Behavioral studies based on *Lsamp*^{-/-} mice reveal the importance of *Lsamp* for the coordination of complex emotional, social behavior, in hippocampal plasticity and during adaptation for modifying environments (Innos et al. 2011, 2012, 2013a, 2013b; Philips et al. 2015; Qiu et al. 2010; Heinla et al. 2015). *Ntm*^{-/-} mice display deficit in emotional learning (Mazitov et al. 2017). Recent studies with *Negr1*^{-/-} mice showed anxiety and depression like behavior due to decreased miniature excitatory post synaptic potential (mEPSP) frequency and lipocalin 2 (*Lcn2*) expression in DG leading to impaired neurogenesis (Noh et al. 2019). Szczurkowska et al. 2018 showed autistic-like core behavior in *Negr1*^{-/-} mice through defective interactions of *Negr1* proteins and FGFR2.

4. IgLONs in association with human diseases

Accumulating evidence suggest the function of *Opcml*, *Lsamp* and *Negr1* as tumor suppressor gene in wide range of cancers such as epithelial ovarian tumors, leukemias, osteosarcomas, breast cancers, colorectal cancers, ovarian cancers, renal carcinomas, cerebellar pilocytic astrocytoma, gliomas etc (Sellar et al. 2003; Ntougkos et al. 2005; Reed et al. 2007; Cui et al. 2008; Barøy et al. 2014; Kim et al. 2014; Coccaro et al. 2015; Zanini et al. 2017; Dong, 2018). On contrary, *Ntm* has been shown to have increased expression in tumors where *Lsamp* have higher expression levels (Ntougkos et al. 2005; Pascal et al. 2009) indicating *Ntm* as an opposite impact in tumorigenesis. One study based on genome wide paired end DNA sequencing method for breakpoint mapping linked *Ntm* with intracranial and aortic aneurysms (Luukkonen et al. 2012).

In humans, genetic variations and altered expressions in the IgLON genes have been associated with various neurological and psychiatric disorders (Must et al. 2008; Pan et al. 2010; Koido et al. 2012; Marauni et al. 2015; Mistry et al. 2013; Ripke et al. 2014; Hyde et al. 2016). Polymorphism in *Lsamp* gene has been found in male contemplated suicide (Must et al. 2008), MDD (Koido et al. 2012) and in SCZ (Koido et al. 2014; Chen et al. 2017). In post mortem brain, the expression of *Lsamp* gene was increased in the dorsolateral prefrontal cortex (DLPFC) of SCZ, BP (Behan et al. 2009), anterior prefrontal cortex (Cox et al. 2016) and in the synaptosomal fraction of orbitofrontal cortex (Velásquez et al. 2017) of SCZ patients. Genetic variations in *Ntm* have been implicated in cognitive functions (Liu et al. 2007), intelligence (Pan et al. 2010), childhood aggressiveness in ADHD (Brevik et al. 2016) and with reduced cognition at late onset of AD (Liu et al. 2007). Significant increased levels of *Ntm* 1b isoform transcript were found in the DLPFC of post mortem schizophrenic brains (Karis et al. 2018). *Opcml* gene variants has been identified in anorexia nervosa (Huckins et al. 2018), SCZ in the Thai population (Panichareon et al. 2012) and with reduced cognition associated with late onset of AD (Liu et al. 2007). Genome-wide association study (GWAS) linked variations in *Negr1* gene with SCZ (Ripke et al. 2014), MDD (Hyde et al. 2016; Amare et al. 2019), intelligence (Sniekers et al. 2017) dyslexia (Veerappa et al. 2013), low white matter integrity (Dennis et al. 2014) and psychological symptoms associated with AD (Westwood et al. 2017; Ni et al. 2018; Raghavan et al. 2019). *Negr1* gene variants have been also involved in obesity, body mass index (Thorleifsson et al. 2009; Speliotes et al. 2010), psychological traits frequently linked with eating disorders (Gamero-Villaruel et al. 2014) and these phenotype could be associated due to *Negr1* protein interaction with Niemann-Pick disease Type C2 (NPC2) protein leads to altered cholesterol transport (Kim et al. 2017). Two siblings having a microdeletion in chromosome 1p31.1, including partial deletion of the *Negr1* gene has been shown to have neuropsychiatric, behavioral and learning difficulties (Genovese et al. 2015), rare deletional cases associated with *Negr1* gene cause severe language impairment and intellectual disability (Tassano et al. 2015). In post mortem PFC and DLPFC the *Negr1* levels are

elevated in SCZ samples (Cox et al. 2016; Karis et al. 2018) and in the DLPFC of MDD patients (Chang et al. 2014). *Negr1* has been picked up in the cerebrospinal fluid proteome signatures for MDD and BP disease exclusive of SCZ (Maccarrone et al. 2013). Another study using human cell lines which are treated with clozapine shown to have increased levels of *Negr1* indicating as a target for antipsychotic drugs (Mustard et al. 2012). When Dark Agouti rats were treated with antidepressant venlafaxine, a serotonin and noradrenaline reuptake inhibitor, *Negr1* upregulation has been noted as a drug response (Tamási et al. 2014). Precise function of IgLON 5 is poorly understood. Anti IgLON 5 disease was first identified in 2014 presenting immune mediated dementia and associated sleep disorders (Sabater et al. 2014). Studies from autopsy samples indicated large number of neuronal loss, with deposition of hyper phosphorylated tau within neurons of the brain stem tegmentum, hypothalamus, and hippocampus and elaborating this disease as unique autoimmune dementia associated with autoimmune encephalitis (Gelpi et al. 2016; Gaig et al. 2017). Another studies described patients with IgLON 5 autoantibodies showing diverse set of neurological symptoms in clinical context - adults with unexplained sleep disorder, movement disorders, bulbar symptoms, CNS hyperexcitability with taupathy (Graus and Santamaria 2017; Honorat et al. 2017). Responses to immunosuppressive treatment are limited in these patients and IgLON 5 also emerges to be associated with a risk of sudden death in sleep (Honorat et al. 2017). Altogether these studies signify the importance of IgLONs adhesion molecules in the neurological and neuropsychiatric disorders.

In order to study the etiopathologies of neuropsychiatric disorders, various traits of disorders could be studied in the rodents that are linked with the susceptible genes through endophenotypes approach. Endophenotype term was coined by Gottesman and Shields, 1967 which later on defined as an internal phenotype between gene and disease which shows their heritability, trait status, cosegregation in families, or frequency in non affected relatives (Gottesman and Gould, 2003; Hasler et al. 2006). Psychiatric disorder related endophenotype approach is proximally, the pathway from genotype to phenotype (Chan et al. 2010). Endophenotypes could be biochemical, neurophysiological, neuroanatomical, endocrine, behavioral or neuropsychological (Gould and Gottesman, 2006). An animal model is likely to display endophenotypes, which are quantified phenotypes relevant to symptoms of the modelled disease (Braff and Freedman, 2002; van den Buuse et al. 2010; Gould and Gottesman, 2006). In the year 2017, National Institute of Mental Health experts have introduced the Research Domains Criteria (RDoC; <https://www.nimh.nih.gov/research/research-funded-by-nimh/rdoc/index.shtml>) framework for categorising psychopathologies which supports endophenotypes oriented studies of psychiatric disorders in animal models. RDoC system employs target assessments at all levels of neurobiological analysis from molecules to circuits and behavior for presenting the biological basis of diagnosis. It has potential to offer etiological understanding into prognosis and the mechanism of gene function (Anderzhanova et al. 2017). The main goal is to understand the psychiatric disorders in

terms of diversified degrees of dysfunctions in general biological systems. In the case of identified susceptible gene, one can analyse the associated endophenotypes to determine disease pathophysiology based on the genotype (Lacono, 2018). For example, an array of animal experiments with knockout animal model in which inactivated CACNA1C (codes for the alpha1C subunit of the voltage gated L type calcium channel $Ca_v1.2$) leads to endophenotypes including impaired cognitive and social processing featuring on how psychiatric endophenotypes can be regulated by gene functions (Dedic et al. 2018).

IgLONs belong to the second most enriched adhesion molecules in the neurons and oligodendrocytes (Sharma et al. 2015). In the rodent brain IgLONs have been found on the developing neurons and glia for the requisition of neural circuit establishment (Mann et al. 1998; Funastu et al. 1999; Miyata et al. 2003). The timing of IgLONs expression and their varied distribution in the brain indicate their significant role in creating diversified neuronal circuitry via intra family interactions (Reed et al. 2004; Schwarz et al. 2009). Genetic variation and expression studies suggest that IgLONs are involved in several psychiatric and diseased conditions in humans (Pan et al. 2010; Koido et al. 2014; Genovese et al. 2015; Hyde et al. 2016; Karis et al. 2018). Animal studies indicated roles of *Lsamp* and *Ntm* in the control of development and activity of neural circuits underlying behavior (Lee et al. 2012; Philips et al. 2015; Mazitov et al. 2017). Recent years, another member of IgLON family, *Negr1* has gained attention after being discovered as a top gene for the major psychiatric disorders and associated with human intelligence (Sniekers et al. 2017). So far, no animal studies have been done on *Negr1* related to brain functions. The purpose of this study was to perform a comprehensive investigation about *Lsamp*, *Ntm* and *Negr1* on neuronal growth, brain structure and behavior related to neuropsychiatric endophenotypes. The main questions are: what are the earliest changes can be traced out after deletion of these crucial adhesion molecules? Is there a possibility that we can correlate brain and behavioral pathologies caused by IgLONs adhesion molecules? Studying IgLONs deletional mice model helps us to gain insight into these questions and aid to target the neuropsychiatric endophenotypes present in animal model of IgLONs adhesion molecules.

AIMS OF THE STUDY

The general aim of the present study was to unravel the effects of IgLON adhesion molecules at the cellular, structural and functional level of the brain. Uncovering these effects of IgLON adhesion molecules helps us to better understand their implications linked with abnormalities in the brain development and connectivity, likely associated with endophenotypes of psychiatric disorders.

More precisely, the aims were as follows:

1. To study the impact of *Lsamp*, *Ntm*, and *Negr1* on the morphology of developing neurons. Morphological phenotyping of developing hippocampal neurons deficient of *Negr1*, *Lsamp*, *Ntm* or both *Lsamp* and *Ntm* includes estimation of structural moities at neurite initiation stage, neurite outgrowth and branching during neuritogenesis process.
2. To examine the effect of *Lsamp*, *Ntm*, *Lsamp/Ntm* and *Negr1* deficiency at the neuroanatomical level.
3. To investigate potential behavioral deviations caused by *Lsamp/Ntm* and *Negr1* deficiencies. Behavioral phenotyping includes testing for exploratory activity, anxiety, learning and memory, and social interactions.
4. To evaluate the relevance of IgLONs deficient mice in relation to neuro-psychiatric endophenotypes.

MATERIALS AND METHODS

1. Experimental Animals

Breeding and housing of the mice was conducted at the animal facility of the Institute of Biomedicine and Translational Medicine, University of Tartu, Estonia. Mice were group housed in standard laboratory cages measuring 42.5 (L) × 26.6 (W) × 15.5 (H) cm, 6–8 animals per cage in the animal colony at 22 ± 1°C, under a 12:12 h light/dark cycle (lights off at 19:00 h). A 2 cm layer of aspen bedding (Tapvei, Estonia) and 0.5 l of aspen nesting material (Tapvei, Estonia) were used in each cage and changed every week. No other enrichment was used besides nesting material. Water and food pellets (R70, Lactamin AB, Sweden) were available *ad libitum*. Breeding and the maintenance of the *Negr1*^{-/-} mice were performed at the animal facility of the Institute of Biomedicine and Translational Medicine, University of Tartu, Estonia. All animal procedures in this study were performed in accordance with the European Communities Directive (2010/63/EU) and permit (No. 29, April 28, 2014) from the Estonian National Board of Animal Experiments.

Male *Lsamp*^{-/-}, *Ntm*^{-/-}, *Lsamp*^{-/-}*Ntm*^{-/-}, *Negr1*^{-/-} mice with mixed genetic background [(129S6/SvEvTac × C57BL/6) × (129S6/SvEvTac × C57BL/6)] were used in this study. As control mice we used their Wild-type (Wt) littermate mice. For primary culture, breeding was done separately for all of the genotypes obtained from the crossings in order to get a sufficient number of new-born pups with particular genotypes and comparable background with control mice. Wt C57BL/6 (Scanbur, Karlslunde, Denmark) mice were used for qPCR analysis and *in situ* RNA hybridization experiment.

1.1 *Lsamp* deficient mice

The scheme for generation of *Lsamp*-deficient (*Lsamp*^{-/-}) mice with a *LacZ* transgene has been described in details by Innos et al. 2011. Briefly, exon 1b of the murine *Lsamp* gene was replaced by an in frame *NLS-LacZ-NEO* cassette resulting in the disruption of all functional *Lsamp* transcripts.

1.2 *Ntm* deficient mice

Ntm gene heterozygous mutant strain (032496-UCD B6;129S5-*Ntm*^{tm1Lex/Mmucd}) was obtained from the Mutant Mouse Regional Resource Centre at UC Davis (https://www.mmrrc.org/catalog/sds.php?mmrrc_id=32496) as described in Mazitov et al. 2017. Briefly, the strategy for the creation of *Ntm*-deficient (*Ntm*^{-/-}) mice was analogous to that of *Lsamp* deficient mice, as exon 1b was deleted, leading to the disruption of all functional *Ntm* transcripts.

1.3 *Lsamp Ntm* double deficient mice

For generation of double deficient (*Lsamp*^{-/-} *Ntm*^{-/-}) mice we followed the scheme: first we generated double heterozygous mice for *Lsamp* and *Ntm* (*Lsamp*^{+/-}/*Ntm*^{+/-}) by crossing *Lsamp*^{-/-} and *Ntm*^{-/-} mice in F2 strain background [(129S5/SvEvBrd × C57BL/6) × (129S5/SvEvBrd × C57BL/6)]. Further crossing the pair of the obtained double heterozygous mice (*Lsamp*^{+/-}/*Ntm*^{+/-}) gave us the entire spectrum of genotypes (including *Lsamp*^{+/+}/*Ntm*^{+/+}, *Lsamp*^{+/+}/*Ntm*^{-/-}, *Lsamp*^{-/-}/*Ntm*^{+/+}, *Lsamp*^{-/-}/*Ntm*^{-/-}).

1.4 *Negr1* deficient mice

The scheme for generation of *Negr1* deficient (*Negr1*^{-/-}) mice has been described earlier in Lee et al. 2012. Briefly, *Negr1* gene was disrupted by generated a targeting vector that replaced exon 2 including the 3' splice site with a neomycin cassette.

2. Morphological study

2.1 Primary hippocampal neuronal culture preparation and neuritogenesis stages

Whole hippocampi of P 0-1 day old mouse pups were used to prepare dissociated hippocampal primary neuronal cultures. The brains were removed, chilled with frozen phosphate buffered saline (PBS), and the hippocampi were micro dissected under sterile conditions according to Chatterjee et al. 2014. The hippocampi were digested with papain/DNase (20 U/ml) solution for 20 min at 37°C periodic stirring. The papain solution was aspirated and the hippocampal pieces were triturated with 1 ml of culture medium. Following centrifugation at 1200 rpm for 2 min the cells were suspended in culture media consisting Dulbecco's modified Eagle's medium F12 Ham supplemented with N1, 10% fetal bovine serum and antibiotic antimycotic solution. Approximately, 20,000–50,000 dissociated neuronal cells were plated and grown onto 35 mm glass bottom dishes (glass surface diameter 14 mm; MatTek, Ashland, MA) precoated with poly D lysine (0.1 mg/ml). All the cultures were grown in a humidified 5% CO₂ incubator at 37°C. Chemicals, culture media and supplements were obtained from Sigma-Aldrich (USA).

Two stages of neuritogenesis were chosen to study the earliest morphological changes during neuronal culture development (1) the neurite initiation stage (*Days in vitro*, DIV 0.25; 6 h post culture), where we investigated the dynamics of cytoskeleton rearrangement and quantified the redistribution of neuronal cytoskeletal actin using phalloidin, an F-actin (filamentous actin) binding compound (Zhang et al. 2016). Microtubule-associated protein (MAP2) which interacts with F-actin during neurite initiation (Roger et al. 2004) was

used as a neuronal cell marker. (2) At DIV 3, we labelled hippocampal neurons with neuron-specific plasmid pAAV-hSyn-RFP (a kind gift from Edward Callaway; Addgene plasmid # 22907), expressing RFP only in neurons from the synapsin promoter and scored for the following morphological characteristics: the number, length and branches of neurites. We also used DIV 3 hippocampal primary culture to elucidate the rate of apoptosis and proliferation during *in vitro* development.

2.2 Immunofluorescent staining and image analysis

For immunofluorescent staining hippocampal neurons grown on glass-bottom dishes were briefly washed twice with cold PBS, and fixed with 4% paraformaldehyde (PFA) for 5–10 min at room temperature (RT). After fixation, the neurons were washed with cold PBS (3 × 5 min), permeabilized with 0.1% Triton X-100 in PBS (PBST) for 10 min, rinsed three times by using PBS and blocked with 1% bovine serum albumin (BSA) in PBS for 1 h at RT. The neurons were incubated with primary antibodies in 1% BSA in PBS in a humidified chamber overnight at 4°C. The primary antibodies used in these studies were: guinea pig anti-MAP2 (dilution 1:500; Synaptic Systems, 188004), rat anti-phospho-histone-H3 (PHH3) (dilution 1:500; Sigma Aldrich, H9908), guinea pig anti-doublecortin (DCX) (dilution 1:300; EMD-Millipore, AB2253), and rabbit anti-synapsin-1 (dilution 1:1000; EMD-Millipore, AB1543P). This was followed by incubation with secondary antibodies in 1% BSA in PBS in a light-proof container for 1–2 h at RT. Secondary antibodies used in dilution 1:1000 were fluorescein (FITC) donkey anti-guinea pig (Jackson, 706-095-148), rhodamine (TRITC) donkey anti-guinea pig (Jackson, 706-025-148), Alexa Fluor 488 donkey anti-mouse (Jackson, 715-545-150) and with dilution 1:2500 were Alexa Fluor 488 goat anti-rat (Molecular Probes, ab 150157), and FITC-conjugated donkey anti-rabbit (Jackson, 711-095-152). Phalloidin-TRITC (Sigma Aldrich) was diluted 1:50 in PBS and incubated for 30 min at RT to selectively stain F-actin. Finally, cells were washed (3 × 20 min in PBS), stained with 0.1 µg/ml of 4',6-diamidino-2-phenylindole (DAPI) for 2–5 min, washed in PBS and mounted with Vectasheild (Vector Laboratories).

LSM 510 META Zeiss laser confocal microscope equipped with x 63/1.4 oil immersion objective was used to capture resulting images of immunostainings. Acquired images were processed using LSM image browser (<http://www.zeiss.co.uk/>) and Photoshop CS4 Extended software (Adobe Systems Inc.). For Phalloidin and synaptic puncta quantification, Imaris 8.1 (Bitplane) was used. 3D reconstructions were build from confocal Z stacks of phalloidin-stained F-actin or synapsin1 immunostained synaptic puncta in the neurons using the “isosurface rendering” function of Imaris. Isosurface was created and the same threshold was set and used for the intensity measurement. These isosurface renderings were used to make quantitative measurements on the volume and surface fluorescent intensity.

2.3 Scanning electron microscopy

DIV 0.25 neuronal cultures grown on poly D lysine coated 12 mm glass coverslips were used for SEM analysis. Neuronal cultures were gently rinsed twice in pre-warmed (37°C) 0.1 M phosphate buffer (pH 7.3). The cultures were fixed with 2.5% glutaraldehyde in the same buffer for 30 min at RT. The samples were then rinsed in 0.1 M phosphate buffer (PB) and post fixed for 30 min at RT in 1% OsO₄ in 0.1 M PB. Dehydration was carried out through series of ethanol solutions each for 5 min from 30% of ethanol solution prepared in 0.1 M PB following 40%, 50%, 70% and 90% in Milli-Q water. The samples were washed once with 99.8% ethanol and stored in 99.8% ethanol at -20°C until critical point dried using liquid CO₂. The samples were then sputter-coated with gold and viewed under scanning electron microscopy Zeiss EVO MA-15.

2.4 Transfection

At DIV 2 primary hippocampal neurons were transiently transfected with plasmid pAAV-hSyn-RFP, using Lipofectamine 2000 according to the instructions of the manufacturer (Invitrogen). Briefly, culture medium was collected and 100 µl of OptiMEM[®] I medium containing 2% Lipofectamine 2000 with 1 µg of plasmid DNA was added directly to the cells grown on the glass bottom dishes and incubated for 3–4 h in a humidified 5% CO₂ incubator at 37°C. The neurons were replenished with collected culture media and maintained for another 24 h to enable the expression of the transfected DNA. All the media and supplements and reagents were obtained from Invitrogen (Carlsbad, CA, USA).

2.5 Neuronal imaging and neurite analysis

At DIV 3, transfection of the pAAV-hSyn-RFP expression plasmid resulted in intense RFP labelling to the entire neurite arbours of individual transfected neurons. Since a small number of individual neurons (~15–20 %) were transfected in each culture, we were able to follow the primary neurite processes of separately labelled neurons. During the image acquisition at DIV 3, the neurons were maintained in sterile PBS solution. Neurons selected for analysis were imaged using an Olympus IX70 inverted microscope equipped with WLSM Plan Apo ×20/1.25 objective and Olympus DP70 CCD camera. For neurite analysis, from 70 to 75 transfected neurons were randomly captured from 3 to 4 independent experiments. For the tracing of neurite number or neurite length per neuron, the total number or total length of projections arising from the cell soma was considered, while branching was determined on the basis of total number of nodes and ends according to Scholl analysis. The morphometric analysis was performed using computer aided neuronal tracing software (NeuroLucida Software; Version 11, MBF Bioscience), and Scholl analysis was performed with Neuroexplorer software (MicroBrightField).

2.6 Apoptosis Assay

At DIV 3 the hippocampal neuronal cultures were fixed with 4% PFA for 5 min at RT, and TUNEL staining was performed using Neuro TACS™ II *in situ* apoptosis detection kit (Trevigen, Inc., Gaithersburg, MD) according to the manufacturer's instructions. Briefly, the fixed neurons were permeabilized with proteinase K (1:100 dilutions). Neurons were then incubated with TdT and biotin-labeled dUTP at 37°C for 1 h. After being washed in PBS, the neurons were incubated with streptavidin-conjugated horseradish peroxidase, and visualized with diaminobenzidine and counterstained with Blue Counterstain (R&D Systems, Minneapolis, MN). The counterstain allowed the visualization of all TUNEL positive nuclei as a dark brown colour, while normal cells appeared as light tan. Neurons were visualized using an Olympus IX70 inverted microscope with ×20/1.25 objective. The number of TUNEL positive cells relative to the total number of cells was determined from 10 randomly selected images from the culture dish from three independent experiments (three culture dishes per experiments) with each genotype.

2.7 qRT-PCR analysis

Total RNA was extracted individually from P3 Wt brains and DIV 3 dissociated hippocampal culture by using Trizol® Reagent (Invitrogen, USA) according to the manufacturer's protocol. First strand cDNA was synthesized by using Random hexamer primer mix (Applied Biosystems) and SuperScript™ III Reverse Transcriptase (Invitrogen, USA). Single strand cDNA was synthesized using Random Hexamers (Applied Biosystems) and SuperScript™ III Reverse Transcriptase (Invitrogen, USA). Quantitative TaqMan Assay with FAM-BHQ-probe was designed for the detection of *Lsamp* 1a/1b and *Ntm* 1a/1b specific transcript by two-step RT-qPCR (qPCR) according to Philips et al. 2015. TaqMan® Universal PCR Master Mix was used in the ABI Prism 7900HT Sequence Detection System (Applied Biosystems, USA). Reactions were carried out in 10 µl reaction volumes in four replicates.

3. Neuroanatomical analysis

3.1 Nissl staining

Nissl staining was carried out on free floating 50 µm coronal cryosections. Brains of Wt, *Lsamp*^{-/-}, *Ntm*^{-/-}, *Lsamp*^{-/-}*Ntm*^{-/-}, *Negr1*^{-/-} and Wt adult mice were dissected and fixed in 4% PFA for 4-5 days followed by cryoprotection with 30% sucrose in 4% PFA/PBS, and subsequently sectioned at 50 µm. Free floating coronal sections were stained with 0.5% Cresyl violet for 7-10 min. The sections were washed with dH₂O, dehydrated with graded alcohols, cleared with xylene, mounted on glass slides using Pertex (Histolab).

Photomicrographs were taken using Olympus BX61 microscope $\times 4$ objective with Olympus DX70 CCD camera (Olympus, Hamburg, Germany).

3.2 Neurofilament immunohistochemical staining

For immunohistochemistry *Lsamp*^{-/-}, *Ntm*^{-/-}, *Lsamp*^{-/-}*Ntm*^{-/-}, *Negr1*^{-/-} and Wt mice were anaesthetised and perfused transcardially with 4% PFA. Dissected brains were post fixed overnight and cryoprotected in 30% sucrose for 24 hours at 4°C and 50 μ m sagittal cryosections were generated. The standard peroxidase anti-peroxidase method was used for neurofilament (NF) immunohistochemical staining. Free floating sections were treated as follows: 1) incubation in 0.3% PBST (PBS with 0.1% Tween-20, pH 7.0) for 40 min; 2) 0.3% H₂O₂ in PBS for 2 h; 3) 5% normal donkey serum (NDS) and 1% BSA in PBST solution (PBST-BSA/5%NGS) for 1h; 4) incubation with anti-NF antibody (1:100; clone 2H3, Developmental Studies Hybridoma Bank) in PBST-0.5%NDS/BSA for 18–24 h at RT with agitation on a shaker table for all incubation and washing steps; 5) washing with PBS/NDS/BSA for 30 min; 6) incubation with anti-mouse IgG (H&L) secondary antibody Peroxidase conjugate (ROCKLAND) in dilution 1:2000 in 0.5% NDS/BSA for 2 h at RT; 7), washing with PBS for 30 min. The sections were then treated with 0.025% diaminobenzidine (DAB)/ 0.05% H₂O₂ solution in PBS. The sections were rinsed, mounted on 0.5% gelatin coated slides and were cover slipped using Pertex (Histolab). Images were captured using inverted light microscope $\times 4$ objective (Olympus BX61 microscope) equipped with Olympus DX70 CCD camera (Olympus, Hamburg, Germany).

3.3 *In situ* RNA hybridisation for *Negr1* transcript

Mouse cDNA fragments specific for *Negr1* (650 bp) transcripts were cloned from a cDNA pool of hippocampi and basal nuclei from four month old male C57BL/6 mice brains and inserted into pBluescript KS+ vector (Stratagene, La Jolla, CA). Following *Negr1* specific primers (containing restriction sites) were used:

Negr1 For TATAGCGGCCGCATGGTGCTCCTGGCGCAGG

Negr1 Rev TATAGTCGACCAGCCTGGTCCCTTGTAATTCCAT

Mouse brains were dissected immediately after decapitation and fixed at 4°C in 4% PFA in 0.1 M PBS, pH 7.4 for 5 days. Subsequently, the brains were immersed in 20% sucrose in 4% PFA/PBS overnight, freezed at -80°C and kept frozen in -80°C until further processing. *In situ* RNA hybridization was carried out on free-floating 40 μ m sagittal cryosections using digoxigenin-UTP (Roche) labelled sense and antisense RNA probes. At first, the sections were rinsed twice in PBST and once in 5 x saline-sodium citrate buffer (SSC), pH 5. Next, the sections were prehybridized for 1 h at 65°C in prehybridization mixture containing 50% formamide, 5X SSC (pH 5), 2% blocking reagent (BR; Roche),

following overnight hybridization in the same conditions with hybridization mixture containing 50% formamide, 5 x SSC, 1% BR and 1 µg/ml probe (heated at 80°C for 5 min and cooled on ice prior to adding to the hybridization mixture). To control the specificity of RNA probe binding, some sections were incubated with the sense probe. After the hybridization, the sections were washed for 30 min at 65°C in solution containing 50% formamide, 5 x SSC and 1% sodium dodecyl sulphate (SDS), following 2 x 30 min at 60°C in 50% formamide, 2 x SSC. Next, the sections were rinsed three times in TBST (25 mM Tris-HCl pH 7.5; 140 mM NaCl; 2.7 mM KCl; 0.1% Tween20) and blocked against non-specific antibody binding for 1h in TBST containing 2% BR. Then, the sections were incubated overnight at 4°C in 1% BR/TBST with 1:2000 anti-digoxigenin antibody conjugated to alkaline phosphatase (Roche). On the third day, the sections were washed three times in TBST, following two washes in NTMT (0.1 M NaCl, 0.1 M Tris-HCl pH 9.5, 50 mM MgCl₂, 0.001% Tween20). Then, the sections were transferred into the BM Purple alkaline phosphate Substrate (Roche) and when sufficient staining had appeared, the reaction was terminated by transferring the sections into PBS. All washing and incubation steps were carried out under rocking. The stained sections were transferred onto slides in 0.5% gelatine, air dried and mounted with Pertex (Histolab).

The stained sections were recorded using Olympus BX61 microscope with Olympus DX70 CCD camera (Olympus, Hamburg, Germany). The abbreviations in all the figures representing anatomical data have been adopted from the mouse brain atlas (Franklin and Paxinos, 1997).

3.4 Magnetic resonance imaging

Negr1^{-/-} and their Wt littermate mice at 7 months of age were used for Magnetic resonance imaging (MRI). Mice were deeply anesthetized and transcardially perfused with 0.1M PBS followed by 4% PFA (4°C). Brains were left in the skulls to preserve the anatomy and incubated in 4% PFA at 4°C for a week with high shaking and then in PBS until 2 days prior to imaging. Skulls were then placed in 2 mM gadovist in PBS and incubated at 4°C with rocking until imaging. For imaging vacuum was created while putting brain in 15ml falcon tubes using PBS solution. A T2 RARE sequence was used for imaging using a 94/20 Bruker BioSpec small animal MRI with the following parameters: Tr, 900 ms; TE, 47.13 ms; imaging matrix, 512 x 360 x 80; spatial resolution, 0.0444 x 0.03 x 0.2 mm for an imaging time of approximately 3 h and 4 min. MRI sequence images were analysed for volume measurements using freely available software ITK-SNAP (V3.2.0). The entire brain and the ventricles were manually delineated for each slice and their 3D volumes were measured by an observer blinded to the genotype according to Bakker et al. 2015 in ITK-SNAP (V3.2.0).

3.5 Immunohistochemical analysis of hippocampus

Fluorescent immunohistochemistry was performed on floating 40 μm thick sagittal sections were collected after every 240 μm to PBS. Sections were permeabilized, blocked and immunostained with mouse pan neuronal anti-NeuN antibody (dilution 1:250, Millipore; MAB377) in combinations with guinea pig anti-Parvalbumin (PV) antibody (dilution 1:200, Synaptic Systems; 195 004) followed by secondary antibody (FITC AffiniPure donkey anti guinea-pig (dilution 1:1000, Jackson ImmunoResearch Lab., 706-095-148, TRITC AffiniPure donkey anti-mouse (dilution 1:1000, Jackson ImmunoResearch Lab., 715-025-150) and DAPI. Subsequently sections were rinsed with PBS and mounted with Fluoromount mounting medium (Sigma Aldrich), and covered with a 0.17-mm coverslip (Deltalab). NeuN positive nuclei, and PV positive cell counting was performed with every 6th section and quantified as the number of NeuN positive or PV positive cells/ area mm² using ImageJ Software (version 1.52a; National Institutes of Health).

4. Behavioral testing

Behavioral testing was performed between 9:00 to 17:00 h under 30 lux light intensity. Before each experiment, mice were let to habituate to the experimental room and the lighting conditions therein for 1 h. The mice were allowed to rest 1–2 weeks between the tests if same mice were used repeatedly. The behavioral experiments with genotypes *Lsamp*^{-/-}, *Ntm*^{-/-} and *Lsamp*^{-/-}*Ntm*^{-/-} were performed with male mice in between 8 to 16 weeks of age. Behavioral testing with *Negr1*^{-/-} mice started when the mice were 12–14 weeks old except scoring of the whiskers length for barbering behavior. Barbering behavior was recorded twice in these mice: before starting the battery of behavioral experiments and after finishing the behavioral experiments.

4.1 Open field test

The Open field test (OFT) of individual mice was measured in a lit room (ca 200 lx) for 30 min in sound proof photoelectric motility boxes measuring 44.8 \times 44.8 \times 45 (H) cm made of transparent Plexiglas and connected to a computer (TSE, Technical & Scientific Equipment GmbH, Germany). Before each experiment mice were let to habituate with the experimental room for 1 h. The floor of the boxes was cleaned with 5% of ethanol and dried thoroughly after each mice experiment. Computer registered the distance travelled, the number of rearings, and the time spent in the central part of the box. Number of mice used as follows: in *Lsamp*^{-/-} mice n=11, in *Ntm*^{-/-} mice n=10, in *Lsamp*^{-/-} *Ntm*^{-/-} mice n=10, and in Wt mice n=14.

4.2 Elevated plus-maze

The elevated plus maze (EPM) test was carried out as described earlier (Innos et al. 2011) to assay anxiety related behaviors. In short, the apparatus consisted of two opposite open (17.5×5 cm) arms without sidewalls and two enclosed arms of the same size with 14 cm high sidewalls and an end wall. The entire plus maze apparatus was elevated to a height of 30 cm and placed in a dim room (15 lx in open arms). Testing began by placing the animal on the central platform (5×5 cm) of the maze, facing a closed arm. An arm entry was counted only when all four limbs were within a given arm. Standard 5 min test duration was employed and the sessions were video recorded. The following parameters were scored by an experienced observer, blind to the experimental group: (1) the number of closed arm entries, (2) the number of open arm entries, (3) the number of protected head dips. Number of mice used as follows: in *Lsamp*^{-/-} n=11, in *Ntm*^{-/-} n=10, in *Lsamp*^{-/-} *Ntm*^{-/-} mice n=10, and Wt n=11.

4.3 Light-dark box test

The light-dark box (TSE, Technical & Scientific Equipment GmbH, Germany) consisted of a quadratic arena made out of dark Plexiglas on three sides and transparent Plexiglas at the front, measuring $30 \times 30 \times 24$ (H) cm. Running from front to back of the arena and situated at its midline was a dark Plexiglas wall containing an opening 3.5 (W) \times 10.0 (H) cm, allowing the mouse to transfer from one compartment of the arena to the other. The wall divided the arena into a lit chamber (ca 200 lx) and a dark chamber (ca 10 lx, with a lid). The Plexiglas arena was surrounded by a soundproof chamber. The apparatus was located in a quiet, dimly (ca 5 lx) illuminated room. An animal was placed in the dark chamber, facing away from the opening, and released. During a 20 min trial, the latency to enter the lit chamber, time spent in the lit chamber, and the numbers of transitions were measured. Number of mice used as follows: in *Lsamp*^{-/-} mice n=10, in *Ntm*^{-/-} mice n=10, in *Lsamp*^{-/-} *Ntm*^{-/-} mice n=10, and Wt mice n=12.

4.4 Morris water maze test

The water maze consisted of a circular pool (diameter 150 cm), escape platform (16 cm in diameter), video camera and computer with software (TSE, Technical & Scientific Equipment GmbH, Germany). The pool (depth 50 cm) was filled with tap water (22°C, to a depth of 40 cm) that was made opaque by adding a small amount of non-toxic white putty. The escape platform was positioned in the centre of the Southwest quadrant (Q2), 20 cm from the wall. The water level was 1 cm above the platform, making it invisible. In each trial, the animals were put into the water, facing the wall, at pseudo-randomly assigned starting positions (East, North, South, or West). The acquisition phase of the experiment consisted of a series of 16 training trials (four trials per day for four consecutive

days, inter-trial interval ca 1 h). Mice were allowed to search for the platform for a maximum of 60 s at which time the mice were gently guided to the platform by means of a metal sieve. The mice remained on the platform for ca 15 s. Posters and furniture around the maze served as visual cues. During testing, the room was dimly lit with diffuse white light (20 lx). Distance travelled during the trial, latency to find the submerged platform and swim velocity were registered. We used average values per day, which was obtained by collapsing data of four trials for each animal. On Day 5 the platform was removed for a probe trial. Mice were placed into the water in the Northeast position (Q4) and were allowed to swim for 60 s. Time spent in all four quadrants (Q1, Q2, Q3, Q4) was measured, with time spent in the target quadrant (Q2) where the platform had been located serving as indicator of spatial memory. Number of mice used as follows: in *Lsamp*^{-/-} mice n=10, in *Ntm*^{-/-} mice n=10, in *Lsamp*^{-/-} *Ntm*^{-/-} mice n=10, and Wt mice n=12. Second set of testing included *Negr1*^{-/-} mice with n=14 and Wt n=13.

4.5 Barbering behavior testing

Barbering behavior was tested on *Negr1*^{-/-} mice at two time points – 8 to 9 weeks and 20 to 21 weeks of age. After weaning at 21 days of age, the mice were group housed by genotypes. At that time point a difference was noted in the appearance of wild-type and *Negr1*^{-/-} mice: while most Wt mice had trimmed whiskers and facial hair, most *Negr1*^{-/-} mice had full sets of whiskers. Barbering behavior was consequently estimated in group-housed mice (7–9 animals per cage) on a three-point scale: (1) no whiskers, (2) partially trimmed whiskers and (3) full whiskers. The percentage of mice having full, partially trimmed and no whiskers was calculated. A total of 67 mice were tested: *Negr1*^{-/-} n=34 and Wt n=33.

4.6 Three-chamber test

Automated three-chamber apparatus were used and the test was performed in three stages, each lasting 10 min, as follows: (1) Habituation: while the doors were open, mice were placed in the center chamber and allowed to freely explore. (2) Sociability: The test mouse was isolated to the center chamber (Chamber 2), while a gender/age-matched stranger (Stranger 1) was placed inside a social enclosure (Noldus) in either Chamber 1 or 3. The other chamber contained an empty social enclosure. The doors were opened, and the test mouse was allowed to freely explore. The times spent in each chamber were recorded. (3) Social novelty: immediately following the second phase, test mice were isolated back in the center chamber. A novel gender/age-matched mouse (Stranger 2) was placed in the previously empty social enclosure and Stranger 1 in the opposite chamber. Doors were opened, and the test mouse was allowed to

freely explore. All stranger mice were Wt males at the same age and habituated to the apparatus during the previous day (30 min habituation three times). The positions of the object and Stranger 1 were alternated between tests to prevent side preference. The tests were video recorded and time spent in each chamber during stages 2 and 3 were measured by the tracking software (EthoVision XT 8.5, Noldus Technology). Numbers of mice used are: *Negr1*^{-/-} n=20 and Wt n=20.

4.7 Social dominance tube test

The test apparatus was adapted from previous work (Koh et al. 2008; Lijam et al. 1997) with some modifications in the experimental design. Two waiting chambers, sized 10 × 10 × 10 cm, were connected by a 30 cm clear plexiglas tube (3 cm diameter). One Wt and one *Negr1*^{-/-} mouse were placed in the waiting chambers at the opposite ends of the tube and were there after simultaneously released into the tube. The mouse that remained in the tube, while its opponent completely backed out from the tube, was declared “winner”. The winner was given a score “1” and the loser a score “0”. Each trial lasted a maximum of 5 min and an even score “0.5” was counted when both opponents remained into the tube. During testing, the room was dimly lit with diffuse white light (20 lx). Each mouse was tested three times with three different weight matched mice of the opposite genotype. Numbers of mice used were: *Negr1*^{-/-} n=20 and Wt n=20.

4.8 Direct social interaction test

The direct social interaction (DSI) test was carried out as described previously (Innos et al. 2011), briefly: 20 *Negr1*^{-/-} mice were matched into 10 pairs of two unfamiliar mice of same genotype according to the body weight and their behaviour was video-recorded for 10 min. The videos were later scored by a trained observer. Three measures (time spent, the number of bouts, and average bout duration) were registered for each mouse for the following parameters: (1) sniffing the body of the other mouse, (2) anogenital sniffing of the other mouse, (3) self-grooming, (4) digging, (5) rearing, (6) aggressive attack, and (7) passive contact. Parameters 1, 2 and 7 were also summarized to get an additional parameter of “total social contact time” for each animal. Altogether, 40 mice were tested: *Negr1*^{-/-} n=20 and Wt n=20.

4.9 Marble burying test

Twenty glass marbles (1.5 cm in diameter) were placed on 5 cm of sawdust bedding as a 4 × 5 grid in a Plexiglas cage measuring 42.5 (L) × 26.6 (W) × 15.5 (H) cm. The mice were placed in the box individually for 30 min, and the

number of marbles buried at least two-thirds deep were counted. A total of 40 mice were tested *Negr1*^{-/-} n=20 and Wt n=20.

4.10 Tail suspension test

Tail suspension test (TST) has been used to assess stress related depression in mice (Lad et al. 2007). Mice were suspended from the edge of a shelf 58 cm above a table top by adhesive tape, placed approximately 1 cm from the tip of the tail. Animals were suspended for 6 min and the duration of immobility was scored during the last 4 min from the recorded videos by an observer blind to the genotype. Mice were considered immobile only when they hung passively and completely motionless for at least 3 seconds. A total of 32 mice were tested: *Negr1*^{-/-} n=16 and Wt n=16.

5. Data presentation and Statistical Analysis

The statistical analysis was performed with Statistica V12 (Statsoft Inc., Oklahoma, USA), R and Graph pad Prism 5 software (Graph Pad, San Diego, CA). The analysis of qRT-PCR data was performed as described previously by Philips et al. 2015. Statistical analysis was performed using unpaired Student's t-test, one-way or two-way analysis for variance (ANOVA) followed by Newman-Keuls *post hoc* test for parametric analysis. Chi-square, Mann-Whitney *U*-test or Wilcoxon Rank Sum test (W) for non-parametric data analysis. Reported correlations were calculated using Spearman's rank-order method. Specific test used per experiments has been specified in figure legends. Values of $p < 0.05$ were considered significant and experimental values represent the mean \pm SEM.

RESULTS

1. Role of IgLONs in morphology of developing neurons

1.1 *Lsamp* and *Ntm* are expressed in developing hippocampus

We used primary hippocampal cultures derived from Wt, *Lsamp*^{-/-}, *Ntm*^{-/-}, and *Lsamp*^{-/-}*Ntm*^{-/-} mice to examine the putative role of *Lsamp*, *Ntm* and their combined effects (interaction) at neuritogenesis stage of neuronal development. The relative amount of *Lsamp* and *Ntm* transcripts was monitored by qPCR analysis from DIV 3 Wt hippocampal neuronal culture and hippocampi of P3 Wt mice (Fig. 2).

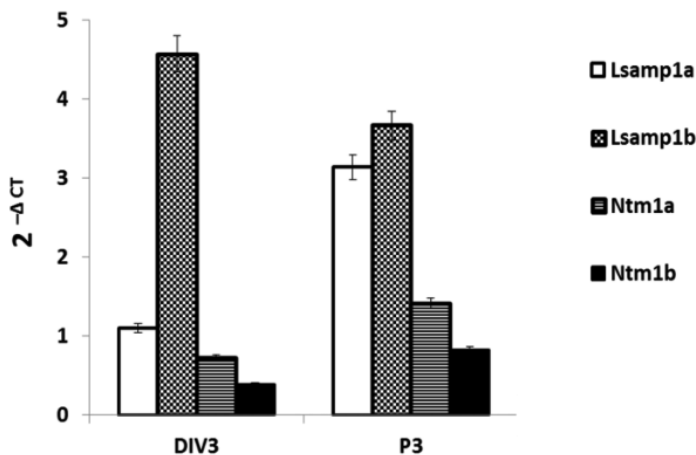


Figure 2. The average mRNA expression level of *Lsamp*1a, 1b and *Ntm*1a, 1b transcripts measured by qPCR. Expression levels are presented for hippocampal neuronal culture at DIV 3 isolated from Wt mice (4 replicates of qPCR from 3 culture dishes) and from P3 Wt mice (n=8) hippocampi based on promoter activity as $2^{-\Delta CT} \pm$ SEM. Data is shown for all 4 active promoters: *Lsamp* 1a and 1b, *Ntm* 1a and 1b.

1.2 Complementary interaction of *Lsamp* and *Ntm* in the regulation of neuritogenesis

At neurite initiation stage (DIV 0.25, 6h post culture) we performed double immunofluorescent labelling with phalloidin, the F-actin-binding compound to label actin filaments or growing protrusions, and neuronal marker, MAP2. These immunostainings demonstrate that *Lsamp*^{-/-} and Wt hippocampal neurons shared a similar neurite initiation phase (Fig. 3a-h), *Ntm*^{-/-} and *Lsamp*^{-/-}*Ntm*^{-/-} double deficient hippocampal neurons had aberrant membrane protrusions and filopodia with one extending neurite, as well as enhanced puncta of F-actin aggregates on the neuron surface (Fig. 3i-p).

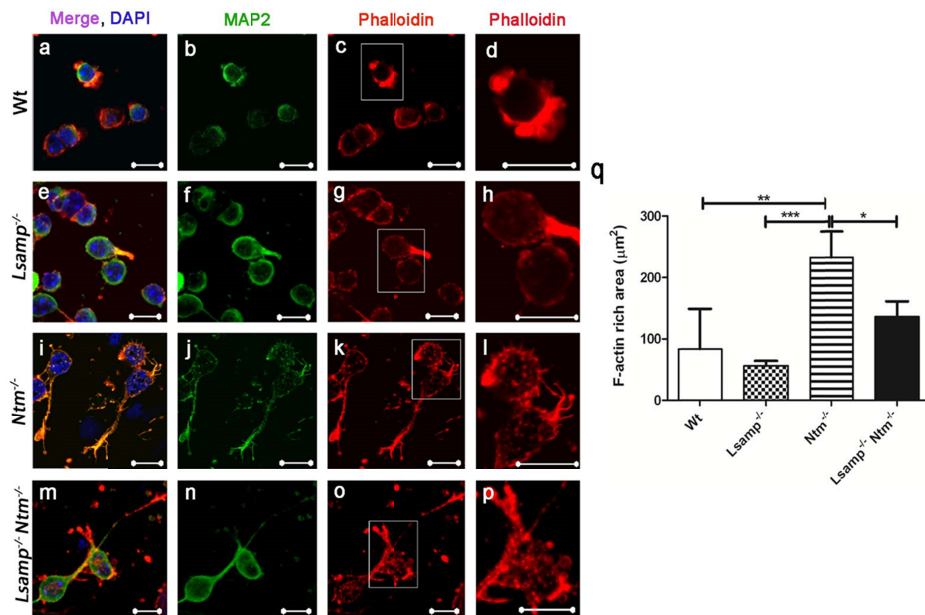


Figure 3. *Lsamp* and *Ntm* deficiency interferes with actin accumulation during the stage of neurite initiation. Confocal fluorescent images of DIV 0.25 hippocampal neurons derived from P0–1 Wt (a–d), *Lsamp*^{-/-} (e–h), *Ntm*^{-/-} (i–l), and *Lsamp*^{-/-}*Ntm*^{-/-} mice (m–p). Phalloidin staining marks F-actin (red), MAP2 neurons (green), and DAPI stains nuclei (blue). Scale bar is 10 µm. Graph (q) represents quantification of F-actin rich accumulation area (µm²) based on phalloidin intensity. n=70–75 neurons evaluated per genotype from three independent experiments. Data represent mean ± SEM, *p<0.05, **p<0.01, ***p<0.001 by one-way ANOVA followed by Newman-Keuls multiple comparisons test.

We performed quantification of the intensity of phalloidin fluorescence on the neuronal surface and found that *Ntm*^{-/-} hippocampal neurons harboured more actin aggregates compared to all other analysed genotypes (*Ntm*^{-/-} vs Wt, p<0.01; *Ntm*^{-/-} vs *Lsamp*^{-/-}, p<0.001; *Ntm*^{-/-} vs *Lsamp*^{-/-}*Ntm*^{-/-}, p<0.05) (Fig 3q). Our statistical analysis did not reveal any significant changes in phalloidin staining intensity between Wt, *Lsamp*^{-/-}, and even in *Lsamp*^{-/-}*Ntm*^{-/-} double deficient hippocampal neurons.

To view the surface topology of hippocampal neurons at the stage of neurite initiation in detail, we visualised the ultrastructure of neurite precursors at DIV 0.25 using scanning electron microscopy. Scanning electron microscopic images revealed that the cultured hippocampal neurons of different genotypes exhibited distinct features (Fig. 4). At the neurite initiation stage, the cultured neurons attach to the substrate surface and give rise to protrusions to form lamellopodia tipped by filopodia.

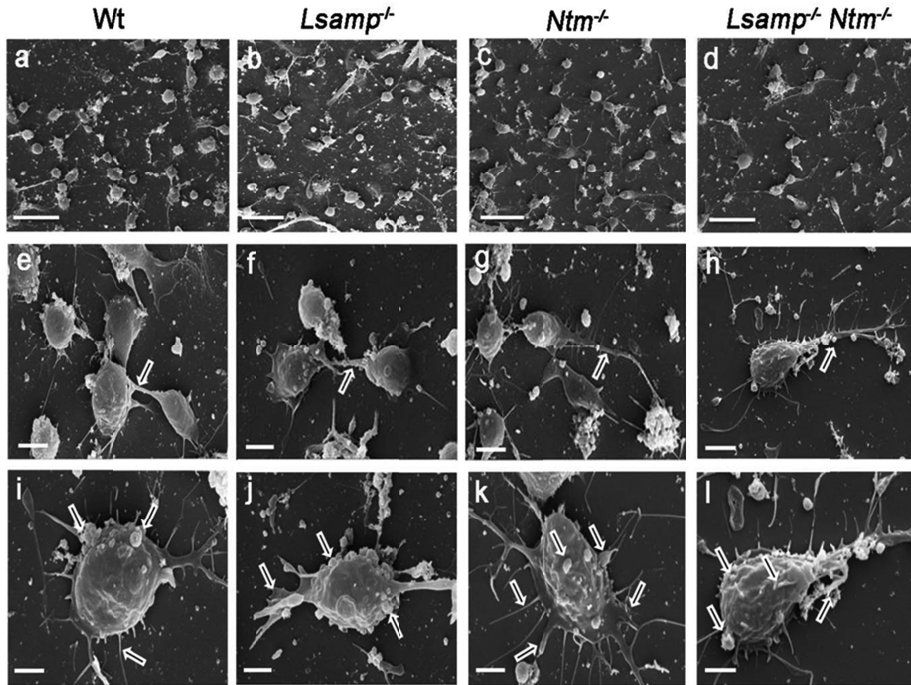


Figure 4. Ultrastructure of hippocampal neurons at neurite initiation stage. Scanning electron microscopy images of Wt (**a, e, i**), *Lsamp*^{-/-} (**b, f, j**), *Ntm*^{-/-} (**c, g, k**), and *Lsamp*^{-/-}*Ntm*^{-/-} (**d, h, l**) hippocampal neurons at DIV 0.25. Arrows at **e-h** point towards growing neurite; and at **i-l** point to the extending protrusions or filopodia on the neuronal surface. Scale bar in **a-d** is 20 μm , in **e-h** is 5 μm , in **i-l** is 2 μm .

Wt neurons were spherical smooth cells surrounded by a thin lamellipodial veil and having few protrusions (Fig. 4a, e, i). Some neurons started establishing focal contacts with neighbouring neurons (Fig. 4a-d). The surface of *Lsamp*^{-/-} neurons was also smooth, but the extending lamellopodia and filopodia appeared broader and thicker in comparison with those of Wt neurons (Fig. 4e-f, i-j). In agreement with the results of our phalloidin staining, scanning electron microscopy analysis revealed the excess of aberrant protrusions and lamellopodia in *Ntm*^{-/-} hippocampal neurons. Moreover, the surface was more ruffled compared to Wt and *Lsamp*^{-/-} neurons. Outgrowth of a single neurite with excessive branches was also observed in *Ntm*^{-/-} neurons (Fig. 4c, g, k). The surface of *Lsamp*^{-/-}*Ntm*^{-/-} double deficient hippocampal neurons was even more ruffled and possessed abnormal filopodium with more aggregates at contact points (Fig. 4d, h, l).

In order to investigate how the deficiency of IgLON molecules further alters neurite outgrowth and branching, we performed morphometric analysis on primary hippocampal neurons at DIV 3. At this stage, the primary hippocampal neurons of all analysed genotypes exhibited well distinct pyramidal shaped somas extending several neurite processes with multiple levels of branching (Fig. 5a-d).

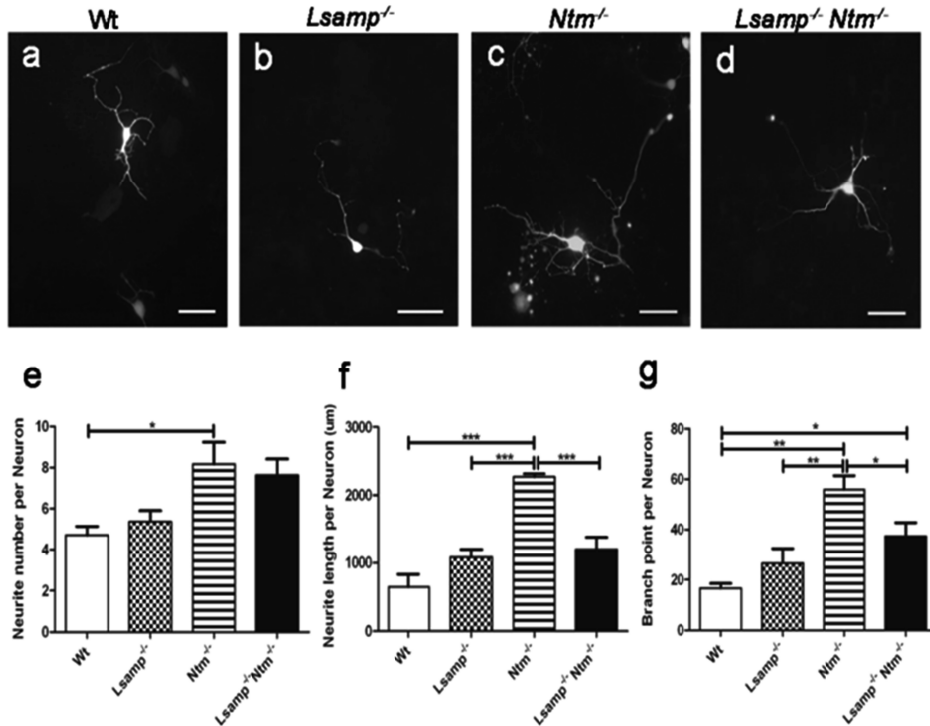


Figure 5. Morphometric analysis of hippocampal neurons in DIV 3 dissociated culture. Representative images of pAAV-hSyn-RFP labelled hippocampal neurons derived from Wt (a), *Lsamp*^{-/-} (b), *Ntm*^{-/-} (c), and *Lsamp*^{-/-} *Ntm*^{-/-} (d) mice. Scale bar is 50 μm. Graphs (e-g) are obtained by neuron tracing Neurolucida and represent the number (e), length (f), and branch points (g) of the neurites per neuron. Data shown as mean ± SEM of (n=70–75) neurons of each genotype from three independent experiments. *p<0.05, **p<0.01, ***p<0.001 by one-way ANOVA followed by Student-Newman-Keuls multiple comparisons test.

Our morphometric analysis revealed that the number of neurites per neuron was higher in *Ntm*^{-/-} hippocampal neurons compared to Wt neurons (p<0.05), but that hippocampal neurons from *Lsamp*^{-/-} and *Lsamp*^{-/-} *Ntm*^{-/-} possessed numbers of neurites per neuron similar to those of the Wt neurons (Fig. 5e). In addition to higher neurite number, the neurons derived from *Ntm*^{-/-} hippocampi also possessed longer neurites compared to Wt (p<0.0001), *Lsamp*^{-/-} (p<0.0001), and to the double deficient *Lsamp*^{-/-} *Ntm*^{-/-} neurons (p<0.0001). No statistically significant differences in neurite length could be observed between other genotypes (Fig. 5f). Quantification of neurite branching points supported our scanning electron microscopy analysis and revealed that the neurites derived from *Ntm*^{-/-} hippocampal neurons branched more than Wt (p<0.01) and *Lsamp*^{-/-} (p<0.01) neurons. Also, the number of branching points of *Ntm*^{-/-} neurites was higher compared to *Lsamp*^{-/-} *Ntm*^{-/-} neurites (p<0.05), but in the last case the

deletion of *Lsamp* reduced the effect of *Ntm*^{-/-}. Significant difference in the number of branching points was detected between *Lsamp*^{-/-}*Ntm*^{-/-} and Wt neurites ($p < 0.05$), and no significant difference was observed between *Lsamp*^{-/-} and Wt neurons (Fig. 5g).

To examine the role of *Lsamp* and *Ntm* on synaptogenesis, we immunostained DIV 14 hippocampal neurons derived from *Lsamp*^{-/-}, *Ntm*^{-/-}, *Lsamp*^{-/-}*Ntm*^{-/-} and Wt with pre synaptic marker, synapsin1 antibody and measured the volume of synaptic puncta (Fig. 6a–d). We did not find any significant difference in the synaptic puncta in any of the genotype (Fig. 6e).

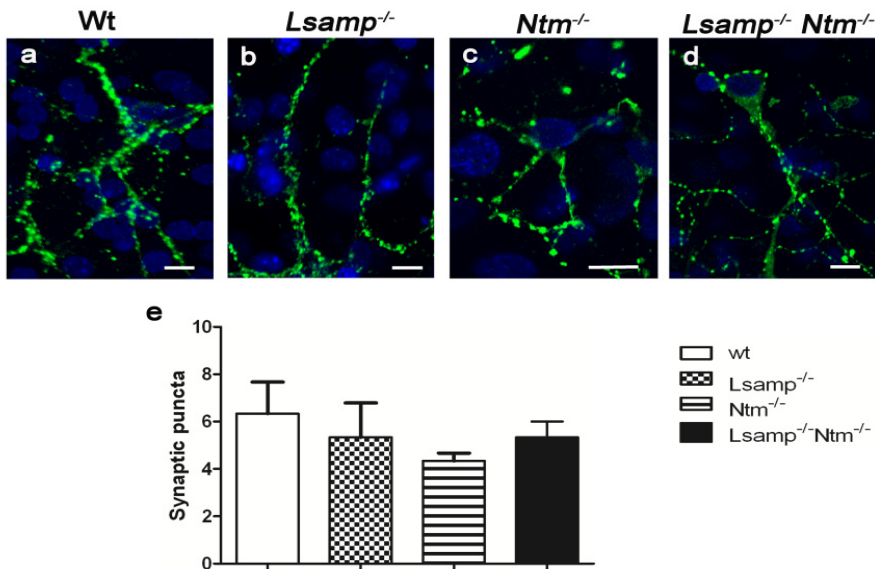


Figure 6. *Lsamp* and *Ntm* deficiency unaffected synaptogenesis during *in vitro* hippocampal neuron development. Representative confocal images of hippocampal neurons (DIV 14) with the presynaptic marker, Synapsin 1 (green) nuclei marker, DAPI (blue) hippocampal neurons cultured from P0-1 (a) Wt, (b) *Lsamp*^{-/-}, (c) *Ntm*^{-/-}, (d) *Lsamp*^{-/-}*Ntm*^{-/-} mice, Scale bar 10 μ m. Graph (e) displays the quantification of synaptic puncta per view or region of interest from three independent experiments (n=30 neurons per genotype). Data represent mean \pm SEM, evaluated per genotype (* $P < 0.05$, ** $P < 0.01$, *** $P < 0.001$ by one-way ANOVA followed by Student-Newman-Keuls multiple comparisons test).

1.3 Coordinated regulation of *Lsamp* and *Ntm* in neuronal homeostasis

In order to understand the role of *Lsamp* and *Ntm* in tissue homeostasis, we compared the rate of proliferation and apoptosis in primary hippocampal cultures at DIV 3 derived from Wt, *Lsamp*^{-/-}, *Ntm*^{-/-}, and *Lsamp*^{-/-}*Ntm*^{-/-} mice.

Proliferation rate was assessed by immunolabelling with mitotic phase marker PHH3 (Fig. 7a), immature and developing neurons were visualised by DCX immunostaining, and the nuclei were stained with DAPI. The proliferating cells were calculated as the percentage of proliferative cells (Fig. 7b). The percentage of proliferative cells in *Ntm*^{-/-} cultures was significantly lower compared to those *Lsamp*^{-/-} cultures (p<0.01) and *Lsamp*^{-/-}*Ntm*^{-/-} (p<0.001) genotypes. The percentage of proliferation in *Lsamp*^{-/-}*Ntm*^{-/-} culture was higher than in Wt (p<0.01) and in *Ntm*^{-/-} (p<0.001) (Fig.7 b-n).

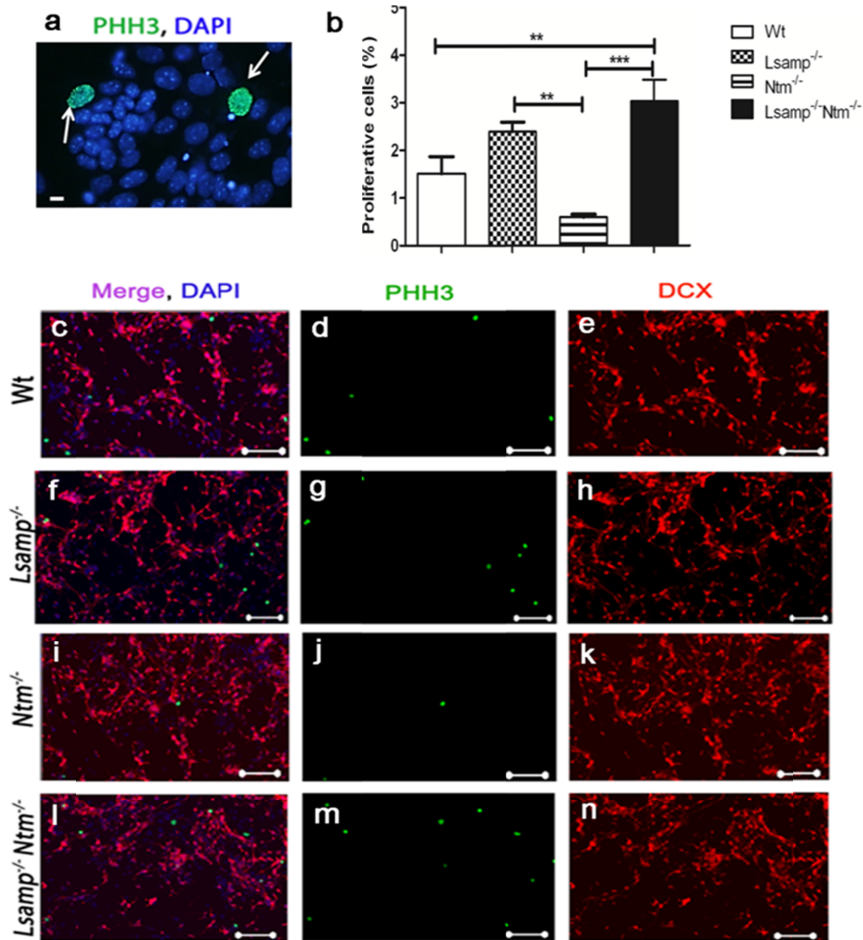


Figure 7. Effects of *Lsamp* and *Ntm* deficiencies on cellular proliferation. (a) High magnification image of PHH3 positive (green) primary cells at DIV 3 undergoing mitosis. Nuclei are stained with DAPI (blue). Graph (b) displays the percentage of proliferative cells. Representative images of DIV 3 hippocampal cultures derived from Wt (c-e), *Lsamp*^{-/-} (f-h), *Ntm*^{-/-} (i-k), and *Lsamp*^{-/-}*Ntm*^{-/-} (l-n) mice show immunostainings with proliferation marker PHH3 (green) and neuronal marker, DCX (red). Scale bar in a is 10 μm in c-n is 100 μm. Data represent mean ±SEM from; *p<0.05, **p<0.01, ***p<0.001 by one-way ANOVA followed by Newman-Keuls multiple comparisons test.

For the detection of apoptotic cells in hippocampal cultures, we used *in situ* TUNEL assay. In *Lsamp*^{-/-} culture, the ratio between all cells to apoptotic cells was significantly lower compared to any other analysed genotype (in all cases p<0.001) (Fig. 8b, e). The percentage of apoptotic cells in *Ntm*^{-/-}, and *Lsamp*^{-/-}*Ntm*^{-/-} cultures at DIV 3 was similar to Wt culture (Fig. 8a, c–e).

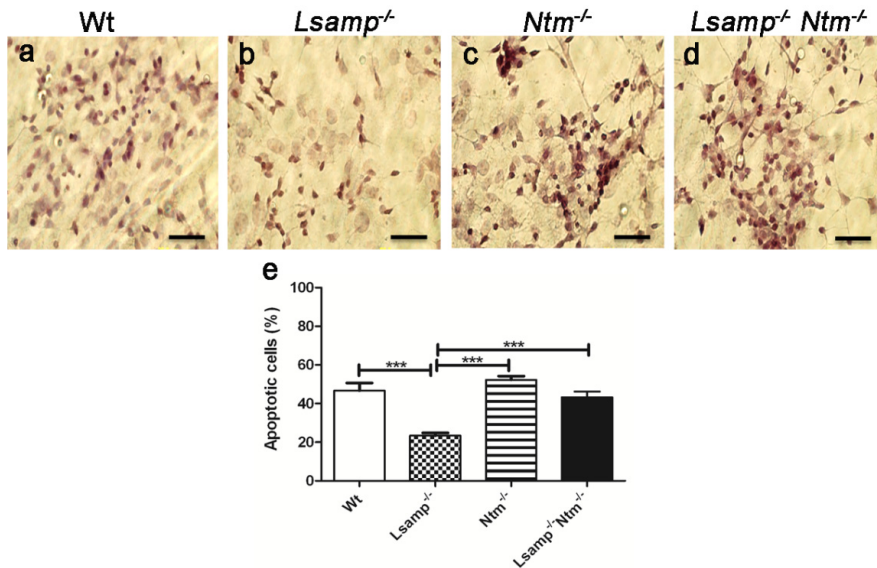


Figure 8. Effects of *Lsamp* and *Ntm* deficiencies on cellular apoptosis. Representative images showing dark brown TUNEL positive hippocampal neurons at DIV 3 derived from Wt (a), *Lsamp*^{-/-} (b), *Ntm*^{-/-} (c), and *Lsamp*^{-/-}*Ntm*^{-/-} (d) mice. Scale bar is 20 μ m. Graph (e) displays the percentage of apoptotic cells among total number of cells. Data represent mean \pm SEM from three independent experiments each with 10 independent image field evaluated per genotype; ***p<0.001 by one-way ANOVA followed by Newman-Keuls multiple comparisons test.

1.4 Implications of *Negr1* during neuritogenesis

To examine the *Negr1* involvement in the initiation stage of the formation of neurites and their outgrowth, we investigated the early neuritogenesis stages with primary hippocampal culture prepared *Negr1*^{-/-} mice and the corresponding Wt mice. We observed that spherical Wt neurons started to develop lamellopodia with few filopodia protrusions (Fig. 9a–d). In contrast, the *Negr1*^{-/-} neurons possess large F-actin rich protrusions that began to aggregate with diffused lamellopodia and a higher number of filopodia that develop faster compared to control neurons (Fig. 9e–h). Quantification of F-actin intensity revealed a significant (p<0.001) increase in neurite initiation sites in *Negr1*^{-/-} hippocampal neurons (Fig. 9i). Similar topographical features of profound filopodia protrusions on the surface and accelerated neurite sprouting in *Negr1*^{-/-} neurons were also visualised by scanning electron microscopic images

(Fig. 9j–m). Tracing of neuronal development were done similarly as described previously using pAAV-hsyn-RFP at DIV2. Morphometric analysis of neurite outgrowth and branching in transfected neurons was examined 24 h after transfection (at DIV 3). Our analysis showed that *Negr1* deficiency led to a significant ($p < 0.0001$) increase in neurite number, neurite length and branching at DIV 3 (Fig. 9n–r).

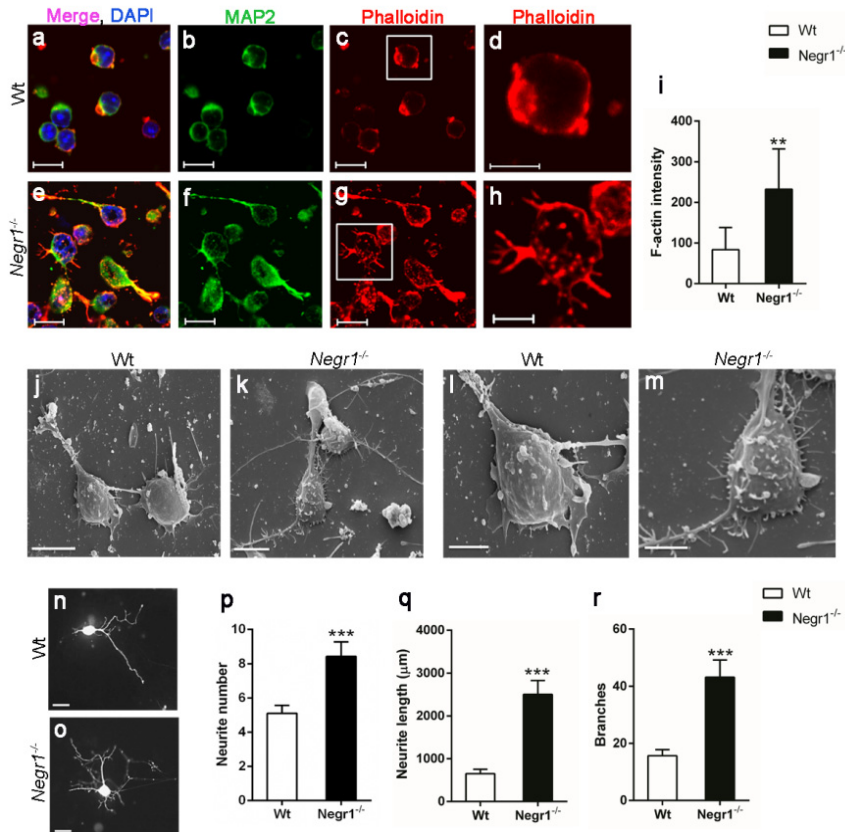


Figure 9. Neuritogenesis is impaired in *Negr1*^{-/-} hippocampal neurons. Confocal images of DIV 0.25 hippocampal neurons derived from P0–1 Wt (a–d) and *Negr1*^{-/-} (e–h) mice. Phalloidin staining marks F-actin (red), MAP2 for neurons (green), and DAPI stains nuclei (blue). Scale bar is 10 μm. Graph (i) represents quantification of F-actin intensity for actin aggregates at the neurite initiation site (μm²). Scanning electron microscopy images of Wt (j, i), *Negr1*^{-/-} (k, m), hippocampal neurons at DIV 0.25. Scale bar in j–k is 5 μm, in l–m 2 μm. Representative images of pAAV-hSyn-RFP transfected hippocampal neurons derived from Wt (n) and *Negr1*^{-/-} (o) mice. Scale bar is 50 μm. Graph (p–r) represents the number (e), length (f), and branch points (g) of the neurites per neuron obtained by neuron tracing Neuroleucida. N = 75–82 neurons evaluated per genotype from three independent experiments. Data represent mean ± SEM, * $p < 0.05$, ** $p < 0.01$, *** $p < 0.001$, Mann–Whitney *U* test (Wilcoxon rank sum test).

2. Neuroanatomy of IgLONs deficient mice

2.1 Gross anatomy of *Lsamp*^{-/-}, *Ntm*^{-/-}, *Lsamp*^{-/-} *Ntm*^{-/-} and *Negr1*^{-/-} brains

Histology of IgLONs deficient adult brains was visualized by Nissl staining and initial screening of sub regional organisation by NF immunostaining. No obvious gross changes in brain anatomy were found by Nissl staining in neither *Lsamp*^{-/-}, *Ntm*^{-/-}, *Lsamp*^{-/-} *Ntm*^{-/-} and *Negr1*^{-/-} brains compared to Wt brain sections (Fig. 10a–e). Anti-NF immunostaining also revealed no obvious disorganisation of the major fiber tracts across genotypes except sign of enlarged ventricles in *Negr1*^{-/-} mice brain (Fig. 10f–j).

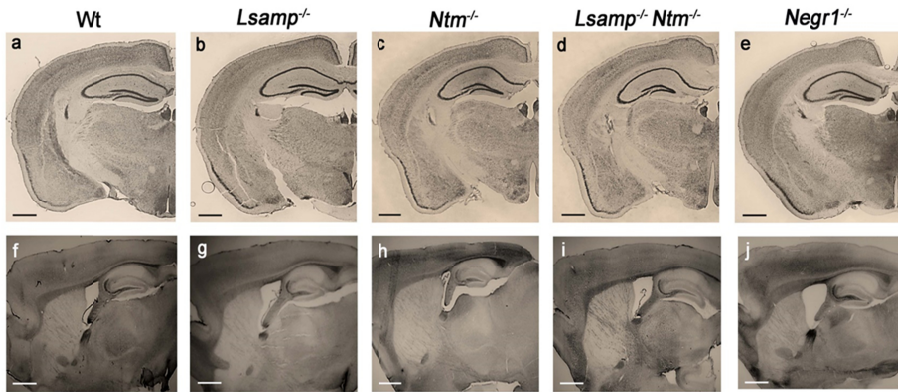


Figure 10. Histological analysis of IgLONs deficient mice brain. Nissl stained adult coronal brain sections of Wt (a), *Lsamp*^{-/-} (b), *Ntm*^{-/-} (c), and *Lsamp*^{-/-} *Ntm*^{-/-} (d) *Negr1*^{-/-} (e) at the level of hippocampus; scale bar: 1.2 mm. Immunostaining for neurofilament (NF) in sagittal brain sections of Wt (f), *Lsamp*^{-/-} (g), *Ntm*^{-/-} (h), and *Lsamp*^{-/-} *Ntm*^{-/-} (i) and *Negr1*^{-/-} (j); scale bar: 1 mm.

2.2 *Negr1* expression in the mice brain

Initial gross anatomy results from *Negr1*^{-/-} mice brain prompted us to study *Negr1* expression and more detailed anatomical analysis of the *Negr1*^{-/-} brain. *In situ* hybridisation was carried out to label the *Negr1* expression in adult mouse brain (Fig. 11). *Negr1* is expressed extensively in the forebrain and cerebellum. Strong expression was observed in all cortical layers in different areas (somatomotor, somatosensory, parietal association area, visual area, retrosplenial area), in the limbic system (hippocampus (DG, CA1-3 sub-fields), entorhinal cortex, subiculum, amygdala, hypothalamus, islands of Calleja, olfactory bulb, olfactory tubercle, lateral geniculate complex and reticular nuclei of thalamus), globus pallidus, and granular layer of cerebellum along with caudate putamen (Fig. 11a, b).

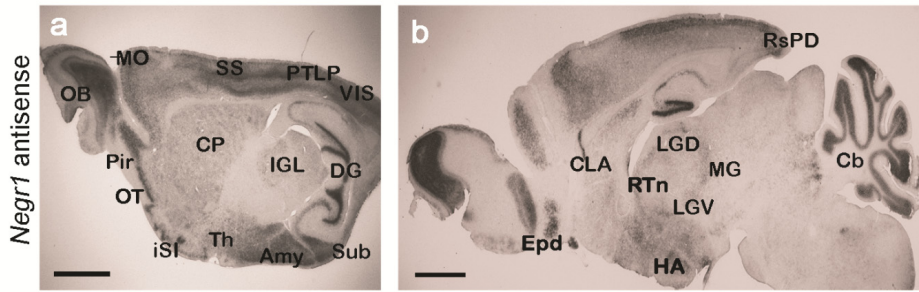


Figure 11. Expression of *Negr1* by *in situ* hybridisation in adult sagittal brain sections (a, b). *OB* olfactory bulb, *Pir* piriform cortex, *OT* olfactory tubercle, *iSI* island of Cajella, *Th* thalamus, *Amy* amygdala, *Sub* subiculum, *DG* dentate gyrus, *IGL* intergeniculate lateral geniculate complex, *CP* caudate putamen, *MO* somatomotor cortex, *SS* somatosensory cortex, *PTLP* posterior parietal association area, *VIS* visual area, *Epd* endopiriform cortex, *HA* hypothalamus, *Cb* cerebellum, *RsPD* retrosplenial cortex, *CLA* claustrum, *RTn* reticular nucleus of thalamus, *LGD/V* dorsal/ventral part of lateral geniculate complex, *MG* medial geniculate nucleus.

2.3 MRI analysis of *Negr1*^{-/-} brain

To study neuroanatomical changes, we analysed the volume of the whole brain and selected brain regions in *Negr1*^{-/-} mice compared to their Wt littermates using high resolution MRI. No significant differences were observed in body weight and brain weight in *Negr1*^{-/-} mice compared to their Wt littermates (Table 2). The analysed brain structures, including the total brain, ventricular system, white matter tracts, and cortical and subcortical grey matter structures were identified according to Bakker et al. 2015 (Table 2). We detected a small but significant (5.7%) reduction in total brain volume in *Negr1*^{-/-} mice as compared to controls (Fig. 12a, b, e). Also, *Negr1*^{-/-} mice had significantly enlarged lateral ventricles (64.6%), third ventricle (37%) and fourth ventricle (35.7%) (Fig. 12c, d, f, g). Regarding white matter areas, the corpus callosum was found to be significantly reduced (15.7%) (Fig. 12h), while other white matter tracts like the anterior commissure (anterior and posterior), internal capsule, fornix and fimbria remained unchanged. Enlargement of the ventricular system in *Negr1*^{-/-} mice might partly reflect the reduction in the volume of other cortical and subcortical areas. We found a significant reduction in the size of the globus pallidus (15.5%) and hippocampus (10%) (Fig. 12i, j). No changes were observed in the frontal cortex, olfactory system (olfactory bulb, olfactory tubercle, lateral olfactory tract and rhinocoele), striatum, hypothalamus, medulla, midbrain, brain stem and cerebellum volume (Table 2).

Table 2. Weight (g) and volume (mm³) measurements (mean±SEM) of selected regions in the *Negr1*^{-/-} compared to the corresponding Wt. *P* values as determined by Mann-Whitney U test (Wilcoxon rank sum test). (Bold *p*-value means significant difference as **p* < 0.05; *p* < 0.01, ****p* < 0.001).**

	Wt	Negr1^{-/-}	% Diff	<i>P</i>-value
Body weight (g)	32.7±3.6	31.2±5	-4.7	0.32
Brain weight	0.45±0.022	0.45±0.028	-0.6	0.88
Total brain volume (mm ³)	493.2±21.5	465±20.4	-5.7	0.03
White matter regions (mm³)				
Corpus callosum	15.71±1.5	13.24±2.1	-15.7	0.04
Ant commissure (anterior)	1.4±0.15	1.3±0.2	-8.9	0.31
Ant commissure (posterior)	0.35±0.9	0.36±0.06	1.9	0.77
Internal capsule	2.1±0.5	1.9±0.56	-10.18	0.31
Fornix	0.49±0.07	0.45±0.06	-7.83	0.47
Fimbria	1.8±0.33	1.7±0.21	-4.7	0.47
Ventricles (mm³)				
Lateral Ventricle	1.5±0.22	2.47±0.73	64.6	0.002
3 rd Ventricle	0.54±0.05	0.74±0.18	37	0.02
4 th Ventricle	0.14±0.02	0.19±0.06	35.7	0.06
Cortical and sub-cortical grey matter regions (mm³)				
Olfactory system	33.5±2.9	32.9±2.1	-1.9	0.66
Frontal cortex	52.6±6.5	48.3±2.8	-8.2	0.11
Striatum	18.5±1.2	17.7±1.2	-4.2	0.19
Globus pallidus	2.2±0.5	1.9±0.18	-15.5	0.03
Hippocampus	23.2±1.6	20.8±2.4	-10	0.02
Thalamus	15.2±0.9	15.1±1.5	-1.04	0.77
Hypothalamus	10.3±0.7	9.9±0.6	-4.21	0.47
Midbrain	8.8±0.5	9.0±1.2	2.03	0.66
Pons	16.7±1.8	15.3±1.5	-8.3	0.31
Medulla	21.0±3.2	22.7±3.7	8.16	0.39
Cerebellum	55.3±1.9	57.5±2.1	3.99	0.19

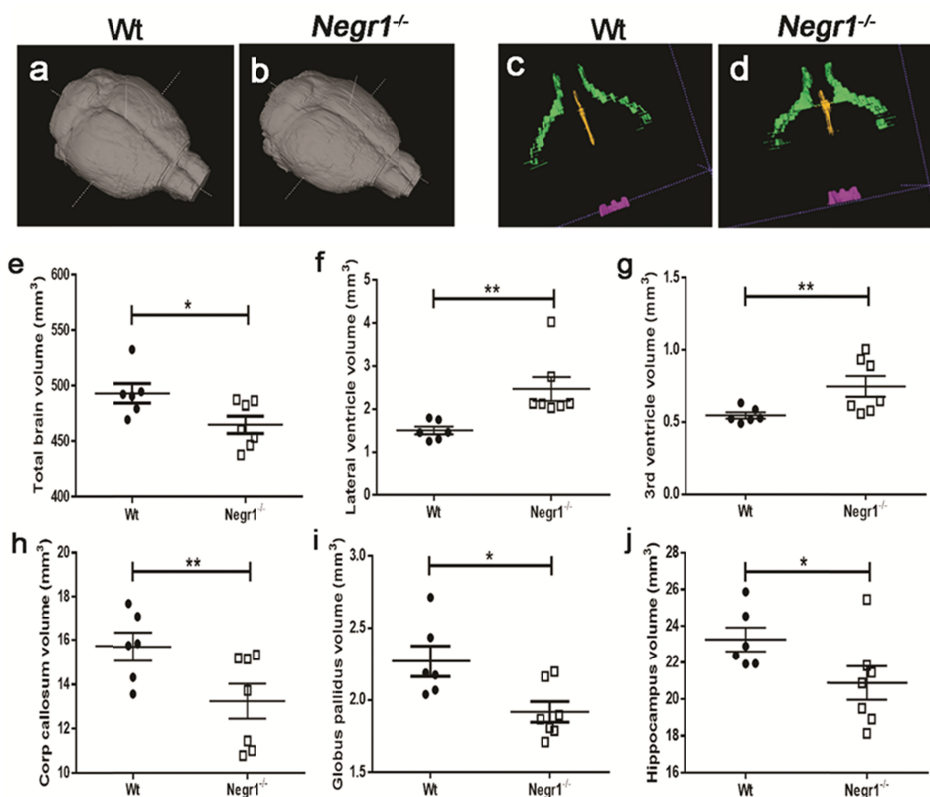


Figure 12. Neuroanatomical abnormalities in *Negr1*^{-/-} mice: A 3D reconstruction of the Wt (a) and *Negr1*^{-/-} (b) brains and ventricles (green: lateral ventricles, yellow: third ventricle and purple: fourth ventricle) in Wt (c) and *Negr1*^{-/-} (d) brains. Ventricle enlargement occurs in the *Negr1*^{-/-} mice. Quantitative analysis of effects of *Negr1* deletion in mice on the volume of total brain (e), lateral ventricles (f), third ventricles (g), corpus callosum (h), globus pallidus (i) and in hippocampus (j). Data represent mean \pm SEM, *p < 0.05, **p < 0.01, ***p < 0.001, Mann-Whitney *U* test (Wilcoxon rank sum test).

2.4 Impact of *Negr1* on hippocampal neuronal population

Since *Negr1* is expressed in hippocampus and we have reduced hippocampal volume in *Negr1*^{-/-} mice, we examined whether *Negr1* deficiency affect the whole neuronal population in hippocampus or some specific neuronal subtypes. We found no significant difference in number of NeuN positive neurons (total hippocampal region, p=0.13; DG=0.40; CA=0.16) (Fig. 13a, b, e, f, k). However, the number of PV positive neurons was found to be significantly reduced (p<0.0001), in the CA (p<0.0001) and in DG (p<0.02) regions of the hippocampus (Fig 13c, d, I, j, l).

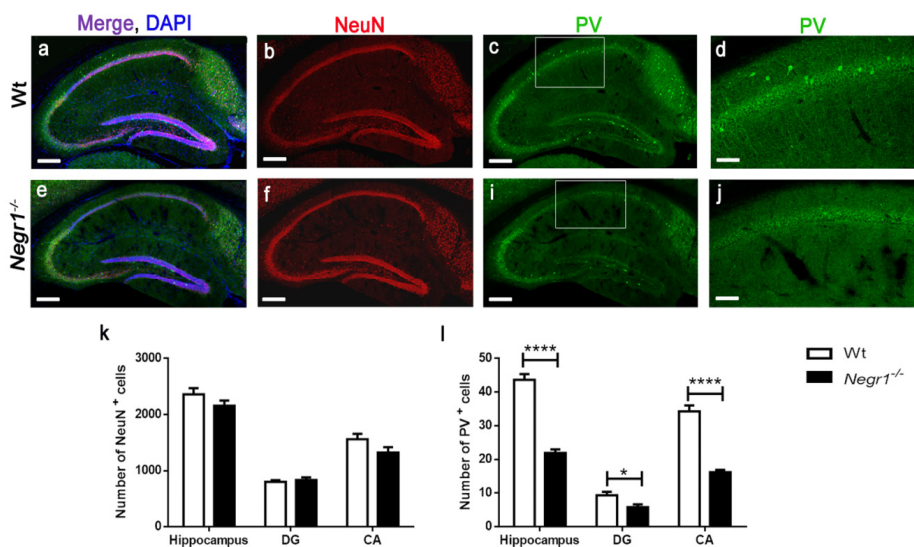


Figure 13. Reduced number of parvalbumin (PV) positive interneurons in the hippocampus of *Negr1*^{-/-} mice. Representative confocal images of the sagittal section of brains of Wt ((a–d) and *Negr1*^{-/-} (e–j) mice for NeuN (red), PV (green) and DAPI (blue) immunostaining. Scale bar is 250 μ m for a–c, e–g and 100 μ m for d and j. Graph represents mean number of NeuN positive cells (k) and PV positive cells (l) in total hippocampus, DG and in CA region. n=3 mice for both genotype with 8–9 sections per brain. Data represent mean \pm SEM, *p < 0.05, **p < 0.01, ***p < 0.001, Mann–Whitney *U* test.

3. Effect of IgLONs deficiency on the mouse behavior

3.1 Coordinated interaction of *Lsamp* and *Ntm* in the regulation of behavior

3.1.1 Open field test

Locomotor and exploratory activity was evaluated through the open field activity test using motility box. The distance travelled in the motility box during the 30 min testing was not dependent on genotype ($F_{(3,41)}=2,1$, $p=0.12$) (Fig. 14a). However, the number of rearings was dependent on genotype ($F_{(3,41)}=3.21$, $p<0.05$). Wt and *Ntm*^{-/-} mice displayed approximately twice as much vertical activity as *Lsamp*^{-/-} mice and *Lsamp*^{-/-}*Ntm*^{-/-} double deficient mice, while, the *post hoc* comparisons remained at the tendency level (Fig. 14b). Distance in centre ($F_{(3,41)}=3.63$, $p<0.05$) was significantly dependent on genotype. The distance travelled in the centre was significantly longer in *Ntm*^{-/-} mice than in all the other three groups (Fig. 14c).

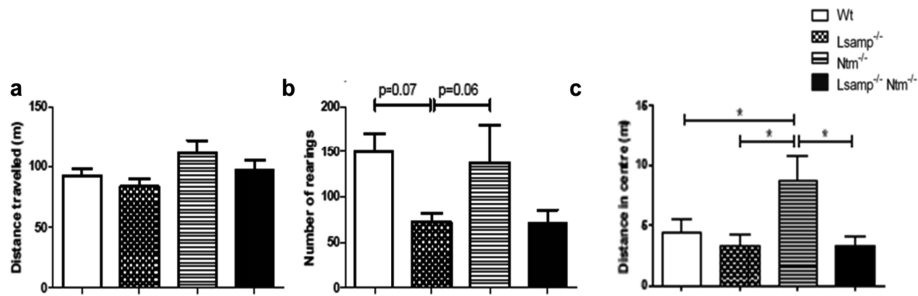


Figure 14. Behavioral analysis of *Lsamp*^{-/-}, *Ntm*^{-/-} and *Lsamp*^{-/-} *Ntm*^{-/-} mice in open field test. Distance travelled (a), the number of rearings performed (b), and distance travelled in the central part of the motility box (c) in the locomotor activity test in *Lsamp*^{-/-} mice (n=11), *Ntm*^{-/-} mice (n=10), *Lsamp*^{-/-} *Ntm*^{-/-} mice (n=10) and Wt mice (n=14). Data are presented as ±SEM (*p<0.05, **p<0.01, ***p<0.001. One-way ANOVA followed by Student-Newman-Keuls multiple comparisons test).

3.1.2 Elevated plus-maze

Elevated plus-maze is used to access anxiety like behavior in mice. The test exploits the avoidance to explore unprotected open arms of the maze at elevated position as an anxiety behavior versus the normal tendency of mice to explore the novel protected area as closed arm. The number of closed arm entries was dependent of genotype ($F_{(3, 38)}=4.05$, $p=0.014$) and according to *post hoc* analysis Wt mice performed significantly less closed arm entries than *Lsamp*^{-/-} *Ntm*^{-/-} mice ($p=0.016$) (Fig. 15a). The number of open arm entries was also dependent on genotype ($F_{(3, 38)}=4.79$, $p=0.006$) and the *post hoc* analysis showed that *Lsamp*^{-/-} *Ntm*^{-/-} mice performed significantly more open arm entries than Wt ($p=0.008$) and *Ntm*^{-/-} mice ($p=0.026$) and the difference compared to *Lsamp*^{-/-} mice verged on significance ($p=0.06$) (Fig. 15b). Protected head dips were dependent on genotype ($F_{(3, 38)}=2.9$, $p=0.047$), but no *post hoc* differences were detected (Fig. 15c).

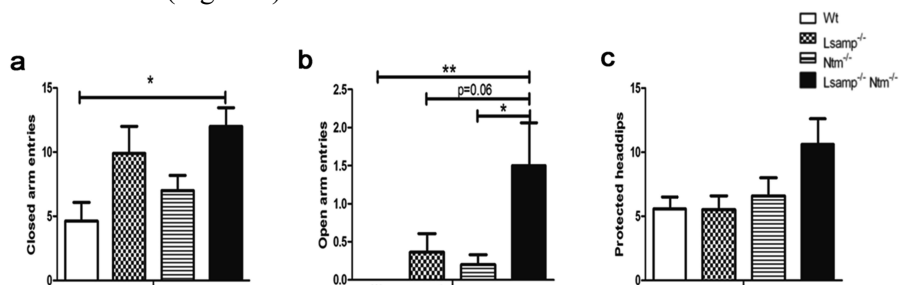


Figure 15. Behavioral analysis of *Lsamp*^{-/-}, *Ntm*^{-/-} and *Lsamp*^{-/-} *Ntm*^{-/-} mice in elevated plus maze. Closed arm entries (a), open arm entries (b), and protected head dips (c) in the elevated plus maze in Wt (n=11), *Lsamp*^{-/-} (n=11), *Ntm*^{-/-} (n=10) and *Lsamp*^{-/-} *Ntm*^{-/-} mice (n=10). Data are presented as ±SEM (*p<0.05, **p<0.01, ***p<0.001. One-way ANOVA followed by Student-Newman-Keuls multiple comparisons test).

3.1.3 Morris water maze

We used Morris water maze to study spatial learning and memory in mice. The test depends on the cues from the start point around the perimeter of open swimming arena to find the submerged escape platform. Spatial learning is evaluated against repeated trials and the reference memory is analysed by preference for the platform area when the platform is absent. For the latency to find the submerged platform in Days 1–4, there was a clear learning (day) effect ($F_{(3,114)}=62.6$, $p<0.0001$) and both genotype effect ($F_{(3,38)}=2.67$, $p=0.061$) and genotype x day interaction ($F_{(9,114)}=1.91$, $p=0.058$) approached significance with $Lsamp^{-/-}Ntm^{-/-}$ double deficient mice tending to display longer latencies in Days 2 and 4 (Fig. 16a–d).

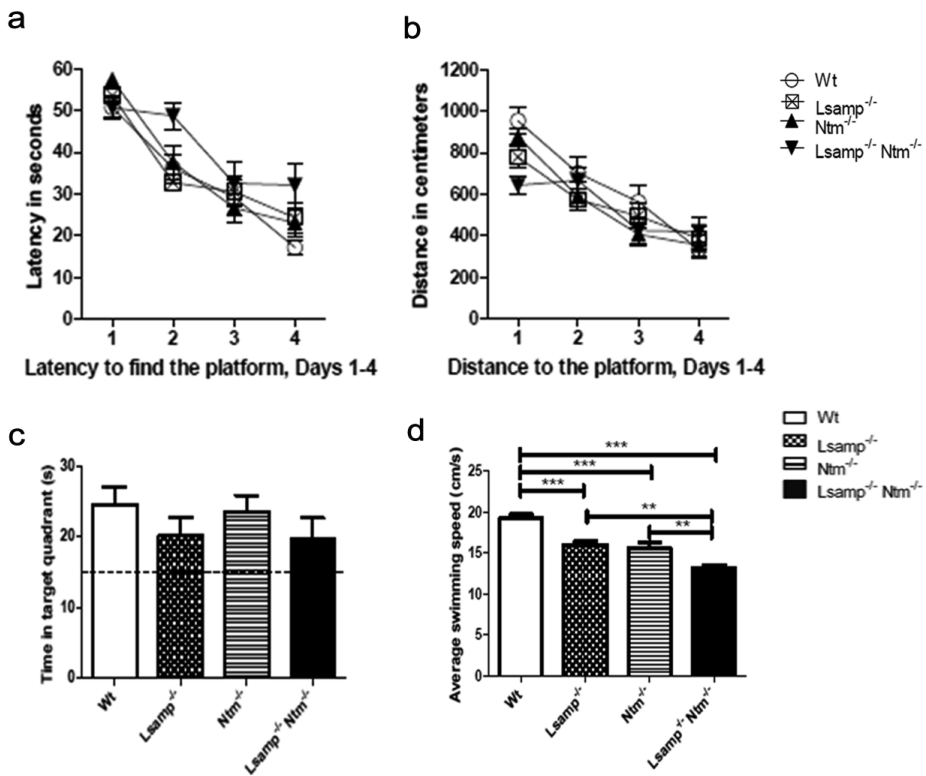


Figure 16. Behavioral analysis of $Lsamp^{-/-}$, $Ntm^{-/-}$, and $Lsamp^{-/-}Ntm^{-/-}$ mice in Morris Water Maze. The learning curve (a, b) showing the time (in s) and distance (in cm) to reach the submerged platform in Days 1–4. Average values per day, obtained by collapsing data of four trials for each animal, are presented in the Morris water maze. Time spent in the target quadrant (c) and swimming speed (cm/s) (d) in $Lsamp^{-/-}$ mice (n=10), $Ntm^{-/-}$ mice (n=10), $Lsamp^{-/-}Ntm^{-/-}$ mice (n=10) and Wt mice (n=12) during Morris water maze. Data are presented as \pm SEM (*p<0.05, **p<0.01, ***p<0.001. One-way ANOVA followed by Student-Newman-Keuls multiple comparisons test). Dotted line in c denotes chance level (15 s).

However, this should not be interpreted as learning deficiency as there were clear differences in swimming speed between the genotype groups (see below). Therefore, distance to the platform is a more objective parameter for expressing the learning curve. The distance was likewise very significantly dependent on day of test ($F_{(3,114)}=46.19$, $p<0.0001$), but not genotype ($F_{(3,38)}=1.67$, $p=0.19$). Genotype x day interaction was significant ($F_{(9,114)}=2.14$, $p=0.031$), but *post hoc* comparisons revealed differences between the groups only in the 1st day (most notably, Wt vs *Lsamp*^{-/-}*Ntm*^{-/-} mice $p=0.004$), which basically reflects differences in swimming speed. Probe trial on Day 5 confirmed the lack of learning deficiency in deficient mice groups as all the genotypes clearly preferred the target quadrant (Fig. 16c) and there were no differences between the groups ($F_{(3,38)}=0.87$, $p=0.47$). Swimming speed was very significantly dependent on genotype ($F_{(3,38)}=24.19$, $p<0.0001$); both single deficient groups swam slower than wild-type mice and the simultaneous deletion of *Lsamp* and *Ntm* genes further aggravated swimming speed deficiency compared to single deficient mice (Fig. 16d).

3.2 Implications of *Negr1* on mouse behavior

Previous publications from our group have shown that deficiency of only *Lsamp* or *Ntm* in mice leads to behavioral changes related to psychiatric endophenotypes (Innos et al. 2011, 2012; Mazitov et al. 2017). Therefore, we next investigated the effect of *Negr1* deficiency on the behavior of mice. We performed battery of behavioral experiments after weaning of the *Negr1*^{-/-} mice.

3.2.1 Barbering behavior test

After weaning, no whisker trimming or barbering behavior was observed in Wt and *Negr1*^{-/-} mice (the mice were group-housed by genotypes). Barbering behavior was consequently estimated in group-housed male mice (7–9 animals per cage) at three-point scale: (1) no whiskers, (2) partially trimmed whiskers, (3) full whiskers. At 8–9 weeks of age, most Wt mice were completely devoid of whiskers and had trimmed facial hair. In contrast to Wt littermates, all *Negr1*^{-/-} mice had full sets of whiskers and facial hair ($\chi^2 = 143.72$, $p < 0.00001$; Fig. 17a). Similar differences in barbering behaviour were evident at 20–21 weeks of age ($\chi^2 = 145.02$, $p < 0.00001$; Fig. 17b). Notably, 100% of *Negr1*^{-/-} mice had a full set of whiskers and facial hairs at both time points.

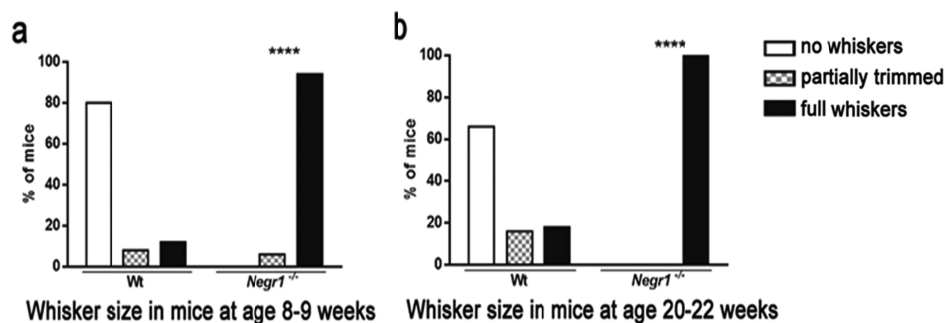


Figure 17. Barbering behavior analysis in *Negr1*^{-/-} mice. Percent of whisker size in mice at 8–9 weeks (**a**), at 20–22 weeks (**b**) of age. Chi-square (χ^2) were used for statistical analysis. * $p < 0.05$, ** $p < 0.01$, *** $p < 0.001$, **** $p < 0.0001$: *Negr1*^{-/-} mice (n=34) compared to Wt mice (n=33).

3.2.2 Three-Chamber test

To evaluate sociability and social novelty, we performed the three-chamber test. Compared to Wt mice, *Negr1*^{-/-} mice spent significantly less time in the chamber with a stranger mouse and spent proportionally more time in the empty central chamber and the chamber containing an inanimate object (Fig. 18a). Normal preference of social novelty was evaluated by social novelty test. Analysis revealed no significant genotype related neither chamber effect differences in Wt mice as compared to *Negr1*^{-/-} mice (Fig. 18b).

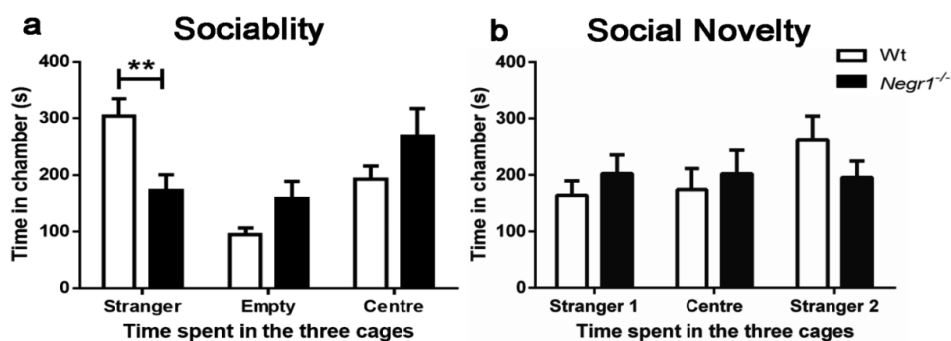


Figure 18. Three-Chamber test analysis in *Negr1*^{-/-} mice. Result of three-chamber sociability (**a**) and social novelty (**b**) test in *Negr1*^{-/-} mice. Time spent in each chamber. Data represent mean \pm SEM, Student's *t*-test. * $p < 0.05$, ** $p < 0.01$, *** $p < 0.001$, **** $p < 0.0001$: *Negr1*^{-/-} mice (n=20) compared to Wt mice (n=20).

3.2.3 Social dominance tube test

To examine social approach avoidance behavior and dominance, mice were subjected to the tube dominance test. While the number of wins achieved by Wt and *Negr1*^{-/-} mice was almost equal (Fig. 19a), the average latency to win calculated by winning time of *Negr1*^{-/-} mice was significantly shorter (Fig 19b).

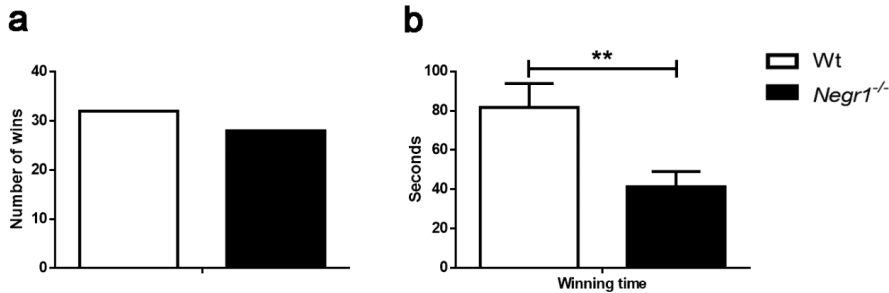


Figure 19. Social dominance tube test in *Negr1*^{-/-} mice. Number of wins (a) and winning time during tube test (b). Data represent mean \pm SEM, Student's *t*-test. **p*<0.05, ***p*<0.01, ****p*<0.001: *Negr1*^{-/-} mice (n=20) compared to Wt mice (n=20).

3.2.4 Direct Social Interaction test between *Negr1*^{-/-} mice

We examined social interaction between two freely moving male mice (12–14 weeks old) of the same genotype as this test is considered to be more sensitive than three-chamber test for studying social interactions in adult mice. During the 10 min direct social interaction test, aggressive behavior, anogenital sniffing, sniffing of other body parts, active contact, passive contact, rearings, digging and self-grooming were assessed. No attacks or aggressive behavior were registered during the interactions in either genotype. Wilcoxon rank sum test (W) revealed that *Negr1*^{-/-} mice spent substantially less time in sniffing of other body parts than genitals (W=82, *p*=0.014) and in active contacts (W=78, *p*=0.035) and tended to have a shorter total social contact bout duration (W=73, *p*=0.08; Fig. 20a–c, g–i, m–o), whereas a higher number of bouts during total social contacts (W=20.5, *p*=0.027) was registered for *Negr1*^{-/-} mice as compared to Wt mice (Fig. 20c). Total social contact is a summarized measure reflecting the sum total of anogenital sniffing, sniffing of other body parts, passive contacts and active contacts. As for non-social activities, *Negr1*^{-/-} mice spent more time on rearings (W=18, *p*=0.014) and had a longer rearing bout duration (W=8, *p*=0.00073); also, *Negr1*^{-/-} mice tended to spend more time digging (W=25, *p*=0.06) and had a larger number of digging bouts (W=13, *p*=0.0057) (Fig. 20d, e, j, k, p, q). In contrast, *Negr1*^{-/-} mice spent less time on self-grooming (W=81, *p*=0.019) and had less self grooming bouts (W=80.5, *p*=0.02) (Fig. 20f, l, r). Assessment of marble burying and tail suspension tests revealed no differences between *Negr1*^{-/-} and Wt mice (Table 3).

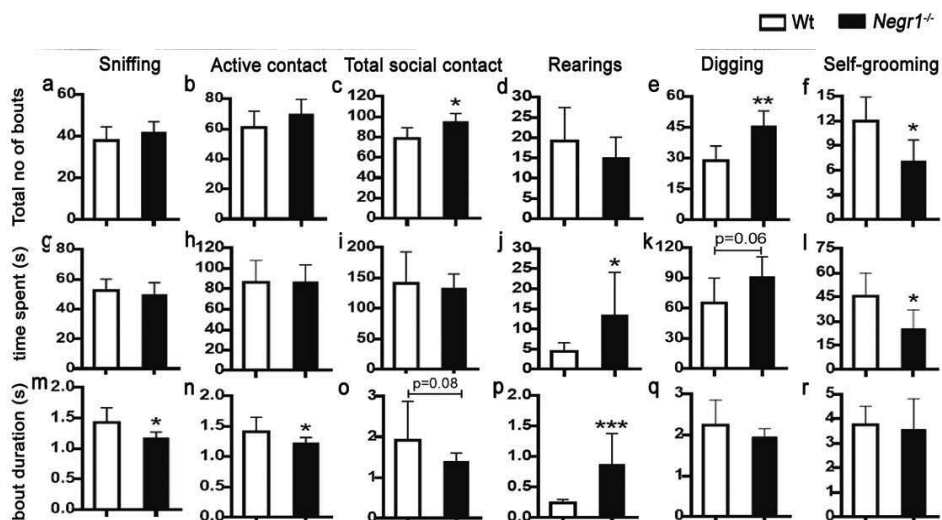


Figure 20. Direct social interaction test. Direct social interactions were scored as sniffing other body parts (a,g,m), active contact (b,h,n), total social contact (c,i,o) comprised of anogenital sniffing, passive contact, active contact and sniffing of other body parts, rearings (d,j,p), digging (e,k,q) and self-grooming (f,l,r). Graph represents total number of bouts (a–f), time spent (g–l) and bout duration (m–r) during each parameter of social interaction. Data represent mean \pm SEM, * $p < 0.05$, ** $p < 0.01$, *** $p < 0.001$, Mann-Whitney U test (Wilcoxon rank sum test).

Table 3. Marble burying and tail suspension test in *Negr1*^{-/-} mice. Marbles burying test (a) and tail suspension test (b). Data represent mean \pm SEM and bold numbers represent significant differences, Mann-Whitney U test (Wilcoxon rank sum test).

(a) Marble burying test {Number of marble buried/displaced in 30 min}	Wt	6.15 \pm 3.55
	<i>Negr1</i> ^{-/-}	4.43 \pm 2.6
(b) Tail suspension test {Immobility time duration (s)}	Wt	133 \pm 25.4
	<i>Negr1</i> ^{-/-}	118 \pm 32.7

3.2.5 Morris Water Maze test

To study the role of *Negr1* in long term spatial memory, we compared the performance of Wt and *Negr1*^{-/-} mice in the hippocampus dependent Morris water maze (Morris et al. 1982).

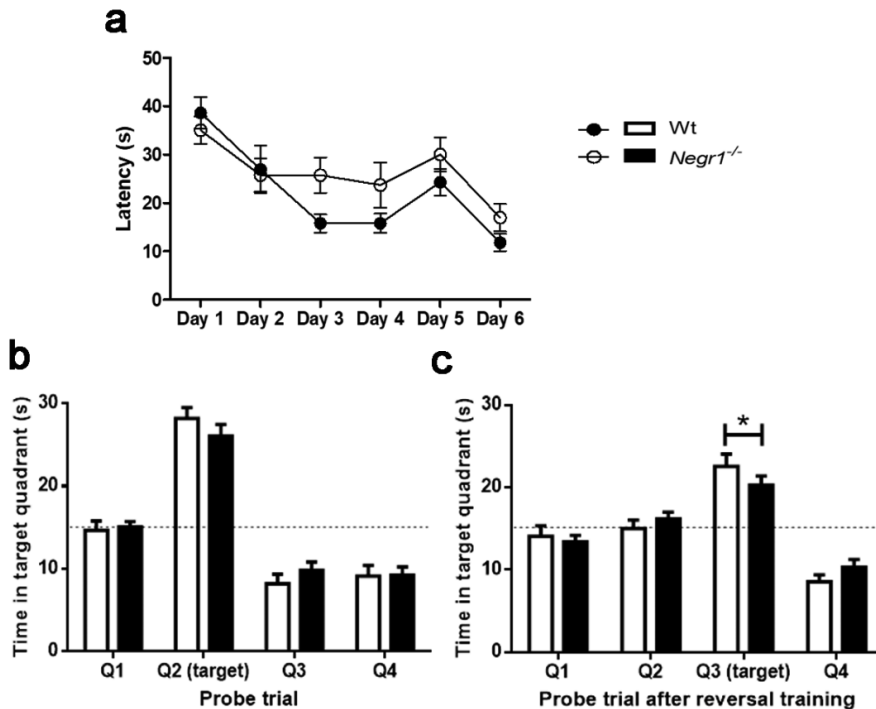


Figure 21. Behavioral analysis of *Negr1*^{-/-} mice in Morris Water Maze. The learning curve in the Morris water maze (**a**) showing the latency time (in s) to reach the submerged platform at days 1–4 (initial learning) and days 5–6 (reversal learning). Average values per day, obtained by collapsing data of four trials for each animal, are presented. In (**b**, **c**) time spent in each of the four quadrants in probe trials after day 4 and day 6, respectively, is presented. In the second probe trial (**c**), following reversal learning, *Negr1*^{-/-} mice spent significantly less time exploring the target quadrant. A total of 27 mice were tested (Wt: n = 13; *Negr1*^{-/-}: n = 14); *p < 0.05, Student’s t-test. Dotted lines denote chance level (15 s).

Wt mice demonstrated improvement in the time required to find the hidden platform (escape latency) over the first three training days and there was a highly significant improvement from day 1 to day 3 ($p = 0.00002$). *Negr1*^{-/-} mice showed less pronounced improvement from day 1 to day 3 ($p = 0.058$) but performed similar to Wt mice at day 4 (Fig. 21a). Thus, *Negr1*^{-/-} mice may have lagged in the learning phase. However, no gross learning impairment was evident as in the probe trial after day 4 the performance of both groups was similar (Fig. 21b). In contrast, the probe trial performed after completion of two days of reversal training at day 6 revealed a statistically significant difference in time spent on scanning the target quadrant with the hidden platform. *Negr1*^{-/-} mice spent significantly less time in the changed target quadrant (Fig. 21c). Overall, these results suggest that *Negr1*^{-/-} mice are slower learners than Wt mice and exhibit an impaired relearning capacity.

3.2.6 Deficits in social behavior correlate with changes in the brain structure of *Negr1*^{-/-} mice

Next, we investigated the correlations between brain regional volumetric changes and social interaction measures. Interestingly, most of the significant correlations were found in *Negr1*^{-/-} mice: reduced total brain volume was negatively correlated with sniffing (bouts) and active contact (bouts and time), and positively correlated with passive and total social contact (length) (Table 4). Reduced hippocampus was positively correlated with passive contact (length) and globus pallidus was negatively correlated with active contact (length) and positively with passive and total contact (length). Thinner corpus callosum was negatively correlated with sniffing (bouts), active contact (bouts and length) and three-chamber sociability test. The size of the 3rd ventricles was positively correlated with sniffing (bouts and length), active contact (bouts and length) and three-chamber sociability test (Table 4). Significant correlations were also found in Wt mice analysis as brain weight is negatively correlated with sniffing and active sniffing length, digging bouts are positively correlated with total brain and hippocampal volume and grooming bout is also positively correlated with 3rd ventricle volume (Table 5). When we combined both the genotype and correlated with brain structures and behavioral parameters we found positively correlations between rearings, grooming with body weight, total brain volume with grooming length and negatively correlations between grooming, rearings with lateral ventricles and brain weight with different sniffings (Table 6).

Table 4. Correlations between the MRI indices and social indices of interest in *Nesgf^{-/-}* mice. The behavioral measures have been presented in either bouts (-B), time (-T) or bout length (-L). Bold *p*-value represents a significant difference, * *p*<0.05, ** *p*<0.01, ****p*<0.001 Spearman's rank-order correlation. Abbreviations: wt – weight, Hippo – hippocampus, CC- corpus callosum, LV - lateral ventricle, 3V – 3rd ventricle, 4V – 4th ventricle, GP- globus pallidus, SNIF – sniffing of other body parts, ACT – active contacts, PAS – passive contacts, TOT – total social contacts, GRO- (self-grooming), DIG- digging, RER- (rearings), 3-Ch_T – three-chamber test sociability time.

	Body wt	Brain wt	Total Brain	Hippo	CC	LV	3V	4V	GP
SNIF-B	-0.58	-0.16	-0.89**	-0.55	-0.98**	-0.25	0.87**	-0.44	-0.77
SNIF-T	-0.42	-0.06	-0.76	-0.71	-0.77	0.04	0.91**	-0.08	-0.77
ACT-B	-0.61	-0.24	-0.92**	-0.59	-0.98**	-0.31	0.85**	-0.53	-0.78
ACT-T	-0.62	-0.32	-0.94*	-0.76	-0.92*	-0.22	0.87**	-0.61	-0.85**
PAS-L	0.88**	0.71	0.85**	0.89	0.73	-0.52	-0.53	0.55	0.95**
TOT-L	0.86**	0.63	0.87**	0.80	0.81	-0.40	-0.56	0.62	0.92**
DIG-L	-0.81**	-0.82**	-0.52	-0.69	-0.34	0.89**	0.06	-0.25	-0.70
3-Ch_T	-0.42	-0.03	-0.79	-0.43	-0.89**	-0.45	0.84**	-0.26	-0.63

Table 5. Correlations between the MRI indices and social indices of interest in Wt mice. The behavioral measures have been presented in either bouts (-B), time (-T) and bout length (-L), bold numbers represent significant differences, * p<0.05 Spearman's rank-order correlation. Abbreviations: wt- weight, Hippo-hippocampus, CC- corpus callosum, LV-lateral ventricle, 3V- 3rd ventricle, 4V-4th ventricle, GP-globus pallidus, SNIF- sniffing of other body parts, ACT- active contacts, GRO- self-grooming, DIG- digging, RER- rearing, 3-Ch_T-three-chamber test sociability time.

	Body wt	Brain wt	Total Brain	Hippo	CC	LV	3V	4V	GP
SNIF-L	-0.19	-0.94*	0.25	0.31	-0.09	-0.19	-0.13	0.28	0.17
ACT-L	-0.19	-0.94*	0.31	0.35	-0.04	-0.16	-0.15	0.32	0.24
GRO-B	0.58	0.55	-0.21	-0.12	0.27	0.25	0.87*	0.01	-0.49
DIG-B	0.63	0.03	0.85*	0.85*	0.47	-0.43	0.02	0.12	0.52
RER-B	0.91*	0.26	0.26	0.38	0.31	-0.25	0.87*	0.07	-0.35
RER-T	0.68	0.31	0.33	0.16	0.42	0.27	0.86*	0.47	-0.13
RER-L	-0.49	-0.05	0.06	-0.34	0.20	0.93*	-0.09	0.67	0.42

Table 6. Correlations between the MRI indices and social indices of interest in both genotype tested. The behavioral measures have been presented in either bouts (-B), time (-T) and bout length (-L), bold numbers represent significant differences, * p<0.05, ** p<0.01, ***p<0.001 (Spearman's rank-order correlation). Abbreviations: wt (weight), Hippo (hippocampus), CC (corpus callosum), LV (lateral ventricle), 3V (3rd ventricle), 4V (4th ventricle), GP (globus pallidus), SNIF- (sniffing of other body parts), ACT- (active contacts), GRO- (self-grooming), RER- (rearings).

	Body wt	Brain wt	Total Brain	Hippo	CC	LV	3V	4V	GP
SNIF-B	-0.04	0.15	-0.23	-0.11	-0.25	-0.03	0.58*	-0.11	-0.23
SNIF-L	-0.01	-0.60*	0.23	0.12	0.13	0.04	-0.11	0.29	0.14
ACT-B	-0.22	-0.03	-0.42	-0.34	-0.48	0.16	0.75*	-0.02	-0.43
ACT-T	-0.37	-0.51	-0.39	-0.35	-0.55	0.17	0.74*	0.01	-0.40
ACT-L	-0.18	-0.75*	0.09	0.03	-0.06	0.05	0.05	0.09	0.04
GRO-T	0.63*	0.55	0.38	0.49	0.50	-0.61*	-0.27	-0.47	0.22
GRO-L	0.66*	0.49	0.59*	0.65*	0.55	-0.76**	-0.44	-0.52	0.46
RER-B	0.65*	0.23	0.37	0.33	0.43	-0.29	0.02	0.02	0.05
RER-T	-0.04	-0.03	-0.13	-0.41	-0.03	-0.72**	0.09	0.51	-0.28
RER-L	-0.19	-0.08	-0.25	-0.50	-0.17	-0.83***	0.09	0.53	-0.32

DISCUSSION

1. *Lsamp* and *Ntm* interact with each other in establishing neuronal morphology and homeostasis

The first step in the direction of establishment of a functional brain during development is the neurite initiation from the newly born neuronal cell. We studied the effects of IgLON molecules on *in vitro* neuritogenesis model by using dissociated hippocampal culture derived from *Lsamp*, *Ntm*, *Negr1* and *Lsamp/Ntm* double deficient mice. Our first goal was to check the impact of *Lsamp* and *Ntm* during neuritogenesis, as both genes have been shown to be coexpressed in the same neurons (Gil et al. 2012). Moreover, during the first postnatal weeks of development, both *Lsamp* and *Ntm* are expressed at the surfaces of neuronal somata, dendrites and axons (Zacco et al. 1990; Chen et al. 2001). *Lsamp* and *Ntm* have been found to be expressed in a complementary fashion in distinct neuronal subpopulations and also coexpressed in some sites (Philips et al. 2015; Gil et al. 2012). A summary of *Lsamp*^{-/-}, *Ntm*^{-/-}, and *Lsamp*^{-/-}*Ntm*^{-/-} neuritogenesis analysis is shown in Table 7.

Table 7. Summarised interactive effects of *Lsamp* and *Ntm* on neuritogenesis of neurons (NC represents no change, ↓* and ↑* denote significantly lower or higher level).

Summary of <i>Lsamp</i> ^{-/-} , <i>Ntm</i> ^{-/-} , and <i>Lsamp</i> ^{-/-} <i>Ntm</i> ^{-/-} neuritogenesis analysis				
Test	<i>Lsamp</i> ^{-/-}	<i>Ntm</i> ^{-/-}	<i>Lsamp</i> ^{-/-} <i>Ntm</i> ^{-/-}	Effects
Neurite initiation (DIV0.25)				
F-actin accumulation	↓*	↑**	↓*	<i>Lsamp</i> dependent <i>Ntm</i> inhibitory effect
Neurite outgrowth (DIV3)				
No of neurites	NC	↑*	NC	<i>Lsamp</i> dependent <i>Ntm</i> inhibitory effect
length of neurites	NC	↑**	NC	<i>Lsamp</i> dependent <i>Ntm</i> inhibitory effect
branching	NC	↑**	↑*	<i>Lsamp</i> enhancer effect on <i>Ntm</i>
Proliferation (DIV3)				
% of cells	NC	↓* *	↑**	<i>Lsamp</i> dependent <i>Ntm</i> positive effect
Apoptosis (DIV3)				
% of cells	↓***	NC	NC	<i>Ntm</i> dependent <i>Lsamp</i> positive effect

Our results from the neurite initiation stage (DIV0.25) showed significantly increased neurite sprouting determined by F-actin rich areas in the *Ntm*^{-/-} hippocampal neurons compared with any other genotype (Wt, *Lsamp*^{-/-} or *Lsamp*^{-/-} *Ntm*^{-/-}), attributing *Ntm* as an inhibitory factor for the initiation of neuritic sprouts. *Lsamp*^{-/-} neurons display a similar pattern of initial dynamics of the cytoskeleton as Wt neurons; however, double-deficient *Lsamp*^{-/-} *Ntm*^{-/-} neurons represent the rescue effect of *Ntm* single deficiency in neurons. Therefore, we hypothesize that *Lsamp* acts as an enhancer of F-actin accumulation during neurite sprouting, as premature accelerated initiation of filopodium were exhibited in *Ntm*^{-/-} hippocampal neurons as compared to *Lsamp*^{-/-} and *Lsamp*^{-/-} *Ntm*^{-/-} neurons.

Morphometric analysis at DIV3 showed accelerated neurite number, length and branching in *Ntm*^{-/-} hippocampal neurons. By contrast, *Lsamp*^{-/-} neurons did not show any changes compared to Wt control. Interestingly, *Lsamp*^{-/-} *Ntm*^{-/-} neurons showed rescue effect of *Ntm*^{-/-} hippocampal neurons and their morphology was similar to the Wt neurons. Therefore, we hypothesize that *Ntm* acts as a negative factor for neurite outgrowth and branching. The vanishing effects of *Ntm* deletion in *Lsamp*^{-/-} *Ntm*^{-/-} neurons indicate that *Lsamp* might be required as an enhancing factor for neuritogenesis in *Ntm*^{-/-} neurons. IgLONs are known to form dimers via homophilic and heterophilic interactions and control neuronal growth and synaptogenesis in differential manner (Reed et al. 2004; Miyata et al. 2002; Hashimoto et al. 2009). *Lsamp* overexpression in hippocampal cell culture had a stimulating effect on synapse formation while *Ntm* overexpression in the same experiment had no effect on the synapse marker, indicating that *Ntm* acts as an inhibiting/neutral factor for synaptogenesis. The concurrent overexpression of *Ntm* and *Lsamp* resulted in a decrease of synapses (Hashimoto et al. 2009), which is another example of how IgLON family members can have antagonistic impact depending on interaction partner. Surprisingly, we found no effects on synaptic number in any of the deficiencies with *Lsamp* and/or *Ntm* in the DIV 14 hippocampal culture. However, there is also a possibility that synaptic contacts in DIV14 neuronal culture did not reflect the physiological cellular contacts in the living brains of young or adult mice. Moreover, our previous study (Vanaveski et al. 2017) using exactly the same genotypes (Wt, *Lsamp*^{-/-} or *Lsamp*^{-/-} *Ntm*^{-/-}) in adult mice hippocampal tissue showed that the expression levels of the marker of synaptogenesis, *Synaptophysin* (*Syp*) was in line with the current results. In *Ntm*^{-/-} adult hippocampi, *Syp* was significantly upregulated. On the other hand, *Syp* was not significantly increased in the hippocampi of mice lacking both *Ntm* and *Lsamp*. Thus, we propose that *Lsamp* is the real enhancer for processes that are correlated with *Syp* activity in the hippocampus. This also suggest that premature neuritogenesis and branching observed in the *Ntm*^{-/-} hippocampal cells during neurite development leads to more cellular contacts and higher synaptic density in adulthood. As the deletion of *Lsamp* along with *Ntm* diminishes the effect of *Ntm*^{-/-} both for neuritogenesis and synapse density, we propose in accordance with Hashimoto et al. 2009 that *Lsamp* acts

as an enhancer for processes that are correlated with both neuritogenesis and *Syp* activity in the hippocampus. Our data combined with previously studies suggest that *Ntm* and *Lsamp* are involved in synaptogenesis with antagonistic functions that could be characteristic for the whole IgLON family.

To elucidate the role of *Lsamp* and *Ntm* in tissue homeostasis where coordination of cellular proliferation and apoptosis is fundamental, we investigated the cellular proliferation and apoptosis in *Lsamp*^{-/-}, *Ntm*^{-/-} and *Lsamp*^{-/-}*Ntm*^{-/-} double deficient hippocampal cultures. Here we found that the deletion of *Lsamp* alone did not affect the proliferation rate. Earlier report showed that over expression of *Lsamp* in cancerous cell lines reduces the rate of proliferation (Barøy et al. 2014). Meanwhile, when *Lsamp* and *Ntm* were deleted together, (*Lsamp*^{-/-}*Ntm*^{-/-} hippocampal culture) it resulted in increased rate of proliferation. However, less proliferation was observed in *Ntm*^{-/-} hippocampal culture, indicating that *Ntm* acted as a positive factor inducing proliferation, but only in the presence of *Lsamp*. In respect to apoptosis rate, we detected a significant decrease of apoptotic cells in *Lsamp* deficient neuronal cultures, whereas previous reports have shown that overexpression of *Lsamp* does not affect apoptosis in cancerous cell lines (Chen et al. 2003; Barøy et al. 2014). On the other hand, *Ntm* deficiency and *Lsamp*/*Ntm* double deficiency had no effect on apoptotic cell percentage. Importantly, our result on *Lsamp* as a positive factor in the apoptosis inducing cellular pathway provides a possible explanation about *Lsamp* as a tumour suppressor which appear only in the presence of *Ntm*. The effects of *Ntm* for cellular homeostasis were determined on the binding partners or specific context. Here we demonstrated that the role of *Ntm* is dependent on *Lsamp*. Previous data shows that *Ntm* has been found to be up-regulated in most of the cancerous tissues (Ntougkos et al. 2005; Makowski et al. 2014; Ogawa et al. 2006). Contrasting data also exist, showing *Ntm* to be downregulated together with *Lsamp* in some tumours, such as medulloblastoma and bladder cancer (Barøy et al. 2014). As a whole, we suggest that the combined effects of *Lsamp* and *Ntm* determine the balancing factor during cellular homeostasis in the course of development and in malignant cellular processes.

Morphometric analysis of *Negr1*^{-/-} hippocampal neurons also showed increased F-actin accumulation as compared to Wt control neurons. Scanning electron microscopy images allowed us to visualise 3D images of defective initial neurite sprouting and altered neuronal surfaces at neurite initiation stage of neuritogenesis present in *Negr1*^{-/-} neurons. Enhanced neurite outgrowth and branching were also recorded in *Negr1*^{-/-} neurons as compared to the corresponding Wt neurons. Altogether these results suggest that IgLONs coordinate the structural molecules of neurite initiation stage during neuritogenesis even before any connections with other neighbouring neurons are made. Neuritogenesis required multiple interactions between the developing neurites and the extracellular matrix. Constructural changes during neuritogenesis were related to abnormal neural circuit development in ASD and SCZ (Bakos et al. 2015; Lang et al. 2014) as endophenotypes.

2. Of IgLON members, only *Negr1* has a profound effect on neuroanatomy

Initial histological sectioning of *Lsamp*^{-/-}, *Ntm*^{-/-}, *Lsamp*^{-/-}*Ntm*^{-/-} and *Negr1*^{-/-} mice brain showed no evidence of gross changes in general organisation of the cortex, hippocampus and other subcortical areas, except ventricular enlargement seen in *Negr1*^{-/-} mice. Therefore, we studied the neuroanatomy of *Negr1*^{-/-} mice in more detail. *In situ* hybridisation using *Negr1* probe showed an expression in the cortical and subcortical brain areas well known for the motivational, affective and cognitive behavior such as the thalamic reticular nucleus and the islands of Calleja. These nuclei are an important component for the information flow in thalamo-cortical circuits and dopaminergic signalling between the PFC and temporal lobe through ventral striatopallidal system. They are crucial for maintaining normal connectivity of the functional brain and their alterations are associated with the pathophysiology of psychiatric disorders (Inta et al. 2011; Steullet et al. 2017). MRI-based brain volumetric analysis revealed neuroanatomical abnormalities such as enlargement of ventricles, and a decrease in the volume of the total brain, hippocampus, globus pallidus and corpus callosum in *Negr1*^{-/-} mice. These abnormalities are in support of neuroanatomical anomalies found in several psychiatric animal models and psychiatric human patients, representing endophenotypes of psychiatric disorders (Table 8).

Affected regions in *Negr1*^{-/-} mouse brain are the fundamental parts of the brain responsible for a wide spectrum of behavioral manifestations and also for functional connectivity between cortical and subcortical areas. Smaller hippocampus is indicative of disturbed functioning of learning, spatial navigation, memory formation, emotional and social behavior via extensive neural circuitry through the prefrontal cortex, thalamus, amygdala, hypothalamus and basal ganglia (Rubin et al. 2014). Atrophied globus pallidus demonstrate disrupted corticobasal ganglia circuitry and/or connections of the limbic pallidum with the dopaminergic system (Ring et al. 2012), and can dysregulate reward prediction, memory, attention and movement planning (Gunadyn et al. 2016; Schechtman et al. 2016). Ventricle enlargement corresponds to the negative symptoms of SCZ (Galderisi et al. 2004), psychotic behavior in depression (Scott et al. 1983), and autistic behavior (Movsas et al. 2013). Similarly, the thinning of corpus callosum is correlative with lower white matter integrity, autism, mental disabilities and SCZ due to imbalanced ratio between excitation and inhibition, called the E/I balance. It has also been related with faulty hemispheric connectivity and linked with impaired sensory motor, social, emotional and cognitive functions (David et al. 1993; Paul et al. 2004).

Table 8. Comparison between structural MRI findings of *Negr1*^{-/-} mice with different animal model of psychiatric disorders and structural MRI findings in human psychiatric patients. (MDD: major depressive disorder, BP: bipolar disorder, ASD: autism spectrum disorder, SCZ: schizophrenia, ADHD: attention deficit hyperactivity disorder, OCD: obsessive compulsory disorder, PTSD: post traumatic stress disorder).

Brain structural anomaly in <i>Negr1</i> ^{-/-} mice	Psychiatric animal model (ref.)	Psychiatric patients (ref.)
Enlarged Ventricles	MDD: (Zubenko et al. 2014), WKY rats (Gormley et al. 2016) SCZ: ckr (Torres et al. 2005), hDISC1 (Pletnikov et al. 2008; Hikida et al. 2007; Clapcote et al. 2007; Shen et al. 2008), <i>Zic2</i> ^{kd/+} (Hatayama et al. 2011), <i>Df16A</i> ^{+/-} , 22q11.2 (Ellegood et al. 2014), CRMP2 (Zhang et al. 2016), NCAM180 (Wood et al. 1998) Down's syndrome: Ts1Cje and Ts2Cje (Ishihara et al. 2010) ASD: 15q13.3 (Kogan et al. 2015) Mental retardation: SrGAP3 (Koschützke et al. 2015)	MDD: (Kempton et al. 2011; Schmaal et al. 2017) BP: (Swayze et al. 1990; Hibar et al. 2016) ASD: (Movsas et al. 2013; Turner et al. 2016) SCZ: (Pina-Camacho et al. 2016; van Erp et al. 2016; Del re et al. 2016) ADHD: (Wang et al. 2007) OCD: (Rosenberg et al. 1997)
Reduced Hippocampus	MDD: (McIntosh et al. 2017); CYP2C19 (Peerson et al. 2014); WKY rats (Gormley et al. 2016) ASD: ITGβ3 (Ellegood et al. 2012) SCZ: (Johnstone et al. 2011) PTSD: (Golub et al. 2011)	MDD: (Kempton et al. 2011, Carballedo et al. 2012; MacMaster et al. 2014; Xue et al. 2015, Schmaal et al. 2017; Durmusoglu et al. 2018) BP: (MacMaster et al. 2014; Hibar et al. 2016) ASD: (Nicolson et al. 2006) SCZ: (Shepherd et al. 2015; van Erp et al. 2016; Lieberman et al. 2018) OCD: (Kwon et al. 2003) PTSD: (O'Doherty et al. 2015)
Reduced Corpus callosum	MDD: (Kumar et al. 2004; Zubenko et al. 2014; Kiesepä et al. 2010) SCZ: MAP6 KO (Gimenez et al. 2017), DISC1 (Shen et al. 2008), <i>Zic2</i> ^{kd/+} (Hatayama et al. 2011; Johnstone et al. 2011) ASD: ITGβ3 (Ellegood et al. 2012)	BP: (Brambila et al. 2004; Kumar et al. 2015) ASD: (Vidal et al. 2006) SCZ: (Kumar et al. 2015; Li et al. 2011; Del re et al. 2016)
Reduced Globus pallidus	ASD: ITGβ3 (Ellegood et al. 2012)	ADHD: (Frodl et al. 2012)
Reduced Frontal cortex	SCZ: <i>Df16A</i> ^{+/-} , 22q11.2 (Ellegood et al. 2014) ASD: ITGβ3 (Ellegood et al. 2012)	SCZ: (James et al. 2004; Arnone et al. 2009; Shepherd et al. 2015; Pina-Camacho et al. 2016) ADHD (Noordermeer et al. 2017)

When investigating the number of parvalbumin (PV) expressing inhibitory interneurons in the hippocampus of *Negr1*^{-/-} mice, we found a significant reduction of this specific cell population in *Negr1*^{-/-} mice as compared to its Wt littermates with no change in the total number of neurons. It has been suggested that reduced excitability of the neurons leads to decrease in the activity of PV expressing interneurons (Le Magueresse et al. 2013; Chen et al. 2018). Hence, the reduction in PV positive interneurons in the hippocampus could be a consequence of total hippocampal activity with reduced inhibitory signalling which leads to hyperactive hippocampus. Another possible mechanism could be the compensatory effects for the reduced excitation (imbalanced E/I ratio) due to a smaller corpus callosum, which is in line with a report showing decreased long term potentiation (LTP) and miniature excitatory post synaptic currents (EPSCs) in the hippocampus of *Negr1*^{-/-} mice (Noh et al. 2019).

Decreased GABAergic signalling has been shown as a relevant etiological finding concerning psychiatric disorders like SCZ, ASD, MDD, stress and anxiety (Lodge et al. 2009; Uchida et al. 2014; Sauer et al. 2015; Lauber et al. 2016; Chen et al. 2018). Taken together, we suggest that the neuroanatomical alterations found in *Negr1*^{-/-} mice are comparable to brain endophenotypes of several neuropsychiatric disorders. *Negr1* deficiency does not directly influence the total number of neurons in the hippocampus; rather it is important in interchanging some specific subtypes of neurons for creating the balance of E/I ratio for proper synaptic functioning.

3. IgLON members cooperate the patterning of complex mouse behavior

3.1 *Lsamp* and *Ntm* interactions in mouse behavior

In order to study the impact of *Lsamp*, *Ntm* and their interactions at the functional level, we performed behavioral phenotyping of *Lsamp*^{-/-}, *Ntm*^{-/-}, and *Lsamp*^{-/-}*Ntm*^{-/-} double deficient mice. A summary of *Lsamp*^{-/-}, *Ntm*^{-/-}, and *Lsamp*^{-/-}*Ntm*^{-/-} behavioral analysis has been shown in Table 9. Initial phenotyping showed no differences in the general locomotor activity between the test groups in the open field test. Even though result from OFT display more time spent and longer distances travelled in the central area by *Ntm*^{-/-} mice. In *Lsamp*^{-/-} mice no exploratory activity in the centre of the open-field was observed which is in line with previous study (Innos et al. 2011). It is noteworthy to observe the disappearance of significant exploratory effect in the *Ntm*^{-/-} mice when *Lsamp* was deleted together with *Ntm* in the *Lsamp*^{-/-}*Ntm*^{-/-} double deficient mice. This indicates that *Lsamp* acts as an enhancer for the exploratory behavior in the central area of the open field. Previous studies pointed out the abolished rearings in the open field in *Lsamp*^{-/-} mice and normal level of rearings in *Ntm*^{-/-} mice (Innos et al. 2011; Mazitov et al. 2017).

Table 9. Summarised interactive effects of *Lsamp* and *Ntm* at behavioral level (NC represents no change, ↓*, ↑* denotes significantly lowered or higher vice versa, ↓t, ↑t denotes lowered or higher trends).

Summary of <i>Lsamp</i>^{-/-}, <i>Ntm</i>^{-/-}, and <i>Lsamp</i>^{-/-}<i>Ntm</i>^{-/-} behavioral analysis				
Test	<i>Lsamp</i>^{-/-}	<i>Ntm</i>^{-/-}	<i>Lsamp</i>^{-/-}<i>Ntm</i>^{-/-}	Effects
Open field				exploratory activity
distance-travelled	NC	NC	NC	no effects
distance in centre	↓*	↑*	↓*	<i>Lsamp</i> enhancer effect
No of rearing	↓t	↑t	↓t	<i>Lsamp</i> enhancer effect
Elevated plus Maze				anxiety related activity
closed arm entries	NC	NC	↑*	combined deletion effect
open arm entries	↓t	↓*	↑**	combined deletion effect
Morris-water maze				learning, memory, swimming
latency training	NC	NC	NC	
swimming speed	↓**	↓**	↓***	combined effect

Decrease in the frequency of rearings has been observed in *Lsamp*^{-/-}*Ntm*^{-/-} double deficient mice which again suggest the effect due to *Lsamp* gene. We used elevated plus maze to study the genotype dependent changes in anxiety. We found drastic reduction in anxiety like behavior in *Lsamp*^{-/-}*Ntm*^{-/-} double deficient mice displayed in the EPM compared to the other tested genotypes. *Lsamp*^{-/-}*Ntm*^{-/-} double deficient mice spent longer time and executed more entries in open arms compared to other genotype tested mice. Hence, we hypothesize that the notable anxiolytic phenotype in *Lsamp*^{-/-}*Ntm*^{-/-} double deficient mice, may demonstrate the amplification of reduced anxiety behavior found in the *Lsamp* and *Ntm* single deletional mice. It can be taken as a model of the architecture of a polygenic psychiatric disease: the carry on effects of single genes that follow the abnormal behavioral features are magnified in the disruption of multiple loci until the behavioral deviation meets diagnostic criteria. It has been frequently shown that *Lsamp*^{-/-} mice are more active and likely to spend more time on the open arm of the EPM (Catania et al. 2008; Innos et al. 2011, 2012).

Ntm^{-/-} mice doesn't show any significant effects in the EPM. Whereas, it has been observed that *Ntm*^{-/-} mice spend more time in the centre of the open field, implying another evidence for reduced anxiety since the Wt control mice normally avoid the centre area of the open field (Bourin et al. 2007). It is constantly unclear in the different behavior paradigms whether the test mice

represent reduced anxiety, excessive behavioral activation or increased locomotor activity (Catania et al. 2008, Innos et al. 2011). All together, these effects (increased time in the open arm of the EPM and in the centre of the open field) indicate the multidimensional structure of anxiety related behavior in mouse (Carola et al. 2002).

In order to analyse the hippocampal dependent learning and memory, we performed Morris water maze. According to our previous studies performed on *Lsamp*^{-/-} and *Ntm*^{-/-} mice (Innos et al. 2011; Mazitov et al. 2017), we observed no gross learning impairments either in *Lsamp*^{-/-}, *Ntm*^{-/-} or in *Lsamp*^{-/-}*Ntm*^{-/-} double deficient mice. Most striking result was observed as amplified deficiency effect in swimming speed: reduction in swimming speed in both *Lsamp* and *Ntm* single deficient mice which is further enhanced in *Lsamp*^{-/-}*Ntm*^{-/-} double deficient mice. Despite of having normal performance in fine motor tests such as rota rod or beam walking test in *Lsamp*^{-/-} mice (Innos et al. 2011), reduction in swimming speed phenotype is very persistent in these mice. There is no adequate explanation of how neural adhesion molecules could impact the speed of movements. The distorted premature myelination recently reported in *Lsamp*^{-/-} mice (Sharma et al. 2015) could be an explanation, since myelination has been associated with processing speed in early childhood (Chevalier et al. 2015). Another hypothesis comes from the evidence that both *Lsamp* (at stage E15.5, Philips et al. 2015) and *Ntm* (at stage P0, Struyk et al. 1995) have strong expression in the developing dorsal striatum (caudate nucleus and putamen) and in the fourth layer of the somatosensory cortex the brain area which has been shown to be involved in the control of speed during execution and mental imagery of sequential movements (Sauvage et al. 2013). The strong signal of both *Lsamp* and *Ntm* in dorsal striatum fades during the first postnatal week and is minimal in adulthood, indicating that these adhesion molecules could perform the specific tasks mediating fine connections between the cells during the development of motor pathways. Taken all together, we hypothesize that the deletional effects of one family member of IgLON molecules is dependent to the another family member and hence represent the complementary and differential effects at the behavioral level.

3.2 Negr1 is involved in regulation of social and cognitive behavior

Our behavior analysis in mice unveiled some novel role of *Negr1* at high order cognitive brain functions such as defective social behavior and memory based plasticity. In fact our study offers *Negr1*^{-/-} mice as a model system to investigate the pathophysiology of neuropsychiatric disorders. A summary of *Negr1*^{-/-} behavioral analysis has been shown in Table 10. Impaired social behavior is typical characteristics of several psychiatric and neurodevelopmental disorders like ASD, SCZ, BPD, and ADHD. Failure of social inter-

action and the withdrawal is one of the most common negative symptoms of SCZ. Here, we showed lack of barbering or whisker trimming behavior in *Negr1*^{-/-} mice, indicating lack of social cooperation, impaired social cognition and inability to build social hierarchy (Strozik et al. 1981; Kalueff et al. 2006; Long, 1972; Sarna et al. 2000). Lack of whiskers trimming has been also seen in *Lsamp*^{-/-} mice (Innos et al. 2011). Three-chamber sociability test also showed impaired voluntary approach for social interaction in *Negr1*^{-/-} mice. Reduced time latency for winning during tube dominance test implies the lack of motivation for dominance or avoidance behavior for competing or hyperactivity during interaction, this can also be additional effects seen due to lack of whiskers trimming by these mice.

Furthermore, direct social interaction test, provided us more extensive evaluation of social and non social activities of mice during interactions. Abnormal total social contact, sniffing to other body part, active contact were observed suggesting the impaired social cognition with hyperactivity, confused and disoriented behavior. Non social activities in *Negr1*^{-/-} mice were further exhibited by the hyperactivity manifestations as increased digging and rearing time were detected which is compensated by reduced self grooming. Animal model of ASD and other neurological disorders like D1A dopamine receptors KO mice, and in 16p11^{+/-} mice (Cormwell et al. 1998; Maillard et al. 2015) also demonstrate decreased self grooming. Increased digging bouts in *Negr1*^{-/-} mice were further evaluated at the scale of obsessive compulsive behavior using marble burying test. Result suggest that *Negr1*^{-/-} mice exhibit no sign of obsessive behavior instead more digging appears to be an effort to escape due to hyperactive behavior perseverations.

The hippocampal functions such as spatial learning and memory test using morris water maze suggest *Negr1*^{-/-} mice as a slower learner and impairments in the relearning ability depicting plasticity defects. We also outlined the correlations between brain structure and observed behavioral parameters. Most important correlations were found is the volumetric changes in the ventricles, hippocampus, globus pallidus, and corpus callosum in *Negr1*^{-/-} mice. These were most significantly correlated with social interaction activities like sniffing bouts of other body parts, the duration of active and passive contact. Reduced brain and hippocampal volume is in lined with impaired learning and sociability effect. We hypothesise that impairments in social behavior leads to behavioral hyperactivity observed in *Negr1*^{-/-} mice were caused by E/I imbalance due to reduced corpus callosum volume. Overall, our findings provide the rationale of the genetic involvement of *Negr1* in the pathogenesis of psychiatric disorders.

Table 10. Summary of *Negr1*^{-/-} mice behavioral analysis and its implications (* represents significant difference; n. =number).

Summary of <i>Negr1</i>^{-/-} behavioral analysis		
Test	Response	Implications
Barbering/Whiskers trimming	nil ****	lack of social hierarchy, social cooperation, & social cognition
3-Chamber test		
Sociability	lower**	impaired voluntary initiation (social approach)
Social-Novelty	no change	
Social dominance		
Tube test	short winning latency**	lack of motivation to compete/interact, withdrawal for social dominance
Direct Social Interaction test		impaired social interactions/social cognition
Total social contact	increased n. of bouts, decreased bout duration	hyperactivity during social engagements &
Sniffing	decreased bout duration	disoriented and confused behavior
Active contact	decreased bout duration	
Rearings	increased time spent & bout duration	hyperactive supported vertical exploration
Digging	increased n. of bouts & time spent	stereotypic repetitive behavior & increased effort to escape
Self-grooming	decreased n. of bouts & time spent	compensatory for hyperactive and repetitive behavior during social interaction
Marble burying	no change	
Tail suspension	no change	
Morris water maze		
latency training	small trend change	slow learner
latency-reversal	decreased **	cognitive (plasticity related relearning inability)

4. IgLONs deficient mice in relation to neuropsychiatric endophenotypes

In the present study, we assessed the morphological, neuroanatomical and behavioral phenotypes of four IgLONs deficient mice models, *Lsamp*^{-/-}, *Ntm*^{-/-}, *Lsamp*^{-/-}*Ntm*^{-/-} and *Negr1*^{-/-} for relevance to the neuropsychiatric disorders. We found that the cytoskeleton abnormalities, neuroanatomical alterations, behavioral impairments found in *Negr1*^{-/-} mice are comparable to brain endophenotypes of several cross disorder neuropsychiatric disorders. *Lsamp*^{-/-}, *Ntm*^{-/-} and *Lsamp*^{-/-}*Ntm*^{-/-} mice can be chosen as a model of polygenic psychiatric disease, where the continued traits of abnormal behavioral due to single genes are amplified in the multiple loci mutations til the abnormal traits carry out the diagnostic criteria.

Accumulating evidence from neuroimaging studies also indicated common volumetric anomalies present in cortical and subcortical brain regions, the most replicated of these being the enlargement of ventricles, and the reduced volume of the hippocampus, frontal cortex and corpus callosum in the neuropsychiatric and neurodevelopmental disorders (Kurokawa et al. 2000; Noordermeer et al. 2017; Wise et al. 2017; Park et al. 2018). Cytoskeleton rearrangements due to actin molecules are very crucial for the neuritogenesis process, synaptic functioning and thereafter proper brain functioning. Abnormalities in actin dysregulation are heavily implicated in several neurodevelopmental and psychiatric disorders (Lang et al. 2014; Bakos et al. 2015; Yan et al. 2016). The pattern of severe behavioral abnormalities in *Negr1*^{-/-} mice is greatly similar to those of existing putative mice models of several neuropsychiatric disorders (Pletnikov et al. 2008; Koh et al. 2008; Hatayama et al. 2011; Zhang et al. 2016; Canitano et al. 2017). This analysis is another promising example encouraging concept that different kinds of genetic variations or mutations may result in similar kind of behavioral manifestations in mice, which could be probably corresponding to the neuropsychiatric syndromes present in humans.

5. Concluding remarks and future prospects

IgLON gene family regulates F-actin accumulation at lamellopodial veils during early stages of neuritogenesis. *Lsamp* and *Ntm* work as a group in balancing cellular homeostasis. We showed that the deletional outcome of one IgLON family member (*Ntm*) is dependent on the presence of another family member (*Lsamp*) which is apparently seen in synaptophysin activity or immature enhanced neurites outgrowth and branching in *Ntm*^{-/-} neurons, and this effect was rescued when both *Lsamp* and *Ntm* genes were deleted, as in the case of *Lsamp*^{-/-}*Ntm*^{-/-} neurons (Fig. 22).

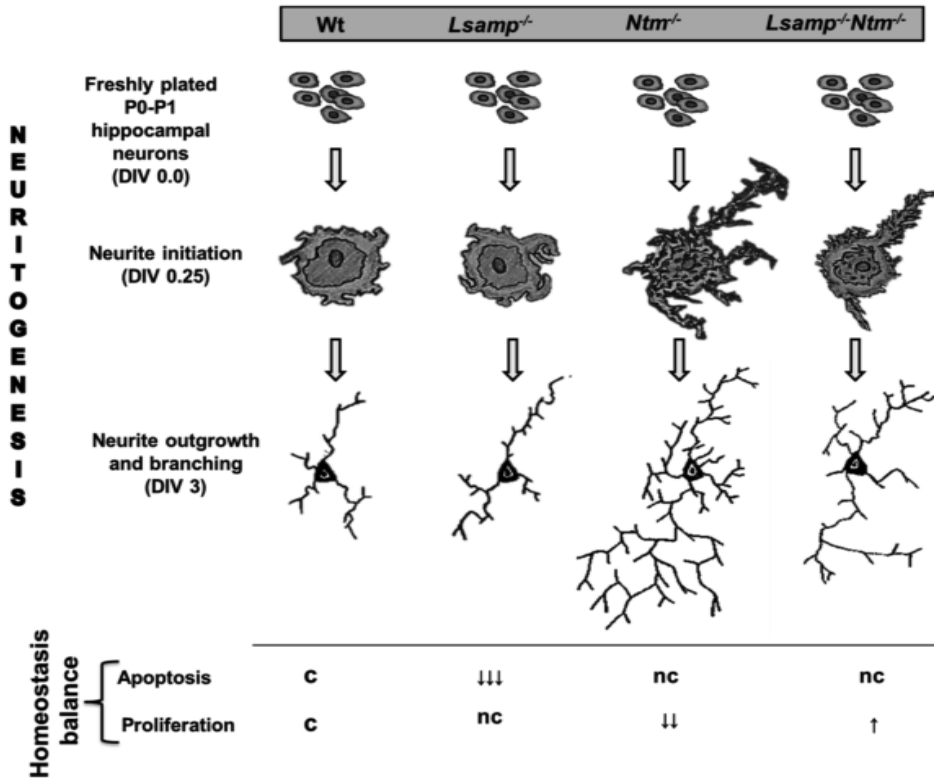


Figure 22. Summary of *Lsamp* and *Ntm* deletional effects on neuritogenesis. Complementary interaction between *Lsamp* and *Ntm* regulate early neuritogenesis and balances the apoptosis and proliferation during neuronal development.

The mechanism driving IgLONs dependent neuritogenesis is unknown and needed further investigations especially of downstream signalling mechanisms which regulate actin cytoskeleton. Actin regulated cytoskeletal mechanisms at synaptic sites would be the promising future prospects to uncover the basic topological significance related to brain functioning. *In vivo* study and detailed cell cycle analysis will provide us more insight towards the effect of *Lsamp* and *Ntm* interactions during tissue homeostasis. It is important to understand what is the function of *Lsamp* and *Ntm* behind the reduced swimming speed in the Morris water maze, in spite of normal efficiency in fine motor performances in the deletional mice. There are few speculations which can be further studied like myelination and somatosensory cortex circuit formation in relation to swimming speed in these mice models.

Deletion of *Negr1* is associated with neuroanatomical anomalies and behavioral alterations that are related to the overlapping symptoms of several psychiatric disorders such as ASD, SCZ and ADHD (Fig. 23). *Negr1*^{-/-} mice may serve as a potential animal model to study pathophysiology of complex neuropsychiatric disorders.

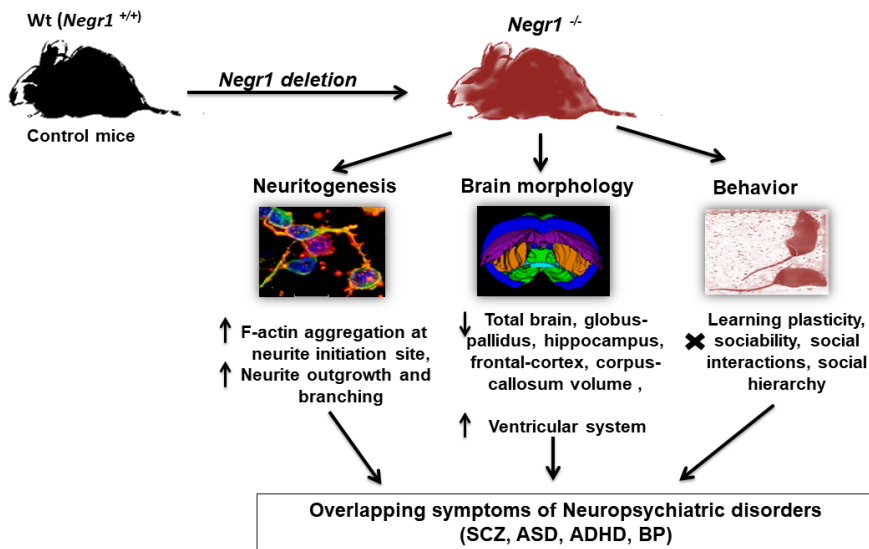


Figure 23. Summary of *Negr1* deletional effects on mice. From Wt (*Negr1*^{+/+}) mice when we delete *Negr1* gene we receive (*Negr1*^{-/-}) mice. *Negr1*^{-/-} exhibit several endo-phenotypes such as abnormal neuritogenesis, brain morphology and behavior. All these impairments congregate in the several psychiatric disorders like SCZ, ASD, ADHD, and BP.

Further investigations are definitively required in order to untangle the putative brain consequences of impaired *Negr1* activity. Detailed studies on neuronal, white matter tract connectivity, myelination process require further exploration. We have proposed hyperactive hippocampus due to imbalanced E/I ratio therefore, it would be interesting to measure electrophysiological changes in hippocampal area of CA1 against inhibitory or excitatory receptors using different pharmacological drugs. Since *Negr1*^{-/-} mice exhibit normal performances in learning during water maze and social novelty test, we believe that other cognitive functions like motivation, food preferences, object recognition or olfactory test need to be checked. Interventions with pharmacological examinations that involve certain neurotransmitter system in social behavior test along with circuit level understanding of endogenous neural activity during social interaction should also be a considerable objectives in the future studies. We believe that further investigations on *Negr1* could land up in the better understanding of the causative and therapeutic implications in neuropsychiatric disorders.

CONCLUSIONS

1. The morphological phenotyping presented in this thesis showed complementary interactions between *Lsamp* and *Ntm* that regulate F-actin accumulation during neurite initiation and balances the speed and rate of neurite outgrowth, branching and cellular homeostasis. Similarly, *Negr1* is also involved in early neuritogenesis and together indicating the role of IgLON family proteins in early neurite sprouting, as cell autonomous, independent of their regulation in cell cell adhesion.
2. Neuroanatomical evidences from *Lsamp*^{-/-}, *Ntm*^{-/-} and double deletional *Lsamp*^{-/-}*Ntm*^{-/-} mice revealed no gross and cytoarchitectural changes. By contrast, *Negr1*^{-/-} brain displayed remarkable brain abnormalities such as ventricle enlargement, decreased volume of hippocampus, globus pallidus, corpus callosum and total brain. Furthermore, immunohistochemical analysis of *Negr1*^{-/-} mice hippocampi showed decreased number of parvalbumin positive inhibitory interneurons indicating decreased activity of hippocampus due to imbalanced E/I ratio. These evidences suggest *Negr1*^{-/-} mice to present neuroanatomical endophenotypes related to neuropsychiatric disorders.
3. The behavioral phenotyping demonstrated test specific differential interactions between *Lsamp* and *Ntm* as the exploratory effects seen in *Ntm*^{-/-} mice dissipated in the case of *Lsamp*^{-/-}*Ntm*^{-/-} mice. Additionally, combined interactions of *Lsamp* and *Ntm* were seen by reduced swimming speed in the morris water maze and altered anxiety in the elevated plus maze *Lsamp*^{-/-}*Ntm*^{-/-} mice. These results implied that activity of *Lsamp* and *Ntm* is dependent on the type of behavioral test used, referring their associative role in coordinating the specific neural circuits manifesting in specific behavioural alterations. *Negr1*^{-/-} mice behavioral profiling revealed significant lack of maintaining social hierarchy due to loss of whiskers trimming, affected hippocampal based spatial learning and deficit in reversal learning behavior, impaired sociability and social interactions. We also provided significant correlations between neuroanatomical and behavioral alterations present in the *Negr1*^{-/-} mice. Collectively, our results suggest role of *Negr1* in neuronal circuit development, connectivity and behavioral deviations related to neuropsychiatric conditions.
4. We evaluated the applicability of IgLONs deficient mice models for endophenotypes of neuropsychiatric disorders. Our analysis from morphological, neuroanatomical and behavioral examinations proposed *Negr1*^{-/-} mice as the best fitted animal model among IgLONs representing various endophenotypes of neuropsychiatric disorders with overlapping symptoms. Most of the neuropsychiatric disorders have heterogeneous symptoms and can have limited similarities with rodent model conditions. It is quite challenging to have an animal model replicating exact similar symptoms, therefore analysing the neuropsychiatric endophenotypes makes it simple to study

diverse traits related to the susceptible genes. *Negr1*^{-/-} mice showed impaired cytoskeleton rearrangements, brain volume and cognitive with social processing abnormalities. Thus, *Negr1*^{-/-} mice model may provide useful tool for studies of etiology of neuropsychiatric disorders.

REFERENCES

- Akeel M, McNamee C J, Youssef S, Moss D (2011). DIgLONs inhibit initiation of neurite outgrowth from forebrain neurons via an IgLON-containing receptor complex. *Brain Res* 1374: 27–35.
- Amare AT, Schubert KO, Tekola-Ayele F, Hsu YH, Sangkuhl K, Jenkins G et al. (2019). The association of obesity and coronary artery disease genes with response to SSRIs treatment in major depression. *J Neural Transm (Vienna)*. 126(1):35–45.
- Anderzhanova E, Kirmeier T, Wotjak CT (2017). Animal models in psychiatric research: The RDoC system as a new framework for endophenotype-oriented translational neuroscience. *Neurobiol. Stress* 7: 47–56.
- Arnone D, Cavanagh J, Gerber D, Lawrie SM, Ebmeier KP, McIntosh AM (2009). Magnetic resonance imaging studies in bipolar disorder and schizophrenia: meta-analysis. *Br J Psychiatry*. 195(3):194–201.
- Bakker R, Tiesinga P, Kötter R (2015). The Scalable Brain Atlas: Instant Web-Based Access to Public Brain Atlases and Related Content. *Neuroinformatics* 13(3):353–366.
- Bakos J, Bacova Z, Grant SG, Castejon AM, Ostatnikova D (2015). Are molecules involved in neuritogenesis and axon guidance related to autism pathogenesis? *Neuromol Med* 17:297–304.
- Barøy T, Kresse S H, Skårn M, Stabell M, Castro R, Lauvrak S et al. (2014). Re-expression of LSAMP inhibits tumor growth in a preclinical osteosarcoma model. *Mol Cancer* 13:93.
- Behan A T, Byrne C, Dunn M J, Cagney G, Cotter D R (2009). Proteomic analysis of membrane microdomain-associated proteins in the dorsolateral prefrontal cortex in schizophrenia and bipolar disorder reveals alterations in LAMP, STXBP1 and BASP1 protein expression. *Mol. Psychiatry* 14:601–613.
- Bourin M, Petit-Demoulière B, Dhonnchadha, BN, Hascöet M (2007). Animal models of anxiety in mice. *Fundam Clin Pharmacol*. 21(6):567–574.
- Braff DL, Freedman R, Schork NJ, Gottesman II (2007). Deconstructing schizophrenia: an overview of the use of endophenotypes in order to understand a complex disorder. *Schizophr Bull*. 33(1):21–32.
- Brambilla P, Nicoletti M, Sassi RB, Mallinger AG, Frank E, Keshavan MS, Soares JC (2004). Corpus callosum signal intensity in patients with bipolar and unipolar disorder. *J Neurol Neurosurg Psychiatry*. 75(2):221–225.
- Brauer AU, Savaskan NE, Plaschke M, Prehn S, Ninnemann O, Nitsch R (2000). IG-molecule Negr1 shows differential expression pattern from LAMP in the developing and adult rat hippocampus. *Hippocampus* 10: 632- 644.
- Brevik E J, van Donkelaar M M, Weber H, Sánchez-Mora C, Jacob C, Rivero O et al. (2016). Genome-wide analyses of aggressiveness in attention-deficit hyperactivity disorder. *Am J Med Genet* 171(5): 733–747.
- Canitano R, Pallagrosi M (2017). Autism spectrum disorders and schizophrenia spectrum disorders: excitation/inhibition imbalance and developmental trajectories. *Front Psychiatry* 8:69.
- Carballedo A, Lisiecka D, Fagan A, Saleh K, Ferguson Y, Connolly G, Meaney J, Frodl T (2012). Early life adversity is associated with brain changes in subjects at family risk for depression. *World J Biol Psychiatry* 13:569–578.

- Carola V, D'Olimpio F, Brunamonti E, Mangia F, Renzi P (2002). Evaluation of the elevated plus-maze and open-field tests for the assessment of anxiety-related behaviour in inbred mice. *Behav Brain Res.* 134(1–2):49–57.
- Casey BJ, Giedd JN, Thomas KM (2000). Structural and functional brain development and its relation to cognitive development. *Biol Psychol.* 54(1–3): 241–57.
- Catania EH, Pimenta A, Levitt P (2008). Genetic deletion of *Lsmp* causes exaggerated behavioral activation in novel environments. *Behav Brain Res* 188(2): 380–390.
- Chan RC, Gottesman II, Ge X, Sham, P C (2010). Strategies for the study of neuropsychiatric disorders using endophenotypes in developing countries: a potential databank from china. *Front Hum Neurosci.*4: 207.
- Chang LC, Jamain S, Lin CW, Rujescu D, Tseng GC, Sibille EA (2014). Conserved BDNF, glutamate- and GABA-enriched gene module related to human depression identified by coexpression meta-analysis and DNA variant genome-wide association studies. *PLOS ONE* 9:e90980.
- Chatterjee S, Sikdar S K (2014). Corticosterone targets distinct steps of synaptic transmission via concentration specific activation of mineralocorticoid and glucocorticoid receptors. *J Neurochem* 12(4):476–490.
- Chen S, Gil O, Ren YQ, Zanazzi G, Salzer LJ, Hillman ED (2001). *Ntm* expression during cerebellar development suggests roles in axon fasciculation and synaptogenesis. *J Neurocytol* 30: 927–937.
- Chen X, Long F, Cai B, Chen X, Chen G (2017). A novel relationship for schizophrenia, bipolar and major depressive disorder Part 3: evidence from chromosome 3 high density association screen. *J. Comp. Neurol.* 526: 59–79.
- Chen CC, Lu J, Yang R, Ding J B, Zuo Y (2018). Selective activation of parvalbumin interneurons prevents stress-induced synapse loss and perceptual defects. *Mol. psychiatry* 23(7): 1614–1625.
- Chesselet MF, Gonzales C, Levitt P (1990). Heterogeneous distribution of the limbic system-associated membrane protein in the caudate nucleus and substantia nigra of the cat. *Neuroscience* 40(3): 725–733.
- Chevalier N, Kurth S, Doucette M R, Wiseheart M, Deoni SCL, Dean DC III et al. (2015). Myelination Is Associated with Processing Speed in Early Childhood: Preliminary Insights. *PLOS ONE* 10(10): e0139897.
- Cho TM, Hasegawa J, Ge B, Loh HH (1986). Purification to apparent homogeneity of a μ -type opioid receptor from rat brain. *Proc. Natl. Acad. Sci. USA* 83: 4138–4142.
- Clapcote SJ, Lipina TV, Millar JK, Mackie S, Christie S, Ogawa F et al. (2007). Behavioral phenotypes of *DISC1* missense mutations in mice. *Neuron* 54:387–402.
- Coccaro N, Zagaria A, Tota G, Anelli L, Orsini P, Casieri P et al. (2015). Overexpression of the *LSAMP* and *TUSC7* genes in acute myeloid leukemia following microdeletion/duplication of chromosome 3. *Cancer Genet.* 10: 517–522.
- Cote PY, Levitt P, Parent A (1995). Distribution of limbic system-associated membrane protein immunoreactivity in primate basal ganglia. *Neuroscience* 69: 71–81.
- Cote PY, Levitt P, Parent A (1996). Limbic system-associated membrane protein (LAMP) in primate amygdala and hippocampus. *Hippocampus* 6: 483–494.
- Corvin A P (2010). Neuronal cell adhesion genes: Key players in risk for schizophrenia, bipolar disorder and other neurodevelopmental brain disorders? *Cell Adh. Migr.* 4(4):511–514.
- Cox DA, Gottschalk M G, Wesseling H, Ernst A, Cooper J D, Bahn S (2016). Proteomic systems evaluation of the molecular validity of preclinical psychosis models compared to schizophrenia brain pathology. *Schizophr Res* 177:98–107.

- Cromwell HC, Berridge KC, Drago J, Levine MS (1998). Action sequencing is impaired in D1A-deficient mutant mice. *Eur J Neurosci* 10:2426–2432.
- Cui Y, Ying Y, van Hasselt A, Ng KM, Yu J, Zhang Q et al. (2008). OPCML is broad tumor suppressor for multiple carcinomas and lymphomas with frequently epigenetic inactivation. *PLOS ONE* 3(8):e2990.
- David AS, Wacharasindhu A, Lishman WA (1993). Severe psychiatric disturbance and abnormalities of the corpus callosum: review and case series. *J Neurol Neurosurg Psychiatry* 56(1): 85–93.
- Dedic N, Pöhlmann ML, Richter JS, Mehta D, Czamara D, Metzger MW et al. (2018). Cross-disorder risk gene CACNA1C differentially modulates susceptibility to psychiatric disorders during development and adulthood. *Mol. Psychiatry* 23(3): 533–543.
- Dennis EL, Jahanshad N, Braskie MN, Warstadt NM, Hibar DP, Kohannim O et al. (2014). Obesity gene NEGR1 associated with white matter integrity in healthy young adults. *Neuroimage* 102:548–557.
- Del Re EC, Gao Y, Eckbo R, Petryshen TL, Blokland GA, Seidman LJ et al. (2016). A New MRI Masking Technique Based on Multi-Atlas Brain Segmentation in Controls and Schizophrenia: A Rapid and Viable Alternative to Manual Masking. *J Neuroimaging*. 26(1):28–36.
- Dong X, Zhang J, Yang F, Wu J, Cai R, Wang Tet al. (2018). Effect of luteolin on the methylation status of the OPCML gene and cell growth in breast cancer cells. *Exp Ther Med*. 16(4):3186–3194.
- Durmusoglu E, Ugurlu O, Akan S, Simsek F, Kizilates G, Kitis O, Ozkul BA, Eker C, Coburn KL, Gonul AS (2018). Hippocampal shape alterations in healthy young women with familial risk for unipolar depression. *Compr Psychiatry* 82:7–13.
- Ellegood J, Henkelman RM, Lerch JP (2012). Neuroanatomical assessment of the integrin $\beta 3$ mouse model related to autism and the serotonin system using high resolution MRI. *Front. Psychiatry* 3: 37.
- Ellegood J, Crawley JN (2015). Behavioral and Neuroanatomical Phenotypes in Mouse Models of Autism. *Neurotherapeutics* 12(3):521–533.
- Flynn K C (2013). The cytoskeleton and neurite initiation. *Bioarchitecture* 3(4): 86–109.
- Franklin KBJ, Paxinos G (1997). The Mouse Brain in Stereotaxic Coordinates. San Diego: Academic Press.
- Frodl T, Skokauskas N (2012). Meta-analysis of structural MRI studies in children and adults with attention deficit hyperactivity disorder indicates treatment effects. *Acta Psychiatr Scand*. 125(2):114–26.
- Funatsu N, Miyata S, Kumanogoh H, Shigeta M, Hamada K, Endo Y et al. (1999). Characterization of a novel rat brain glycosylphosphatidylinositolanchored protein (Negr1), a member of the IgLON cell adhesion molecule family. *J Biol Chem* 274:8224–8230.
- Gaig C, Graus F, Compta Y, Högl B, Bataller L, Brüggemann N et al. (2017). Clinical manifestations of the anti-IgLON5 disease. *Neurology* 88(18):1736–1743.
- Galderisi S, Quarantelli M, Volpe U, Mucci A, Cassano GB, Invernizzi G et al. (2008). Patterns of structural MRI abnormalities in deficit and nondeficit schizophrenia. *Schizophr Bull* 34:393–401.
- Gamero-Villarrol C, Gonzalez LM, Gordillo I, Carrillo JA, Garcia-Herraiz A, Flores I et al. (2015). Impact of NEGR1 genetic variability on psychological traits of patients with eating disorders. *Pharmacogenom J* 15:278–283.

- Gandal MJ, Haney JR, Parikshak NN, Leppa V, Ramaswami G, Hartl C et al. (2018). Shared molecular neuropathology across major psychiatric disorders parallels polygenic overlap. Common Mind Consortium; PsychENCODE Consortium; iPSYCH-BROAD Working Group, Horvath S, Geschwind DH. *Science* 359(6376):693–697.
- Garver LS, Xi Z, Dimopoulos G (2008). Immunoglobulin superfamily members play an important role in the mosquito immune system. *Dev Comp Immunol.* 32:519–531.
- Gelpi E, Höftberger R, Graus F, Ling H, Holton JL, Dawson T et al. (2016). Neuropathological criteria of anti-IgLON5-related tauopathy. *Acta Neuropathol.* 132(4): 531–43.
- Genovese A, Cox DM, Butler MG (2015). Partial deletion of chromosome 1p31.1 including only the neuronal growth regulator 1 gene in two siblings. *J Pediatr Genet* 4:23–28.
- Gil OD, Zanazzi G, Struyk AF, Salzer JL (1998). *Ntm* Mediates Bifunctional Effects on Neurite Outgrowth via Homophilic and Heterophilic Interactions. *J Neurosci* 18:9312–9325
- Gil OD, Zhang L, Chen S, Ren YQ, Pimenta A, Zanazzi G et al (2002). Complementary Expression and Heterophilic Interactions between IgLON Family Members *Ntm* and LAMP. *J Neurobiol* 51:190–204.
- Gimenez U, Boulan B, Mauconduit F, Taurel F, Leclercq M, Denarier E et al. (2017). 3D imaging of the brain morphology and connectivity defects in a model of psychiatric disorders, MAP6–KO mice. *Sci Rep* 7:10308.
- Golub Y, Kaltwasser SF, Mauch CP, Herrmann L, Schmidt U, Holsboer F et al. (2011). Reduced hippocampus volume in the mouse model of Posttraumatic Stress Disorder. *J Psychiatr Res* 45:650–659.
- Gormley S, Rouine J, McIntosh A, Kerskens C, Harkin A (2016). Glial fibrillary acidic protein (GFAP) immunoreactivity correlates with cortical perfusion parameters determined by bolus tracking arterial spin labelling (bt-ASL) magnetic resonance (MR) imaging in the Wistar Kyoto rat. *Physiol Behav.* 160:66–79.
- Gottesman II & Gould TD (2003), The endophenotype concept in psychiatry: etymology and strategic intentions. *Am J Psychiatry* 160(4):636–45.
- Gould TD & Gottesman II (2006). Psychiatric endophenotypes and the development of valid animal models. *Genes Brain Behav.* 5(2):113–119.
- Graus F & Santamaría J (2017). Understanding anti-IgLON5 disease. *Neurol Neuroimmunol Neuroinflamm.* 4(5):e393.
- Grimwood J, Gordon L A, Olsen A, Terry A, Schmutz J, Lamerdin J et al. (2004). The DNA sequence and biology of human chromosome 19. *Nature* 428: 529–535.
- Gunaydin LA, Kreitzer AC (2016). Cortico-basal ganglia circuit function in psychiatric disease. *Annu Rev Physiol* 78:327–350.
- Hasler G, Drevets WC, Gould TD, Gottesman II, Manji HK (2006). Toward constructing an endophenotype strategy for bipolar disorders. *Biol Psychiatry.* 60(2):93–105.
- Heinla I, Leidmaa E, Kongi K, Pennert A, Innos J, Nurk K et al. (2015). Gene expression patterns and environmental enrichment-induced effects in the hippocampi of mice suggest importance of *Lsamp* in plasticity. *Front. Neurosci* 9: 205.
- Hachisuka A, Nakajima O, Yamazaki T, Sawada J (2000). Developmental expression of opioid-binding cell adhesion molecule (OBCAM) in rat brain. *Brain Res. Dev. Brain Res.* 122: 183–191.
- Hashimoto T, Maekawa S, Miyata S (2009). IgLON cell adhesion molecules regulate synaptogenesis in hippocampal neurons. *Cell Biochem Funct* 27: 496–498.

- Hatayama M, Ishiguro A, Iwayama Y, Takashima N, Sakoori K, Toyota T et al. (2011). *Zic2* hypomorphic mutant mice as a schizophrenia model and *ZIC2* mutations identified in schizophrenia patients. *Sci Rep* 1:16.
- Hibar DP, Westlye LT, van Erp TG, Rasmussen J, Leonardo CD, Faskowitz J et al. (2016). Subcortical volumetric abnormalities in bipolar disorder. *Mol. Psychiatry* 21(12):1710–1716.
- Hikida T, Jaaro-Peled H, Seshadri S, Oishi K, Hookway C, Kong S et al. (2007). Dominant-negative *DISC1* transgenic mice display schizophrenia-associated phenotypes detected by measures translatable to humans. *Proc Natl Acad Sci USA* 104: 14501–14506.
- Honorat JA, Komorowski L, Josephs KA, Fechner K, St Louis EK, Hinson SR et al. (2017). IgLON5 antibody: Neurological accompaniments and outcomes in 20 patients. *Neurol Neuroimmunol Neuroinflamm.* 4(5):e385.
- Horton H L and Levitt P (1988). A unique membrane-protein is expressed on early developing limbic system axons and cortical targets. *J Neurosci.* 8: 4653–4661.
- Huckins LM, Hatzikotoulas K, Southam L, Thornton LM, Steinberg J, Aguilera-McKay F et al. (2018). Investigations of common, low frequency and rare genome-wide variation in anorexia nervosa. *Mol. Psychiatry* 23(5):1169–1180.
- Hyde CL, Nagle M W, Tian C, Chen X, Paciga SA, Wendland JR, Tung JY et al. (2016). Identification of 15 genetic loci associated with risk of major depression in individuals of European descent. *Nat Genet* 48: 1031–1036.
- Iacono WG (2018). Endophenotypes in psychiatric disease: prospects and challenges. *Genome Med.* 10(1):11.
- Innos J, Philips MA, Leidmaa E, Heinla I, Raud S, Reemann P et al (2011). Lower anxiety and a decrease in agonistic behaviour in *Lsamp*-deficient mice. *Behav Brain Res* 217: 21–31.
- Innos J, Philips MA, Raud S, Lilleväli K, Kõks S, Vasar E (2012). Deletion of the *Lsamp* gene lowers sensitivity to stressful environmental manipulations in mice. *Behav Brain Res* 228:74–81.
- Innos J, Koido K, Philips MA, Vasar E (2013). Limbic system associated membrane protein as a potential target for neuropsychiatric disorders. *Front Pharmacol* 4: 32.
- Innos J, Leidmaa E, Philips MA, Sütt S, Alftoa A, Harro J et al (2013). *Lsamp* (-/-) mice display lower sensitivity to amphetamine and have elevated 5-HT turnover. *Biochem Biophys Res Commun* 430: 413–418.
- Inta D, Meyer-Lindenberg A, Gass P (2011). Alterations in Postnatal Neurogenesis and Dopamine Dysregulation in Schizophrenia: A Hypothesis. *Schizophr Bull* 37(4): 674–680.
- Ishihara K, Amano K, Takaki E, Shimohata A, Sago H, Epstein CJ et al. (2010). Enlarged brain ventricles and impaired neurogenesis in the *Ts1Cje* and *Ts2Cje* mouse models of Down syndrome. *Cereb. Cortex* 20: 1131–1143.
- James AC, James S, Smith DM, Javaloyes A (2004). Cerebellar, prefrontal cortex, and thalamic volumes over two time points in adolescent-onset schizophrenia. *Am. J. Psychiatry* 161 (6):1023–1029.
- Johnstone M, Thomson PA, Hall J, McIntosh AM, Lawrie SM, Porteous DJ (2011). *DISC1* in schizophrenia: genetic mouse models and human genomic imaging. *Schizophr Bull* 37: 14–20.
- Kalueff AV, Minasyan A, Keisala T, Shah ZH, Tuohimaa P (2006). Hair barbering in mice: implications for neurobehavioural research. *Behav Processes* 71:8–15.

- Karis K, Eskla KL, Kaare M, Täht K, Tuusov J, Visnapuu T et al. (2018). Altered expression profile of IgLON family of neural cell adhesion molecules in the dorsolateral prefrontal cortex of schizophrenic patients. *Front Mol Neurosci* 11:8.
- Kempton MJ, Salvador Z, Munafò MR, Geddes JR, Simmons A, Frangou S et al. (2011). Structural neuroimaging studies in major depressive disorder. Meta-analysis and comparison with bipolar disorder. *Arch Gen Psychiatry* 68:675–690.
- Kiesepä T, Eerola M, Mäntylä R, Neuvonen T, Poutanen VP, Luoma K et al. (2010). Major depressive disorder and white matter abnormalities: a diffusion tensor imaging study with tract-based spatial statistics. *J Affect Disord* 120:240–244.
- Kim H, Hwang JS, Lee B, Hong J, Lee S (2014). Newly Identified Cancer-Associated Role of Human Neuronal Growth Regulator 19 (NEGR1). *J Cancer* 5(7): 598–608.
- Kim H, Chun Y, Che L, Kim J, Lee S, Lee S (2017). The new obesity-associated protein, neuronal growth regulator 1 (NEGR1), is implicated in Niemann-Pick disease Type C (NPC2)-mediated cholesterol trafficking. *Biochem Biophys Res Commun* 482:1367–1374.
- Keller F, Rimvall K, Barbe M F, Levitt P (1989). A membrane glycoprotein associated with the limbic system mediates the formation of the septo-hippocampal pathway in vitro. *Neuron* 3: 551–561
- Kogan JH, Gross AK, Featherstone RE, Shin R, Chen Q, Heusner CL et al. (2015). Mouse Model of Chromosome 15q13.3 Microdeletion Syndrome Demonstrates Features Related to Autism Spectrum Disorder. *J Neurosci* 35:16282–16294.
- Koschützke L, Bertram J, Hartmann B, Bartsch D, Lotze M, von Bohlen et al. (2015). SrGAP3 knockout mice display enlarged lateral ventricles and specific cilia disturbances of ependymal cells in the third ventricle. *Cell Tissue Res* 361:645–650.
- Koh HY, Kim D, Lee J, Lee S, Shin HS (2008). Deficits in social behavior and sensorimotor gating in mice lacking phospholipase Cbeta1. *Genes Brain Behav* 7(1):120–8.
- Koido K, Janno S, Traks T, Parksepp M, Ljubajev U, Veiksaar P, et al. (2014). Associations between polymorphisms of LSAMP gene and schizophrenia. *Psychiatry Res* 215(3):797–8.
- Koido K, Traks T, Balotsev R, Eller T, Must A, Koks S et al. (2012). Associations between LSAMP gene polymorphisms and major depressive disorder and panic disorder. *Transl Psychiatry* 2:e152.
- Kubick N, Brösamle D, Mickael ME (2018) Molecular Evolution and Functional Divergence of the IgLON Family. *Evol Bioinform Online*. 14:1176934318775081.
- Kumar A, Gupta RC, Thomas MA, Alger J, Wyckoff N, Hwang S (2004). Biophysical changes in normal-appearing white matter and subcortical nuclei in late-life major depression detected using magnetization transfer. *Psychiatry Res* 130:131–140.
- Kurokawa K, Nakamura K, Sumiyoshi T, Hagino H, Yotsutsuji T, Yamashita I et al. (2000). Ventricular enlargement in schizophrenia spectrum patients with prodromal symptoms of obsessive-compulsive disorder. *Psychiatry Res* 99(2):83–91.
- Kwon JS, Shin YW, Kim CW, Kim YI, Youn T, Han MH, Chang KH, Kim JJ (2003). Similarity and disparity of obsessive-compulsive disorder and schizophrenia in MR volumetric abnormalities of the hippocampus-amygdala complex. *J Neurol Neurosurg Psychiatry* 74(7):962–964.
- Lad HV, Liu L, Payá-Cano JL, Fernandes C, Schalkwyk LC (2007). Quantitative traits for the tail suspension test: automation, optimization, and BXD RI mapping. *Mamm Genome* 18(6–7):482–491.

- Lang B, Pu J, Hunter I, Liu M, Martin-Granados C, Reilly TJ et al. (2014). Recurrent deletions of ULK4 in schizophrenia: a gene crucial for neurogenesis and neuronal motility. *J Cell Sci* 127:630–640.
- Lauber E, Filice F, Schwaller B (2016). Prenatal Valproate Exposure Differentially Affects Parvalbumin-Expressing Neurons and Related Circuits in the Cortex and Striatum of Mice. *Front Mol Neurosci* 9:150.
- Le Magueresse C, Monyer H (2013). GABAergic interneurons shape the functional maturation of the cortex. *Neuron* 77: 388–405.
- Lee SH, Ripke S, Neale BM, Faraone SV, Purcell SM, Perlis RH et al. (2013). Genetic relationship between five psychiatric disorders estimated from genome-wide SNPs. *Nat Genet* 45: 984–994.
- Lee AWS, Hengstler H, Schwald K, Berriel-Diaz M, Loreth D, Kirsch M et al. (2012). Functional inactivation of the genome-wide association study obesity gene neuronal growth regulator 1 in mice causes a body mass phenotype. *PLOS ONE* 7:e41537.
- Levitt P (1984). A monoclonal antibody to limbic system neurons. *Science* 223: 299–301.
- Lieberman JA, Girgis RR, Brucato G, Moore H, Provenzano F, Kegeles L et al. (2018). Hippocampal dysfunction in the pathophysiology of schizophrenia: a selective review and hypothesis for early detection and intervention. *Mol. Psychiatry* 23(8):1764–1772.
- Lijam N, Paylor R, McDonald MP, Crawley JN, Deng CX, Herrup K et al (1997). Social interaction and sensorimotor gating abnormalities in mice lacking Dvl1. *Cell* 90:895–905.
- Liu F, Arias-Vásquez A, Slegers K, Aulchenko YS, Kayser M, Sanchez-Juan P et al. (2007). A genomewide screen for late-onset Alzheimer disease in a genetically isolated Dutch population. *Am J Hum Genet.* 81(1):17–31.
- Lodge DJ, Behrens MM, Grace AA (2009). A loss of parvalbumin-containing interneurons is associated with diminished oscillatory activity in an animal model of schizophrenia. *J Neurosci* 29(8):2344–2354.
- Long SY (1972). Hair-nibbling and whisker-trimming as indicators of social hierarchy in mice. *Anim Behav* 20(1):10–12.
- Luukkonen TM, Pöyhönen M, Palotie A, Ellonen P, Lagström S, Lee JH et al. (2012). A balanced translocation truncates Neurotrimin in a family with intracranial and thoracic aortic aneurysm. *J Med Genet.* 49(10):621–9.
- Maccarrone G, Ditzen C, Yassouridis A, Rewerts C, Uhr M, Uhlen M et al. (2013). Psychiatric patient stratification using biosignatures based on cerebrospinal fluid protein expression clusters. *J Psychiatr Res* 47:1572–1580.
- MacMaster FP, Langevin LM, Jaworska N, Kemp A, Sembo M (2014). Corpus callosal morphology in youth with bipolar depression. *Bipolar Disord.* 16(8):889–93.
- Maillard AM, Ruef A, Pizzagalli F, Migliavacca E, Hippolyte L, Adaszewski S et al. (2015). The 16p11.2 locus modulates brain structures common to autism, schizophrenia and obesity. *Mol. Psychiatry* 20:140–147.
- Makowski L, Zhou C, Zhong Y, Kuan P F, Fan C, Sampey BP et al. (2014). Obesity increases tumor aggressiveness in a genetically engineered mouse model of serous ovarian cancer. *Gynecol Oncol* 133(1):90–97.
- Mann F, Zhukareva V, Pimenta A, Levitt P, Bolz J (1998). Membrane-associated molecules guide limbic and nonlimbic thalamocortical projections. *J Neurosci* 18: 9409–9419.

- Maruani A, Huguet G, Beggiato A, ElMaleh M, Toro R, Leblond CS et al. (2015). 11q24.2–25 micro-rearrangements in autism spectrum disorders: Relation to brain structures. *Am J Med Genet A* 167A(12):3019–3030.
- Mazitov T, Bregin A, Philips M A, Innos J, Vasar, E (2016). Deficit in emotional learning in Neurotrimin knockout mice. *Behav Brain Res* 28: 311–318.
- McNamee C J, Youssef S, Moss D (2011) IgLONs form heterodimeric complexes on forebrain neurons. *Cell Biochem Funct* 29: 114–119.
- McIntosh AL, Gormley S, Tozzi L, Frodl T, Harkin A (2017). Recent advances in translational magnetic resonance imaging in animal models of stress and depression. *Front Cell Neurosci* 11:150.
- Mistry M, Gillis J, Pavlidis P (2013). Genome-wide expression profiling of schizophrenia using a large combined cohort. *Mol. Psychiatry* 18(2): 215–225.
- Miyata S, Matsumoto N, Taguchi K, Akagi A, Iino T, Funatsu N, Maekawa S (2003). Biochemical and ultrastructural analyses of IgLON cell adhesion molecules, Kilon and OBCAM in the rat brain. *Neuroscience* 117: 645–658.
- Movsas TZ, Pinto-Martin JA, Whitaker AH, Feldman JF, Lorenz JM, Korzeniewski SJ et al. (2013). Autism Spectrum Disorder is associated with ventricular enlargement in a Low Birth Weight Population. *J Pediatr* 163(1):73–78.
- Munno DW & Syed N I (2003). Synaptogenesis in the CNS: an odyssey from wiring together to firing together. *J Physiol* 552(1): 1–11.
- Must A, Tasa G, Lang A, Vasar E, Kõks S, Maron E, Väli M (2008) Association of limbic system-associated membrane protein (LSAMP) to male completed suicide. *BMC Med Genetics* 9: 34.
- Mustard CJ, Whitfield PD, Megson IL, Wei J (2012). The effect of clozapine on the expression of obesity genes. *Eur Psychiatry* 27(1):1104.
- Ni H, Xu M, Zhan GL, Fan Y, Zhou H, Jiang HY et al. (2018). The GWAS Risk Genes for Depression May Be Actively Involved in Alzheimer's Disease. *J Alzheimers Dis* 64(4):1149–1161.
- Nicolson R, DeVito TJ, Vidal CN, Sui Y, Hayashi KM, Drost DJ, Williamson PC, Rajakumar N, Toga AW, Thompson PM (2006). Detection and mapping of hippocampal abnormalities in autism. *Psychiatry Res.* 148(1):11–2117056234.
- Noh K, Lee H, Choi TY, Joo Y, Kim SJ, Kim H et al. (2019) Negr1 controls adult hippocampal neurogenesis and affective behaviors. *Mol. Psychiatry*. [Epub ahead of print]
- Noordermeer SDS, Luman M, Greven CU, Veroude K, Faraone SV, Hartman CA et al. (2017). Structural brain abnormalities of attention-deficit/hyperactivity disorder with oppositional defiant disorder. *Biol Psychiatry* 82(9):642–650.
- Ntougkos E, Rush R, Scott D, Frankenberg T, Gabra H, Smyth J F et al. (2005). The IgLON family in epithelial ovarian cancer: expression profiles and clinicopathologic correlates. *Clin Cancer Res* 11:5764–5768.
- O'Doherty DC, Chitty KM, Saddiqui S, Bennett MR, Lagopoulos J. (2015). A systematic review and meta-analysis of magnetic resonance imaging measurement of structural volumes in posttraumatic stress disorder. *Psychiatry Res.* 232(1):1–33.
- Ogawa K, Utsunomiya T, Mimori K, Tanaka F, Haraguchi N, Inoue H, et al. (2006). Differential gene expression profiles of radioresistant pancreatic cancer cell lines established by fractionated irradiation. *Int J Oncol* 28(3):705–13.
- Pan Y, Wang K S, Aragam N (2010). NTM and NR3C2 polymorphisms influencing intelligence: family-based association studies. *Prog Neuropsychopharmacol Biol Psychiatry* 35(1):154–160.

- Panichareon B, Nakayama K, Thurakitwannakarn W, Iwamoto S, Sukhumsirichart W (2012). OPCML gene as a schizophrenia susceptibility locus in Thai population. *J Mol Neurosci*. 46(2):373–7.
- Park MTM, Raznahan A, Shaw P, Gogtay N, Lerch JP, Chakravarty MM (2018). Neuroanatomical phenotypes in mental illness: identifying convergent and divergent cortical phenotypes across autism, ADHD and schizophrenia. *J Psychiatry Neurosci* 43(2):170094.
- Pascal LE, Goo YA, Vêncio R Z, Page L S, Chambers A A, Liebeskind E S et al. (2009). Gene expression down-regulation in CD90+ prostate tumor-associated stromal cells involves potential organ-specific genes. *BMC Cancer* 9: 317.
- Paul LK, Schieffer B, Brown WS (2004). Social processing deficits in agenesis of the corpus callosum: Narratives from the Thematic Apperception Test. *Arch Clin Neuropsychol* 19:215–225.
- Persson A, Sim SC, Viriding S, Onishchenko N, Schulte G, Ingelman-Sundberg M (2014). Decreased hippocampal volume and increased anxiety in a transgenic mouse model expressing the human CYP2C19 gene. *Mol. Psychiatry* 19(6):733–41.
- Petryszak R, Burdett T, Fiorelli B et al. (2014). Expression Atlas update – a database of gene and transcript expression from microarray- and sequencing-based functional genomics experiments. *Nucleic Acids Res*. 42:D926–D932.
- Philips MA, Lilleväli K, Heinla I, Luuk H, Hundahl CA, Kongi K et al (2015). *Lsamp* is implicated in the regulation of emotional and social behavior by use of alternative promoters in the brain. *Brain Struct Funct* 220:1381–1393.
- Pimenta AF, Fischer I, Levitt P (1996a). cDNA cloning and structural analysis of the human limbic-system-associated membrane protein (LAMP). *Gene* 170: 189–195.
- Pimenta AF, Reinoso BS, Levitt P (1996b). Expression of the mRNAs encoding the limbic system-associated membrane protein (LAMP). II. Fetal rat brain. *J Comp Neurol* 375: 289–302.
- Pimenta AF, Zhukareva V, Barbe MF, Reinoso BS, Grimley C, Henzel W et al. (1995). The limbic system-associated membrane protein is an Ig superfamily member that mediates selective neuronal growth and axon targeting. *Neuron* 15(2):287–297.
- Pimenta AF and Levitt P (2004). Characterization of the genomic structure of the mouse limbic system-associated membrane protein (*Lsamp*) gene. *Genomics* 83: 790–801.
- Pina-Camacho L, Del Rey-Mejías Á, Janssen J, Bioque M, González-Pinto A, Arango C et al. (2016). Age at First Episode Modulates Diagnosis-Related Structural Brain Abnormalities in Psychosis. *Schizophr Bull*. 42(2): 344–357.
- Pischedda F, Szczerkowska J, Cîrnaru M D, Giesert F, Vezzoli E, Ueffing M, et al (2014). A cell surface biotinylation assay to reveal membrane-associated neuronal cues: *negrl* regulates dendritic arborization. *Mol Cell Proteomics* 13: 733–748.
- Pletnikov MV, Ayhan Y, Nikolskaia O, Xu Y, Ovanesov MV, Huang H et al. (2008). Inducible expression of mutant human *DISC1* in mice is associated with brain and behavioral abnormalities reminiscent of schizophrenia. *Mol. Psychiatry* 13(2):173–186.
- Poplawski GHD, Lie R, Hunt M, Kumamaru H, Kawaguchi R, Lu P et al. (2018). Adult rat myelin enhances axonal outgrowth from neural stem cells. *Sci Transl Med*. 10 (442).
- Qiu S, Champagne D L, Peters M, Catania E H, Weeber E J, Levitt P et al. (2010). Loss of limbic system-associated membrane protein leads to reduced hippocampal

- mineralocorticoid receptor expression, impaired synaptic plasticity, and spatial memory deficit. *Biol Psychiatry* 68: 197–204.
- Raghavan NS, Vardarajan B, Mayeux R (2019). Genomic variation in educational attainment modifies Alzheimer disease risk. *Neurol Genet.* 5(2):e310.
- Ranaivoson FM, Turk LS, Ozgul S, Kakehi S, von Daake S, Lopez N et al. (2019). A Proteomic Screen of Neuronal Cell-Surface Molecules Reveals IgLONs as Structurally Conserved Interaction Modules at the Synapse. *Structure.* pii: S0969–2126(19)30082–6.
- Reed J, McNamee C, Rackstraw S, Jenkins J, Moss D (2004). Diglons are heterodimeric roteins composed of IgLON subunits, and diglon-CO inhibits neurite outgrowth from cerebellar granule cells. *J Cell Sci* 117: 3961–3973.
- Reinoso BS, Pimenta AF, Levitt P (1996). Expression of the mRNAs encoding the limbic system-associated membrane protein (LAMP). I. Adult rat brain. *J Comp Neurol* 375: 274–288.
- Ring HA, Serra-Mestres J (2002). Neuropsychiatry of the basal ganglia. *J Neurol Neurosurg Psychiatry* 72:12–21.
- Ripke S, Neale BM, Corvin A, Walters JT, Farh KH, Holmans PA et al. (2014). Biological insights from 108 schizophrenia-associated genetic loci. *Nature* 511:421–427.
- Roger B, Al-Bassam J, Dehmelt L, Milligan RA, Halpain S (2004). MAP2c, but not tau, binds and bundles F-actin via its microtubule binding domain. *Curr Biol* 14(5):363–71.
- Rosenberg DR, Keshavan MS, O’Hearn KM, Dick EL, Bagwell WW, Seymour AB et al. (1997). Frontostriatal measurement in treatment-naive children with obsessive-compulsive disorder. *Arch Gen Psychiatry.* 54(9):824–830.
- Rubin RD, Watson PD, Duff MC, Cohen NJ (2014). The role of the hippocampus in flexible cognition and social behavior. *Front in Hum Neurosci* 8:742.
- Sabater L, Gaig C, Gelpi E, Bataller L, Lewerenz J, Torres-Vega E et al. (2014). A novel non-rapid-eye movement and rapid-eye-movement parasomnia with sleep breathing disorder associated with antibodies to IgLON5: a case series, characterisation of the antigen, and post-mortem study. *Lancet Neurol* 13(6):575–86.
- Salzer JL, Rosen CL, Struyk AF (1996). GPI-anchored proteins in neural cell adhesion. In: C DR, editor. *Advences in Molecular and Cellular Biology. Cell adhesion* Greenwich, CT: 193–222.
- Sanz R, Ferraro G B, Fournier A E (2015). IgLON cell adhesion molecules are shed from the cell surface of cortical neurons to promote neuronal growth. *J Biol Chem* 290: 4330–4342.
- Sarna JR, Dyck RH, Whishaw IQ (2000). The Dalila effect: C57BL6 mice barber whiskers by plucking. *Behav Brain Res* 108:39–45.
- Sauer JF, Strüber M, Bartos M (2015). Impaired fast-spiking interneuron function in a genetic mouse model of depression. *eLife* 4: e04979.
- Sauvage C, Jissendi P, Seignan S, Manto M, Habas C (2013). Brain areas involved in the control of speed during a motor sequence of the foot: real movement versus mental imagery. *J Neuroradiol.* 40(4): 267–280.
- Schäfer M, Bräuer AU, Savaskan NE, Rathjen FG, Brümmendorf T (2005). Neurotractin/kilon promotes neurite outgrowth and is expressed on reactive astrocytes after entorhinal cortex lesion. *Mol Cell Neurosci* 29:580–590.

- Schechtman E, Noblejas MI, Mizrahi AD, Dauber O, Bergman H (2016). Pallidal spiking activity reflects learning dynamics and predicts performance. *Proc Natl Acad Sci U S A* 113 (41):E6281–E6289.
- Schmaal L, Hibar DP, Sämann PG, Hall GB, Baune BT, Jahanshad N et al. (2017). Cortical abnormalities in adults and adolescents with major depression based on brain scans from 20 cohorts worldwide in the ENIGMA Major Depressive Disorder Working Group. *Mol. Psychiatry* 22: 900–909.
- Schmidt E R, Brignani S, Adolfs Y, Lemstra S, Demmers J, Vidaki M et al. (2014). Subdomain-mediated axon-axon signaling and chemoattraction cooperate to regulate afferent innervation of the lateral habenula. *Neuron* 83(2):372–87.
- Scott ML, Golden CJ, Ruedrich SL, Bishop RJ (1983). Ventricular enlargement in major depression. *Psychiatry Res* 8(2):91–93.
- Schofield P R, McFarland K C, Hayflick JS, Wilcox J N, Cho TM, Roy S, et al. (1989). Molecular characterization of a new immunoglobulin superfamily protein with potential roles in opioid binding and cell contact. *EMBO J.* 8: 489–495.
- Sellar G C, Watt K P, Rabiasz G J, Stronach EA, Li L, Miller EP et al. (2003). OPCML at 11q25 is epigenetically inactivated and has tumor suppressor function in epithelial ovarian cancer. *Nat Genet.* 34: 337–343.
- Sharma K, Schmitt S, Bergner CG, Tyanova S, Kannaiyan N, Manrique-Hoyos N et al. (2015). Cell type- and brain region-resolved mouse brain proteome. *Nat Neurosci* 18: 1819–1831.
- Shen S, Lang B, Nakamoto C, Zhang F, Pu J, Kuan S et al. (2008). Schizophrenia-related neural and behavioral phenotypes in transgenic mice expressing truncated Disc1. *J Neurosci* 28(43):10893–10904.
- Shepherd AM, Quidé Y, Laurens KR, O'Reilly N, Rowland JE, Mitchell PB, Carr VJ, Green MJ (2015). Shared intermediate phenotypes for schizophrenia and bipolar disorder: neuroanatomical features of subtypes distinguished by executive dysfunction. *J Psychiatry Neurosci.* 40(1):58–68.
- Sniekers S, Stringer S, Watanabe K, Jansen PR, Coleman JRI, Krapohl E et al. (2017). Genome-wide association meta-analysis of 78,308 individuals identifies new loci and genes influencing human intelligence. *Nat Genet* 49:1558.
- Speliotes EK, Willer CJ, Berndt SI, Monda KL, Thorleifsson G, Jackson AU et al. (2010). Association analyses of 249,796 individuals reveal 18 new loci associated with body mass index. *Nat Genet* 42:937–948.
- Steullet P, Cabungcal JH, Bukhari SA, Ardelt MI, Pantazopoulos H et al. (2017). The thalamic reticular nucleus in schizophrenia and bipolar disorder: role of parvalbumin-expressing neuron networks and oxidative stress. *Mol. Psychiatry* 1–9.
- Strozik E & Festing MF (1981). Whisker trimming in mice. *Lab Anim* 15:309–312.
- Struyk A F, Canoll P D, Wolfgang M J, Rosen C L, D'Eustachio P, Salzer J L (1995). Cloning of Ntm defines a new subfamily of differentially expressed neural cell adhesion molecules. *J Neurosci* 15: 2141–2156.
- Sugimoto C, Maekawa S, Miyata S (2010). OBCAM, an immunoglobulin superfamily cell adhesion molecule, regulates morphology and proliferation of cerebral astrocytes. *J Neurochem.* 112: 818–828.
- Swayze VW, II, Andreasen NC, Alliger RJ, Ehrhardt JC, Yuh WT (1990). Structural brain abnormalities in bipolar affective disorder. Ventricular enlargement and focal signal hyperintensities. *Arch. Gen. Psychiatry.* 47:1054–1059.

- Szczurkowska J, Pischedda F, Pinto B, Managò F, Haas CA, Summa M et al. (2018). NEGR1 and FGFR2 cooperatively regulate cortical development and core behaviours related to autism disorders in mice. *Brain* 141(9): 2772–2794.
- Takamori S, Holt M, Stenius K, Lemke EA, Grønborg M, Riedel D et al. (2006). Molecular anatomy of a trafficking organelle. *Cell* 127:831–846.
- Tan RPA, Leshchyns'ka I, Sytnyk V (2017). Glycosylphosphatidylinositol- anchored immunoglobulin superfamily cell adhesion molecules and their role in neuronal development and synapse regulation. *Front Mol Neurosci* 10:378.
- Tamási V, Petschner P, Adori C, Kirilly E, Ando RD, Tothfalusi L et al. (2014). Transcriptional evidence for the role of chronic venlafaxine treatment in neurotrophic signaling and neuroplasticity including also glutamatergic- and insulin-mediated neuronal processes. *PLOS ONE* 9:e113662.
- Tassano E, Gamucci A, Celle ME, Ronchetto P, Cuoco C, Gimelli G (2015). Clinical and molecular cytogenetic characterization of a de novo interstitial 1p31.1p31.3 deletion in a boy with moderate intellectual disability and severe language impairment. *Cytogenet Genome Res* 146:39–43.
- Thorleifsson G, Walters GB, Gudbjartsson DF, Steinthorsdottir V, Sulem P, Helgadóttir A et al. (2009). Genome-wide association yields new sequence variants at seven loci that associate with measures of obesity. *Nat Genet* 41:18–24.
- Togashi H, Sakisaka T, Takai Y (2009). Cell adhesion molecules in the central nervous system. *Cell Adh. Migr.* 3(1): 29–35.
- Torres G, Meeder BA, Hallas BH, Sperryak JA, Mazurchuk R, Jones C et al. (2005). Ventricular size mapping in a transgenic model of schizophrenia. *Brain Res Dev Brain Res.* 154: 35–44.
- Turner TN, Hormozdiari F, Duyzend MH, McClymont SA, Hook PW, Iossifov I et al. (2016). Genome Sequencing of Autism-Affected Families Reveals Disruption of Putative Noncoding Regulatory DNA. *Am J Hum Genet.* 98(1):58–74.
- Uchida T, Furukawa T, Iwata S, Yanagawa Y, Fukuda A (2014). Selective loss of parvalbumin positive GABAergic interneurons in the cerebral cortex of maternally stressed Gad1 heterozygous mouse offspring. *Transl Psychiatry* 4: e371.
- Van den Buuse M (2010). Modeling the positive symptoms of schizophrenia in genetically modified mice: pharmacology and methodology aspects. *Schizophr. Bull.* 36: 246–27.
- Van Erp TGM, Hibar DP, Rasmussen JM, Glahn DC, Pearlson GD, Andreassen OA et al. (2016). Subcortical brain volume abnormalities in 2028 individuals with schizophrenia and 2540 healthy controls via the ENIGMA consortium. *Mol. Psychiatry* 21:547–553.
- Vanaveski T, Singh K, Narvik J, Eskla K-L, Visnapuu T, Heinla I et al. (2017). Promoter-Specific Expression and Genomic Structure of IgLON Family Genes in mouse. *Front Neurosci* 11:38.
- Vawter P M (2000). Dysregulation of the neural cell adhesion molecule and neuropsychiatric disorders. *Eur. J. Pharmacol.* 405 (1–3): 385–395.
- Veerappa AM, Saldanha M, Padakannaya P, Ramachandra NB (2013). Family-based genome-wide copy number scan identifies five new genes of dyslexia involved in dendritic spinal plasticity. *J Hum Genet* 58:539–547.
- Velásquez E, Nogueira F C S, Velásquez I, Schmitt A, Falkai P, Domont G B et al. (2017). Synaptosomal proteome of the orbitofrontal cortex from schizophrenia patients using quantitative label-free and iTRAQ-based shotgun proteomics. *J. Proteome Res.* 16: 4481–4494.

- Vidal CN, Nicolson R, DeVito TJ, Hayashi KM, Geaga JA, Drost DJ et al. (2006). Mapping corpus callosum deficits in autism: an index of aberrant cortical connectivity. *Biol Psychiatry*. 60(3):218–225.
- Wang J, Jiang T, Cao Q, Wang Y (2007). Characterizing anatomic differences in boys with attention-deficit/hyperactivity disorder with the use of deformation-based morphometry. *AJNR Am J Neuroradiol* 28:543–547.
- Wang T, Zhang X, Li A, Zhu M, Liu S, Qin W et al. (2017). Polygenic risk for five psychiatric disorders and cross-disorder and disorder-specific neural connectivity in two independent populations. *Neuroimage Clin* 14:441–449.
- Westwood S, Liu B, Baird AL, Anand S, Nevado-Holgado AJ, Newby D et al. (2017). The influence of insulin resistance on cerebrospinal fluid and plasma biomarkers of Alzheimer's pathology. *Alzheimers Res Ther* 9(1):31.
- Wise T, Radua J, Via E, Cardoner N, Abe O, Adams TM et al. (2017). Common and distinct patterns of grey-matter volume alteration in major depression and bipolar disorder: evidence from voxel-based meta-analysis. *Mol. Psychiatry* 22(10):1455–1463.
- Wood GK, Tomasiewicz H, Rutishauser U, Magnuson T, Quirion R, Rochford J, Srivastava LK (1998). NCAM-180 knockout mice display increased lateral ventricle size and reduced prepulse inhibition of startle. *Neuroreport*. 9(3):461–466.
- Yamada M, Hashimoto T, Hayashi N, Higuchi M, Murakami A, Nakashima T et al. (2007). Synaptic adhesion molecule OBCAM; synaptogenesis and dynamic internalization. *Brain Res* 1165: 5–14.
- Yan Z, Kim E, Datta D, Lewis DA, Soderling S H (2016). Synaptic Actin Dysregulation, a Convergent Mechanism of Mental Disorders? *J. Neurosci* 36(45): 11411–11417.
- Zacco A, Cooper V, Chantler P D, Fisher-Hyland S, Horton HL, and Levitt P (1990). Isolation, biochemical characterization and ultrastructural analysis of the limbic system associated membrane protein (LAMP), a protein expressed by neurons comprising functional neural circuits. *J. Neurosci* 10: 73–90.
- Zanini E, Louis LS, Antony J, Karali E, Okon IS, McKie AB et al. (2017). The Tumor-Suppressor Protein OPCML Potentiates Anti-EGFR- and Anti-HER2-Targeted Therapy in HER2-Positive Ovarian and Breast Cancer. *Mol Cancer Ther*. 16(10): 2246–2256.
- Zhang Y, Chen K, Sloan SA et al. (2014). An RNA-sequencing transcriptome and splicing database of glia, neurons, and vascular cells of the cerebral cortex. *J. Neurosci* 34:11929–11947.
- Zhang X, Hu X, Lei H, Hu J, Zhang Y (2016). Mechanical force-induced polymerization and depolymerization of F-actin at water/solid interfaces. *Nanoscale* 8(11): 6008–13.
- Zhang H, Kang E, Wang Y, Yang C, Yu H, Wang Q et al. (2016). Brain-specific Crmp2 deletion leads to neuronal development deficits and behavioural impairments in mice. *Nat Commun* 7:11773.
- Zhukareva VV, Cherevskaya N, Pimenta A, NowyckyM, Levitt P (1997). Limbic system-associated membrane protein (LAMP) induces neurite outgrowth and intracellular Ca²⁺ increase in primary fetal neurons. *Mol Cell Neurosci* 10: 43–55.
- Zubenko GS, Hughes HB, Jordan RM, Lyons-Weiler J, Cohen BM (2014). Differential hippocampal gene expression and pathway analysis in an etiology-based mouse-model of major depressive disorder. *Am J Med Genet B Neuropsychiatr Genet* 165B (6):457–466.

SUMMARY IN ESTONIAN

Neuropsühhiaatriliste endofenotüüpide seos IgLON adhesioonimolekulidega hiire aju

Psühhiaatriliste häirete multifaktoriaalse patogeneesi mõistmine on suur väljakutse. Neuropsühhiaatriliste häirete modelleerimine loomudelites annab võimaluse uurida, kuidas närviringete düsfunktsionaalsus põhjustab patoloogiliste fenotüüpide avaldumist. Erinevad ülegenoomsed assotsiatsiooniuuringud (GWAS) ning ekspressiooniuringud on näidanud IgLON perekonda kuuluvate adhesioonimolekulide (*Lsamp*, *Ntm*, *Opcml*, *Negr1*, *IgLON 5*) seost inimese neuropsühhiaatriliste häiretega ning käitumiskatsed *Lsamp* ja *Ntm* puudulike hiirtega on näidanud IgLON molekulide osalust emotsionaalse ja sotsiaalse käitumise kujunemises. Funktsionaalsed uuringud on näidanud, et IgLON valgud osalevad närviringete kujunemisel ja toimimisel nii arenevas kui ka täiskasvanud aju. On teada, et tsütoskeleti dünaamilised ümberkorraldused arenevates neuronites on aluseks neuraalsete ringete kujunemisele, kuid IgLON perekonna molekulide roll arenevate neuronite tsütoskeleti reguleerimises on olnud siiani teadmata.

Käesoleva töö eesmärk oli selgitada *Lsamp* ja *Ntm* vaheliste vastastoitmete ja *Negr1* mõju aju struktuurile ja funktsioonidele, kasutades vastavate geenide suhtes mutantseid hiiremudeleid. Analüüsisime neuropsühhiaatriliste häiretega seotud morfoloogilisi, anatoomilisi ja käitumuslikke parameetreid *Lsamp*^{-/-}, *Ntm*^{-/-}, *Lsamp*^{-/-}*Ntm*^{-/-} ja *Negr1*^{-/-} hiirtes. Mitmetasandiline lähenemine aitab selgitada, kuidas aju struktuursed kõrvalekalded mõjutavad käitumist. Näitasime, et *Lsamp* ja *Ntm* mõjutavad varajast neuriitide väljakasvu ja rakkude jagunemist ning apoptoosi teineteisest sõltuvalt ning samasugused vastasmõjud on jälgitavad ka mutanthiirte käitumuslikes reaktsioonides. Leidsime, et *Negr1*^{-/-} hiirtel on kõrvalekalded neuritogeneesis, neuroanatomias ja et nende hipokampuses on vähem inhibitoorseid neuroneid, mis võivad olla sellele hiireliinile iseloomuliku puuduliku sotsiaalse ja tunnetusliku käitumise põhjuseks. Lisaks näitavad käesoleva väitekirja tulemused, et IgLON adhesioonimolekulide toime võib olla sõltumatu rakkudevahelisest adhesioonist.

Meie uurimistulemused aitavad mõista, kuidas IgLON adhesioonivalgud, mille geenipiirkonnad on olulised riskilookused paljudele psühhiaatrilistele häiretele, reguleerivad närviringete kujunemist, mõjutades neuronite morfoloogiat ja omadusi ning aju anatoomiat. Neid neuronaalseid muutusi, mis seostuvad muutustega käitumises, võib vaadata kui psühhiaatriliste häiretega seotud endofenotüüpe. Oleme näidanud erinevate IgLON puudulikkusega hiiremudelite sobivust psühhiaatriliste häirete modelleerimiseks ning nende mudelite edasine uurimine aitab neuropsühhiaatriliste häirete kujunemist paremini mõista.

ACKNOWLEDGEMENT

This thesis owes its existence to the help, support and inspiration of several people. Firstly, I would like to express my sincere appreciation and gratitude to my supervisor Mari-Anne Philips, who found me apt for this PhD work and invited me to Tartu. She has been a constant source of encouragement and enthusiasm, during this Ph.D. project. Thank you for being my mentor, ally, friend, and for all the discussions we have shared throughout this journey, both academic and non-academic. My greatest gratitude goes to my co-supervisor Kersti Lilleväli who was always available to answer my questions on a daily basis, however great or stupid they may have been and for constantly guiding me at work and overcome the challenges in the personal front. I am also greatly indebted to my co-supervisor Eero Vasar for his valuable guidance during my research. His support and inspiring suggestions have been precious for the development of this thesis. Without all of you, this thesis would not have been possible.

I am very thankful to all of my colleagues from Department of Physiology. Thank you for making every day a great day academically. I am also grateful to my collaborators especially Scott Gilbert (Swarthmore College), Mart Rahi (The Estonian University of Life Sciences), Michael E Schäfer (Johannes Gutenberg-University Mainz), and all the members of Allen Kaasik Lab, Department of Pharmacology, University of Tartu, for always being enthusiastic and for letting me use their facility. I would also like to thank internal reviewers for giving insight look into this thesis.

My deepest gratitude goes to my family and friends who have always been there for me. I would like to thank ChandraShekhar for introducing me to Mari-Anne and without that this could have never been possible. Thanks Chandra for always being such a nice and supporting friend. I am also very thankful to our Indian community at Tartu for making me feel homely even far away from home country. Thanks for all the group parties, festivals, delicious food and chit chat we have shared together.

Most importantly, I would like to thanks my parents Shri S. P. Singh and Smt. Pushpa Singh for showering all their love, care, support throughout my life, and for raising me to become an inquisitive person. You two are truly my biggest strength and guide. Special thanks go to Manisha, Snigdha, Rupesh, Gautam, Manashwi, Aalya and Shambhawi for their love, cherishing and stimulating positive family values. I also want to thank my in-laws Smt. Rathnamma, Shri H. Jayaram, Smt. J. Jayalakshmi and Karthik for their support, care and encouragement to pursue my dreams. Last but not the least, I would like to express my deepest appreciation to my beloved husband Mohan Jayaram for his unconditional love, support, patience, and for always putting the extra into ordinary.

Finally, my heartiest thanks for the mice which have been sacrificed for this research work, without them this work would not have been possible.

Above all else, I would like to express my deepest gratitude and regards to Almighty who has been with me at every moment.

PUBLICATIONS

CURRICULUM VITAE

Name: Katyayani Singh
Date of Birth: February 20, 1983
Address: Department of Physiology,
Ravila19, 50411 Tartu, Estonia
Telephone: +372 5845 7000
E-mail: singhkat@ut.ee, katyayani.micro@gmail.com

Education:

1998 10th from CBSE board, Kendriya Vidyalaya no-2, Gaya, India.
2000 12th from CBSC board, Kendriya Vidyalaya no-2, Gaya, India.
2002–2006 B. Sc in Microbiology with Honors, Allahabad Agricultural
University, India.
2006–2008 M.Sc. in Applied Microbiology, Vellore Institute of Techno-
logy, India.
2009–2011 M.Phil in NeuroScience, National Institute of Mental Health
and Neurosciences (NIMHANS), Bangalore India.
2014–2019 Doctoral studies in Neurosciences, University of Tartu, Faculty
of Medicine, Estonia

Career:

2007–2009 Project assistant (1,00), Department of Neuroimmunology,
NIMHANS, India
2011–2012 Research scholar (1,00) Institute of Cell Biology, University of
Bern, Switzerland.
2013–2014 Project assistant (1,00), Centre for Nano Science &
Engineering, Indian Institute of Sciences, India.
2018- Junior Researcher (0,5), Institute of Biomedicine and
Translational Medicine, University of Tartu, Estonia.

Professional training and meetings

2009 36th Annual Conference of Indian Immunology Society, NIMHANS,
India. (Oral presentation).
2010 Indo- French Symposium on “Recent Trends in Brain Tumor Treatments
and Research”, NIMHANS, India.
2011 Course on Cutting edge Microscopy at Microscopy Imaging Centre,
University of Bern, Switzerland.
2012 Training course on “Education and Training of Persons conducting
Animal Experiments, University of Zurich, Switzerland.
2015 Scientific discussion meeting on “Release of Chemical transmitters from
cell bodies and dendrites of nerve cells” at the Royal Society London,
UK.

- 2016 Workshop on Behavioral phenotyping of rodent disease models – Potential and Pitfalls, University of Tartu, Estonia.
- 2017 Cortical development Conference – Neural stem cells to neural circuits, Chania, Greece (Poster).
- 2018 5th International Seminar on Behavioral Methods, Krakow, Poland (Poster).
- 2019 EMBO Workshop on Molecular neuroscience: From genes to circuits in health disease, Bangalore, India (Poster).

List of Publications:

1. **Singh K***, Jayaram M, Kaare M, Leidmaa E, Jagomäe T, Heinla I, Hickey M A, Kaasik A, Schäfer, MKE, Innos J, Lilleväli K, Philips MA, Vasar E (2019). Neural cell adhesion molecule *Negr1* deficiency in mouse results in structural brain endophenotypes and behavioral deviations related to psychiatric disorders. *Scientific Reports*, 9(1), 5457. doi: 10.1038/s41598-019-41991-8.
2. **Singh K**, Lilleväli K, Gilbert SF, Bregin A, Narvik J, Jayaram M, Rahi M, Innos J, Kaasik A, Vasar E, Philips MA (2018). The combined impact of IgLON family proteins *Lsamp* and *Neurotrimin* on developing neurons and behavioral profiles in mouse. *Brain Research Bulletin*, 140, 5–18. doi: 10.1016/j.brainresbull.2018.03.013.
3. **Singh K**, Loreth D, Pottker B, Hefti K, Innos J, Schwald K, Hengstler H, Menzel L, Sommer CJ, Radyushkin K, Kretz O, Philips MA, Haas CA, Frauenknecht K, Lilleväli K, Heimrich B, Vasar E, Schäfer MKE (2018). Neuronal Growth and Behavioral Alterations in Mice Deficient for the Psychiatric Disease-Associated *Negr1* Gene. *Frontiers in Molecular Neuroscience*, 11 (30), 1–14. doi: 10.3389/fnmol.2018.00030.
4. Vanaveski T, **Singh K**, Narvik J, Eskla KL, Visnapuu T, Heinla I, Jayaram M, Innos J, Lilleväli K, Philips MA, Vasar E (2017). Promoter-Specific Expression and Genomic Structure of IgLON Family Genes in Mouse. *Frontiers in Neuroscience*, 11 (38), 1–15. doi: 10.3389/fnins.2017.00038.
5. Heinla I, Leidmaa E, Kongi K, Pennert A, Innos J, Nurk K, Tekko T, **Singh K**, Vanaveski T, Reimets R, Mandel M, Lang A, Lilleväli K, Kaasik A, Vasar E, Philips MA (2015). Gene expression patterns and environmental enrichment-induced effects in the hippocampi of mice suggest importance of *Lsamp* in plasticity. *Frontiers in Neuroscience*, 9 (205), 1–8. doi: 10.3389/fnins.2015.00205.
6. George JB, Abraham GM, **Singh K**, Ankolekar SM, Amrutur B, Sikdar SK (2014). Input coding for neuro-electronic hybrid systems. *Biosystems*, 126, 1–11. doi: 10.1016/j.biosystems.2014.08.002.
7. Saxena S, Roselli F, **Singh K**, Leptien K, Julien JP, Gros-Louis F, Caroni P. (2013). Neuroprotection through Excitability and mTOR Required in ALS Motoneurons to Delay Disease and Extend Survival. *Neuron*, 80(1),80–96. doi: 10.1016/j.neuron.2013.07.027.

8. Patil SA, **Katyayani S**, Sood A, Kavitha AK, Marimuthu P, Taly AB (2013). Possible significance of anti-heat shock protein (HSP-65) antibodies in autoimmune myasthenia gravis. *Journal of neuroimmunology*, 257 (1–2), 107–109. doi: 10.1016/j.jneuroim.2013.02.001.
9. Patil S A, **Katyayani S**, Arvind N (2012). Significance of antibody detection in the diagnosis of cryptococcal meningitis. *Journal of immunoassay & immunochemistry*, 33 (2), 140–148. doi: 10.1080/15321819.2011.606862.

ELULOOKIRJELDUS

Nimi: Katyayani Singh
Sünniaeg: 20. veebruar 1983
Aadress: Department of Physiology,
Ravila19, 50411 Tartu, Estonia
Telefon: +372 5845 7000
E-mail: singhkat@ut.ee, katyayani.micro@gmail.com

Haridustee:

1998 10th from CBSE board, Kendriya Vidyalaya no-2, Gaya, India.
2000 12th from CBSC board, Kendriya Vidyalaya no-2, Gaya, India.
2002–2006 B. Sc in Microbiology with Honors, Allahabad Agricultural
University, India.
2006–2008 M.Sc. in Applied Microbiology, Vellore Institute of Technology,
India.
2009–2011 M.Phil in NeuroScience, National Institute of Mental Health and
Neurosciences (NIMHANS), Bangalore India.
2014–2019 Tartu Ülikool, Arstiteaduste valdkond, neuroteaduste doktorantuur

Teenistuskäik:

2007–2009 Project assistant (1,00), Department of Neuroimmunology,
NIMHANS, India
2011–2012 Research scholar (1,00) Institute of Cell Biology, University of
Bern, Switzerland.
2013–2014 Project assistant (1,00), Centre for Nano Science & Engineering,
Indian Institute of Sciences, India.
2018– Noorem teadur (0,5), Institute of Biomedicine and Translational
Medicine, University of Tartu, Estonia.

Erialane enesetäiendus:

2009 36th Annual Conference of Indian Immunology Society, NIMHANS,
India. (Oral presentation).
2010 Indo- French Symposium on “Recent Trends in Brain Tumor
Treatments and Research”, NIMHANS, India.
2011 Course on Cutting edge Microscopy at Microscopy Imaging Centre,
University of Bern, Switzerland.
2012 Training course on “Education and Training of Persons conducting
Animal Experiments, University of Zurich, Switzerland.
2015 Scientific discussion meeting on “ Release of Chemical transmitters
from cell bodies and dendrites of nerve cells” at the Royal Society
London, UK.
2016 Workshop on Behavioral phenotyping of rodent disease models-
Potential and Pitfalls, Tartu Ülikool, Estonia.

- 2017 Cortical development Conference – Neural stem cells to neural circuits, Chania, Greece (Poster).
- 2018 5th International Seminar on Behavioral Methods, Krakow, Poland (Poster).
- 2019 EMBO Workshop on Molecular neuroscience: From genes to circuits in health disease, Bangalore, India (Poster).

Publikatsioonid:

1. **Singh K***, Jayaram M, Kaare M, Leidmaa E, Jagomäe T, Heinla I, Hickey M A, Kaasik A, Schäfer, MKE, Innos J, Lilleväli K, Philips MA, Vasar E (2019). Neural cell adhesion molecule *Negr1* deficiency in mouse results in structural brain endophenotypes and behavioral deviations related to psychiatric disorders. *Scientific Reports*, 9(1), 5457. doi: 10.1038/s41598-019-41991-8.
2. **Singh K**, Lilleväli K, Gilbert SF, Bregin A, Narvik J, Jayaram M, Rahi M, Innos J, Kaasik A, Vasar E, Philips MA (2018). The combined impact of IgLON family proteins Lsamp and Neurotrimin on developing neurons and behavioral profiles in mouse. *Brain Research Bulletin*, 140, 5–18. doi: 10.1016/j.brainresbull.2018.03.013.
3. **Singh K**, Loreth D, Pottker B, Hefti K, Innos J, Schwald K, Hengstler H, Menzel L, Sommer CJ, Radyushkin K, Kretz O, Philips MA, Haas CA, Frauenknecht K, Lilleväli K, Heimrich B, Vasar E, Schäfer MKE (2018). Neuronal Growth and Behavioral Alterations in Mice Deficient for the Psychiatric Disease-Associated *Negr1* Gene. *Frontiers in Molecular Neuroscience*, 11 (30), 1–14. doi: 10.3389/fnmol.2018.00030.
4. Vanaveski T, **Singh K**, Narvik J, Eskla KL, Visnapuu T, Heinla I, Jayaram M, Innos J, Lilleväli K, Philips MA, Vasar E (2017). Promoter-Specific Expression and Genomic Structure of IgLON Family Genes in Mouse. *Frontiers in Neuroscience*, 11 (38), 1–15. doi: 10.3389/fnins.2017.00038.
5. Heinla I, Leidmaa E, Kongi K, Pennert A, Innos J, Nurk K, Tekko T, **Singh K**, Vanaveski T, Reimets R, Mandel M, Lang A, Lilleväli K, Kaasik A, Vasar E, Philips MA (2015). Gene expression patterns and environmental enrichment-induced effects in the hippocampi of mice suggest importance of Lsamp in plasticity. *Frontiers in Neuroscience*, 9 (205), 1–8. doi: 10.3389/fnins.2015.00205.
6. George JB, Abraham GM, **Singh K**, Ankolekar SM, Amrutur B, Sikdar SK (2014). Input coding for neuro-electronic hybrid systems. *Biosystems*, 126, 1–11. doi: 10.1016/j.biosystems.2014.08.002.
7. Saxena S, Roselli F, **Singh K**, Leptien K, Julien JP, Gros-Louis F, Caroni P. (2013). Neuroprotection through Excitability and mTOR Required in ALS Motoneurons to Delay Disease and Extend Survival. *Neuron*, 80(1),80–96. doi: 10.1016/j.neuron.2013.07.027.
8. Patil SA, **Katyayani S**, Sood A, Kavitha AK, Marimuthu P, Taly AB (2013). Possible significance of anti-heat shock protein (HSP-65) antibodies

in autoimmune myasthenia gravis. *Journal of neuroimmunology*, 257 (1-2), 107–109. doi: 10.1016/j.jneuroim.2013.02.001.

9. Patil S A, **Katyayani S**, Arvind N (2012). Significance of antibody detection in the diagnosis of cryptococcal meningitis. *Journal of immunoassay & immunochemistry*, 33 (2), 140–148. doi: 10.1080/15321819.2011.606862.

DISSERTATIONES NEUROSCIENTIAE UNIVERSITATIS TARTUENSIS

1. **Sirli Raud.** Cholecystokinin₂ receptor deficient mice: changes in function of GABA-ergic system. Tartu, 2005.
2. **Kati Koido.** Single-nucleotide polymorphism profiling of 22 candidate genes in mood and anxiety disorders. Tartu, 2005.
3. **Dzhamilja Safulina.** The studies of mitochondria in cultured cerebellar granule neurons: characterization of mitochondrial function, volume homeostasis and interaction with neurosteroids. Tartu, 2006.
4. **Tarmo Areda.** Behavioural and neurogenetic study of mechanisms related to cat odour induced anxiety in rodents. Tartu, 2006.
5. **Aleksei Nelovkov.** Behavioural and neurogenetic study of molecular mechanisms involved in regulation of exploratory behaviour in rodents. Tartu, 2006.
6. **Annika Vaarmann.** The studies on cystatin B deficient mice: neurochemical and behavioural alterations in animal model of progressive myoclonus epilepsy of Unverricht-Lundborg type. Tartu, 2007.
7. **Urho Abramov.** Sex and environmental factors determine the behavioural phenotype of mice lacking CCK₂ receptors: implications for the behavioural studies in transgenic lines. Tartu, 2008.
8. **Hendrik Luuk.** Distribution and behavioral effects of WFS1 protein in the central nervous system. Tartu, 2009.
9. **Anne Must.** Studies on molecular genetics of male completed suicide in Estonian population. Tartu, 2009.
10. **Kaido Kurrikoff.** Involvement of cholecystokinin in chronic pain mechanisms and endogenous antinociception. Tartu, 2009.
11. **Anu Aonurm-Helm.** Depression-like phenotype and altered intracellular signalling in neural cell adhesion molecule (NCAM)-deficient mice. Tartu, 2010.
12. **Silva Sütt.** Role of endocannabinoid system and *Wfs1* in regulation of emotional behaviour: behavioural, pharmacological and genetic studies. Tartu, 2010.
13. **Mari-Anne Philips.** Characterization of *Myg1* gene and protein: expression patterns, subcellular localization, gene deficient mouse and functional polymorphisms in human. Tartu, 2010.
14. **Ranno Rätsep.** Genetics of psoriasis and vitiligo, focus on IL10 family cytokines. Tartu, 2010.
15. **Kairit Joost.** Selective screening of metabolic diseases in Estonia: the application of new diagnostic methods. Tartu, 2012, 143 p.
16. **Monika Jürgenson.** A complex phenotype in mice with partial or complete deficiency of the NCAM protein. Tartu, 2012, 117 p.

17. **Ene Reimann.** Description of the cytokines and cutaneous neuroendocrine system in the development of vitiligo. Tartu, 2012, 117 p.
18. **Jürgen Innos.** Behavioural, pharmacological and neurochemical characterisation of limbic system-associated membrane protein (LSAMP) deficient mice. Tartu, 2013, 113 p.
19. **Kaili Anier.** The role of DNA methylation in the development of cocaine-induced behavioural sensitisation. Tartu, 2013, 147 p.
20. **Maarika Liik.** Cognitive functioning, perceived cognition, subjective complaints and symptoms of depression in patients with epilepsy: neuropsychological assessment and spet brain imaging study. Tartu, 2014, 124 p.
21. **Sten Ilmjärv.** Estimating differential expression from multiple indicators. Tartu, 2015, 125 p.
22. **Paula Reemann.** The effects of microenvironment on skin cells. Tartu, 2015, 146 p.
23. **Tanel Visnapuu.** Pharmacological and behavioral characterization of the monoaminergic and GABA-ergic systems of *Wfs1*-deficient mice. Tartu, 2015, 107 p.
24. **Indrek Heinla.** Behavioural and genetic comparison of B6 and 129Sv mouse lines focusing on the anxiety profile and the expression of *Lsamp* gene. Tartu, 2016, 115 p.
25. **Liina Haring.** Cognitive functioning after first psychotic episode. Tartu, 2017, 146 p.
26. **Triin Tekko.** Neurodevelopmental Approach in the Study of the Function of *Wfs1* and *Lsamp*, Potential Targets in the Regulation of Emotional Behaviour. Tartu, 2018, 194 p.
27. **Alina Altpere.** Targeting of mechanisms of elevated anxiety in female *Wfs1*-deficient mice. Tartu, 2018, 98 p.
28. **Maarja Toots.** Pharmacological challenge in rodent models of Wolfram syndrome with emphasis on diabetic phenotype. Tartu, 2018, 114 p.